

University of New Hampshire

## University of New Hampshire Scholars' Repository

---

Doctoral Dissertations

Student Scholarship

---

Fall 1982

### A STUDY OF THE THERMODYNAMICS OF ANION BINDING TO HUMAN SERUM TRANSFERRIN

DONALD ALLEN FOLAJTAR

Follow this and additional works at: <https://scholars.unh.edu/dissertation>

---

#### Recommended Citation

FOLAJTAR, DONALD ALLEN, "A STUDY OF THE THERMODYNAMICS OF ANION BINDING TO HUMAN SERUM TRANSFERRIN" (1982). *Doctoral Dissertations*. 1333.  
<https://scholars.unh.edu/dissertation/1333>

This Dissertation is brought to you for free and open access by the Student Scholarship at University of New Hampshire Scholars' Repository. It has been accepted for inclusion in Doctoral Dissertations by an authorized administrator of University of New Hampshire Scholars' Repository. For more information, please contact [Scholarly.Communication@unh.edu](mailto:Scholarly.Communication@unh.edu).

## INFORMATION TO USERS

This reproduction was made from a copy of a document sent to us for microfilming. While the most advanced technology has been used to photograph and reproduce this document, the quality of the reproduction is heavily dependent upon the quality of the material submitted.

The following explanation of techniques is provided to help clarify markings or notations which may appear on this reproduction.

1. The sign or "target" for pages apparently lacking from the document photographed is "Missing Page(s)". If it was possible to obtain the missing page(s) or section, they are spliced into the film along with adjacent pages. This may have necessitated cutting through an image and duplicating adjacent pages to assure complete continuity.
2. When an image on the film is obliterated with a round black mark, it is an indication of either blurred copy because of movement during exposure, duplicate copy, or copyrighted materials that should not have been filmed. For blurred pages, a good image of the page can be found in the adjacent frame. If copyrighted materials were deleted, a target note will appear listing the pages in the adjacent frame.
3. When a map, drawing or chart, etc., is part of the material being photographed, a definite method of "sectioning" the material has been followed. It is customary to begin filming at the upper left hand corner of a large sheet and to continue from left to right in equal sections with small overlaps. If necessary, sectioning is continued again—beginning below the first row and continuing on until complete.
4. For illustrations that cannot be satisfactorily reproduced by xerographic means, photographic prints can be purchased at additional cost and inserted into your xerographic copy. These prints are available upon request from the Dissertations Customer Services Department.
5. Some pages in any document may have indistinct print. In all cases the best available copy has been filmed.

**University  
Microfilms  
International**

300 N. Zeeb Road  
Ann Arbor, MI 48106



8320642

**Folajtar, Donald Allen**

A STUDY OF THE THERMODYNAMICS OF ANION BINDING TO HUMAN  
SERUM TRANSFERRIN

*University of New Hampshire*

PH.D. 1982

University  
Microfilms  
International

300 N. Zeeb Road, Ann Arbor, MI 48106



A STUDY OF THE THERMODYNAMICS OF ANION  
BINDING TO HUMAN SERUM TRANSFERRIN

BY

DONALD A. FOLAJTAR  
A.B., Franklin & Marshall College, 1978

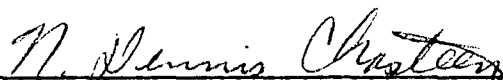
A DISSERTATION

Submitted to the University of New Hampshire  
in Partial Fulfillment of  
the Requirements for the Degree of

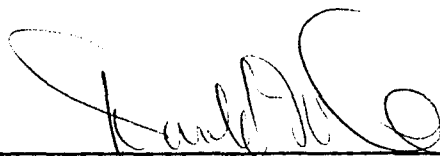
Doctor of Philosophy  
in  
Chemistry

September, 1982

This thesis has been examined and approved.



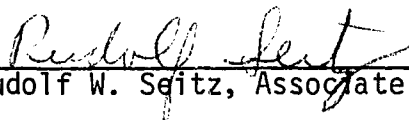
Thesis director, N. Dennis Chasteen  
Professor of Chemistry



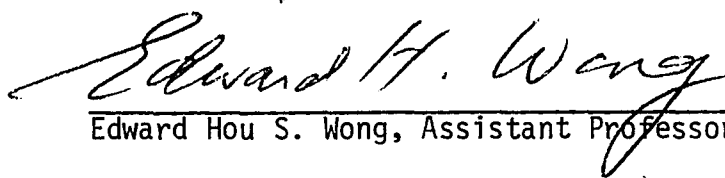
Donald M. Green, Professor of Biochemistry



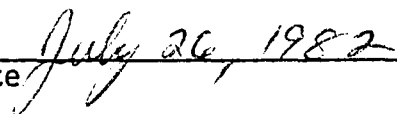
Paul R. Jones, Professor of Chemistry



Rudolf W. Seitz, Associate Professor of Chemistry



Edward Hou S. Wong, Assistant Professor of Chemistry

Date  July 26, 1982

To Janet,  
For Listening  
For Sharing  
For Caring



## TABLE OF CONTENTS

LIST OF TABLES.....	v
LIST OF FIGURES.....	vi
ABSTRACT.....	ix
I. INTRODUCTION TO THE TRANSFERRINS AND THEIR ANION BINDING PROPERTIES.....	1
Physical Properties.....	2
Effect of Inorganic Anions on Transferrin.....	4
II. STUDY OF ANION BINDING TO HUMAN SERUM TRANSFERRIN BY EPR DIFFERENCE SPECTROSCOPY.....	7
Experimental Procedure.....	10
Results.....	14
Discussion.....	41
III. THERMODYNAMICS OF IRON BINDING TO TRANSFERRIN.....	45
Experimental Procedure.....	48
Results.....	55
Determination of b.....	56
Determination of c.....	60
Determination of a.....	63
Determination of Q.....	71
Discussion.....	81
IV. STUDY OF ATP AND PYROPHOSPHATE BINDING TO TRANSFERRIN BY <sup>31</sup> -P NMR SPECTROSCOPY.....	87
Experimental.....	87
Results.....	91
<sup>31</sup> -P Spectroscopy of ATP Binding to Transferrin.....	91
<sup>31</sup> -P Spectroscopy of Pyrophosphate Binding to Transferrin.....	101
Distance Calculation.....	104
Discussion.....	109
V. SUMMARY.....	112
REFERENCES.....	115

## LIST OF TABLES

2.1	% Reduction of EPR Signal Amplitude.....	21
2.2	Binding Data for Anions with Human Transferrin.....	27
2.3	Results of Model Calculations for Chloride Binding.....	34
3.1	Possible Reactions of Iron(III) and Pyrophosphate at pH 7.5.....	68
3.2	Titratable Protons released during Fe(III) complexation.....	70
3.3	Summary of Equilibrium Constants $Q_1$ and $Q_2$ .....	77
3.4	Stepwise Site Equilibrium Constants.....	80
4.1	Summary of Binding Data of ATP to Transferrin.....	100
4.2	Calculated Metal-Anion Distances.....	111

## LIST OF FIGURES

2.1	X-band Spectrum of Diferric Transferrin at pH 7.5 and 77 K.....	8
2.2	Iron(III) Energy Level Diagram.....	9
2.3	Effect of Chloride Ion on the X-band spectrum of Diferric Transferrin.....	15
2.4	Computer Subtracted EPR Difference Spectra as a Function of Chloride.....	16
2.5	Effect of Thiocyanate on 77 K X-band EPR Spectrum of Diferric Transferrin.....	18
2.6	Frozen Solution 77 K EPR Spectrum of Iron(III) and Pyrophosphate at pH 7.5.....	19
2.7	Effect of Microwave Power on the EPR Amplitude of Diferric Transferrin.....	22
2.8	X-band EPR Spectrum of Diferric Transferrin at 1 mW and pH 7.5.....	23
2.9	Difference Spectrum Parameter $\Delta A$ as a Function of Anion Concentration.....	25
2.10	EPR Titration of Diferric Transferrin with NaSCN at pH 7.4.....	26
2.11	Hill Plots of Anion Binding.....	29
2.12	Hill Plots of SCN <sup>-</sup> Binding to Diferric Transferrin.....	30
2.13	Effect of Chloride on the X-band EPR Spectra of the Monoferric Transferrins.....	35
2.14	Hill Plot of Chloride Binding to N-terminal Monoferric Transferrin.....	37
2.15	Hill Plot of Chloride Binding to C-terminal Monoferric Transferrin.....	38
2.16	Effect of Chloride on the X-band EPR Spectrum of Diferric Ovotransferrin.....	39
2.17	Hill Plot of Chloride Binding to Diferric Ovotransferrin.....	40

3.1	Frozen Solution 77 K EPR Spectrum of Pyrophosphate, Transferrin and Iron(III), pH 7.5.....	51
3.2	X-band EPR Spectrum of Fe-Pyrophosphate Complex at 77 K and pH 7.5.....	52
3.3	X-band EPR Spectrum of Transferrin Bound Iron(III) at 77 K and pH 7.5.....	53
3.4	Dependence of Iron Saturation of Transferrin on Pyrophosphate Concentration.....	57
3.5	Determination of b.....	59
3.6	Dependence of Iron Saturation on pH.....	61
3.7	Determination of c.....	62
3.8	Schematic of Urea/Polyacrylamide-Gel Electro- phoresis as a Function of pH.....	64
3.9	Dependence of Iron Saturation on Concentration of Added Bicarbonate.....	65
3.10	Determination of a.....	66
3.11	Determination of Q.....	73
3.12	Effect of $Q_1$ and $Q_2$ as a Function of pH.....	76
3.13	Predicted % Fe-saturation as a Function of Protein and Pyrophosphate Concentration.....	85
4.1	$^{31}\text{P}$ NMR Spectrum of ATP.....	92
4.2	$(1/T_1)_p$ vs $[\text{FeTfFe}]$ for Alpha Phosphorus of ATP.....	93
4.3	$(1/T_1)_p$ vs $[\text{FeTfFe}]$ for Beta Phosphorus of ATP.....	94
4.4	$(1/T_1)_p$ vs $[\text{FeTfFe}]$ for Gama Phosphorus of ATP.....	95
4.5	$(1/T_1)_p$ vs $[\text{ATP}]$ at Constant Protein.....	97
4.6	$(1/T_1)_p$ vs $[\text{ATP}]$ at Constant Protein.....	98
4.7	$(1/T_1)_p$ vs $[\text{ATP}]$ at Constant Protein.....	99
4.8	$(1/T_1)_p$ vs $[\text{NTA/TF}]$ .....	102
4.9	$(1/T_1)_p$ vs $[\text{Fe}]/[\text{Tf}]$ .....	103

4.10	$(1/T_1)_p$ vs $[PP_i]$ at Constant Protein.....	105
4.11	$(1/T_1)_p$ vs $[TF]$ at Constant Pyrophosphate.....	106
4.12	Dahlquist-Raftery Plot of $(1/T_1)_p$ at Constant Protein Concentration.....	107
4.13	Dahlquist-Raftery Plot of $(1/T_1)_p$ at Constant Pyrophosphate Concentration.....	108

## ABSTRACT

### A STUDY OF THE THERMODYNAMICS OF ANION BINDING TO HUMAN SERUM TRANSFERRIN

by

DONALD A. FOLAJTAR

University of New Hampshire, September, 1982

Electron paramagnetic resonance difference spectroscopy of diferric human serum transferrin indicates that certain inorganic anions alter the electronic environment of the iron centers of the protein by binding to specific anion sites. The binding of these anions (thiocyanate, perchlorate, adenosinetriphosphate, pyrophosphate, and chloride) is shown to occur pairwise with high positive cooperativity, an observation unique to nonstereospecific anion-protein interactions. It is shown that human serum transferrin has binding sites for four non-synergistic anions, two in each domain. The association constants are reported.

It is unlikely that the anions bind to a significant extent at the sites occupied by the synergistic anion since none of them facilitates iron binding in the absence of bicarbonate.

It is more likely that these anions bind to positively charged amino acids or possibly to amide dipoles of the protein. The free energy of association of these anions follows the lyotropic series which is approximately the same sequence for the affinity of anions for positively charged sites on proteins.

$^{31}\text{-P}$  NMR spectroscopy reveals that the locus of interaction is near the iron centers and confirms that both sites are effected. In solutions containing an NTA:transferrin concentration of 4:1 no paramagnetic enhancement in the  $^{31}\text{-P}$  relaxation rate is observed. NTA also negates the response of the EPR spectrum to the above anions. Cooperativity in anion binding is also observed at pH 7.5 but at pH 9, no cooperativity is evident.

A competitive binding study between pyrophosphate and transferrin for iron is presented. The results reveal that the thermodynamics of iron binding to transferrin is dependent on the concentration of pyrophosphate, the pH of the solution and the bicarbonate concentration.

## CHAPTER I

### INTRODUCTION TO THE TRANSFERRINS AND THEIR ANION BINDING PROPERTIES

The transferrins are a class of metal binding proteins widely distributed in the physiological fluids and cells of vertebrates. Serum transferrin plays an active role in iron metabolism, being the only protein known to carry iron from sites of adsorption and storage to sites of utilization and excretion (1). Ovotransferrin and lactoferrin, transferrins found in the white of avian eggs and in mammalian milk, respectively, appear to provide a defense mechanism against infection by denying iron, an essential nutrient, to invading organisms (2).

All transferrins are B-globulins capable of binding two atoms of iron as high spin Fe(III). The protein will also bind a variety of other trace metals such as Cu(II), VO(II), Gd(III), Co(III), and Zn(II). Metal binding is facilitated by the binding of certain synergistic organic anions possessing a carboxylate group and a second electron-withdrawing group. It is well established that, in physiological media, the synergistic anion is carbonate (or bicarbonate) and that the protein cannot sequester iron in the absence of a suitable anion (3-6). Determination of the physiological roles of the two metal binding sites, the role of the synergistic anions in binding, the identity of the coordinating ligands, and of the mechanism of metal association



and dissociation are focal points in transferrin research. Several reviews of the transferrin literature have been published in recent years (7-12).

### Physical Properties

Transferrin consists of a single polypeptide chain with two prosthetic carbohydrate groups. It has a molecular weight of 78,000 and has no subunits. The protein consists of two similar domains, each containing one metal binding site, as evidenced by the high degree of internal homology (13) and by the production of fragments of various transferrins by partial proteolysis. These fragments have approximately half the molecular weight of the whole protein and a single Fe(III) site (14-17). The complete amino acid sequence of human serum transferrin and ovotransferrin has recently been published, and about 40% of the amino acids are identical in the N- and C-terminal domains (18,19). Studies of human lactoferrin reveal similar internal homologies (20). Transferrin, which contains two Fe-binding sites, has clearly evolved by duplication of the structural gene from an ancestral protein that had a single Fe-binding site and a molecular weight of 40,000 (18). Nonetheless, the two domains show some interesting differences including the presence of more disulfide bonds in the C-terminal domain. Why transferrin has evolved as a two-sited protein and the biological advantage obtained in this evolution remain mysteries.

Preliminary X-ray crystal structures of human serum transferrin, lactoferrin, and rabbit transferrin have been reported (21-23).

The rabbit protein consists of two lobes, resembling ellipsoids with major axes inclined at about 30 degrees to each other (23). The overall dimensions are consistent with hydrodynamic measurements.

Oxygen and nitrogen donor atoms have been implicated in the binding of iron to the protein. Ultraviolet difference spectra of various metallothioneins display two prominent bands attributed to the binding of ionized phenolate groups (24-27). Presumably, two or possibly three tyrosines are coordinated to the metal. Fluorescent lifetime measurements of lanthanide metallothioneins suggest two tyrosines (28). On the other hand, titration data on tyrosine in apo- and diferric metallothioneins and nitration of tyrosine suggest three residues per metal site (29). The visible absorption spectra of Fe(III), Cu(II), and Co(III) complexes reflect electron donor-acceptor interactions between the metal and tyrosine (30). Transitions in the resonance Raman spectrum also implicate tyrosine and histidine in the binding process (31,32). The EPR spectrum of copper metallothionein exhibits a three component splitting attributed to a superhyperfine interaction from coordinated nitrogen, presumably from imidazole (33). Proton relaxation studies confirm that solvent water molecules have access to the metal-binding site (34).

The role of the synergistic anion in the binding of metals to metallothionein is an area of great interest. It appears that the anion is ligated directly to the metal and most likely to the protein as well (35-37). It is not known whether carbonate

or bicarbonate is the anion preferred by transferrin; a recent NMR study has implicated both (38).

Transferrin contains two completely functional metal binding sites located in the N- and C- terminal domains of the protein. Originally the optical spectra of the two sites were thought to be identical (16). Recent successes in proteolytically cleaving transferrin into two monoferric fragments have revealed small but definite differences in the visible region (14-17). Differences have also been observed by EPR and NMR spectroscopy. VO(II) EPR spectra of transferrin exhibit up to three spectroscopic species depending on pH, but at physiological pH of 7.5, only two species are identifiable (35,41). Further distinctions can be made from EPR spectra of isotopically pure Cu(II) transferrin and from single-site monoferric transferrins (42,43).

The binding of iron to transferrin and the distribution of iron between the two sites is dependent upon pH, the form of the added iron, and whether small chelates are present or not. Iron, added as a ferric salt, gives variable and unpredictable nonspecific binding due to hydrolysis and polynuclear complex formation. More reliable loading is achieved by the use of ferric chelates or freshly prepared ferrous salts. Below pH 7.0, C-terminal binding is favored whereas at higher pH values, the N-terminal site is preferred.

#### Effect of Inorganic Anions on Transferrin

The binding of inorganic ions to proteins has long been recognized. Anion binding to proteins is usually relatively

weak, having site affinity constants in the range of  $0.1 \text{ M}^{-1}$  to  $1000 \text{ M}^{-1}$ , although much higher values have been reported for polyvalent electrolytes (44,45). The dialysis-resistant binding of NTA and citrate to transferrin is probably an example of multidentate attachment to the protein (40).

Recently, Williams and Moreton observed that dialysis of serum against buffer caused iron, preferentially bound in the N-terminal site, to migrate to the C-terminal site in equilibrated samples of fresh serum (46). The low molecular weight component largely responsible for this effect has been identified as the chloride ion (47). Other anions can also bring about this change, perchlorate being most effective. In combination, an increase in anion concentration and pH markedly enhances the stability of iron-binding in the N-terminal domain relative to the C-terminal domain (48).

The effect of inorganic anions on the properties of transferrin is not limited to their influence on the thermodynamic stabilities of iron binding to the two sites of the protein. Because iron is held so tightly to the protein, a kinetic barrier to the release of iron from the protein must be overcome before transfer of iron is achieved. Chloride has been found to be very effective at accelerating the kinetics of iron release from the C-terminal site of diferric transferrin but retards the release from the N-terminal site (47). Similar results have been observed for the two monoferric transferrins (49). In addition to chloride, other anions, including perchlorate, fluoride,

EDTA, and NTA, are capable of affecting the kinetics of iron release.

Of particular interest are phosphorus containing chelates and nucleotides which are present as potential iron ligands and transport agents in the cytosol of the iron requiring reticulocyte. Efficiency of iron removal in vitro by such chelates follows the order pyrophosphate > adenosinetriphosphate (ATP) > adenosinediphosphate (ADP) > 2,3-diphosphoglycerate. Adenosinemonophosphate (AMP) and orthophosphate are ineffective as catalysts for the release of iron from transferrin (50,51).

The pronounced influence of physiologically relevant inorganic anions on the metal binding properties of transferrin prompted the investigations reported in this dissertation.

## CHAPTER II

### A STUDY OF ANION BINDING TO HUMAN SERUM TRANSFERRIN BY EPR DIFFERENCE SPECTROSCOPY

Figure 2.1 shows the frozen solution Fe(III) EPR spectrum of diferric transferrin. The intense resonance at an effective g-value of 4.3 (150 mT) and the weaker signal at  $g'=9.7$  (70 mT) is typical of non-heme iron proteins and rhombic Fe(III)-complexes. The fingerprint of iron specifically bound to transferrin is the detailed splittings of the  $g'=4.3$  resonance (9,52). This fine structure is unique to transferrin iron. Small complexes exhibit broad featureless spectra in this region while uncomplexed Fe(III) exists as a polymeric hydroxide and is EPR silent at 77° K (3).

From X-band and Q-band line position measurements, the ratio of axial to rhombic components of the zero field (E/D) has been determined to be 0.31-0.32 (53). The value of E/D near 1/3 reflects the low symmetry environment of the metal ion. E/D ratios of 1/3 with a zerofield splitting greater than the energy of the spectrometer ( $D > h\nu$ ) give rise to spectra with effective g-values of 4.3 (49). In a spherical ligand field environment, Fe(III) has six degenerate spin states (Figure 2.2), but axial or rhombic perturbations of the ligand field remove some degeneracy, producing three pairs of degenerate spin states ( $m_S = \pm 1/2, \pm 3/2, \pm 5/2$ ) known as Kramer's doublets (54). The degeneracies of this zero-field state are removed by application of an external magnetic field. EPR transitions observed at X-

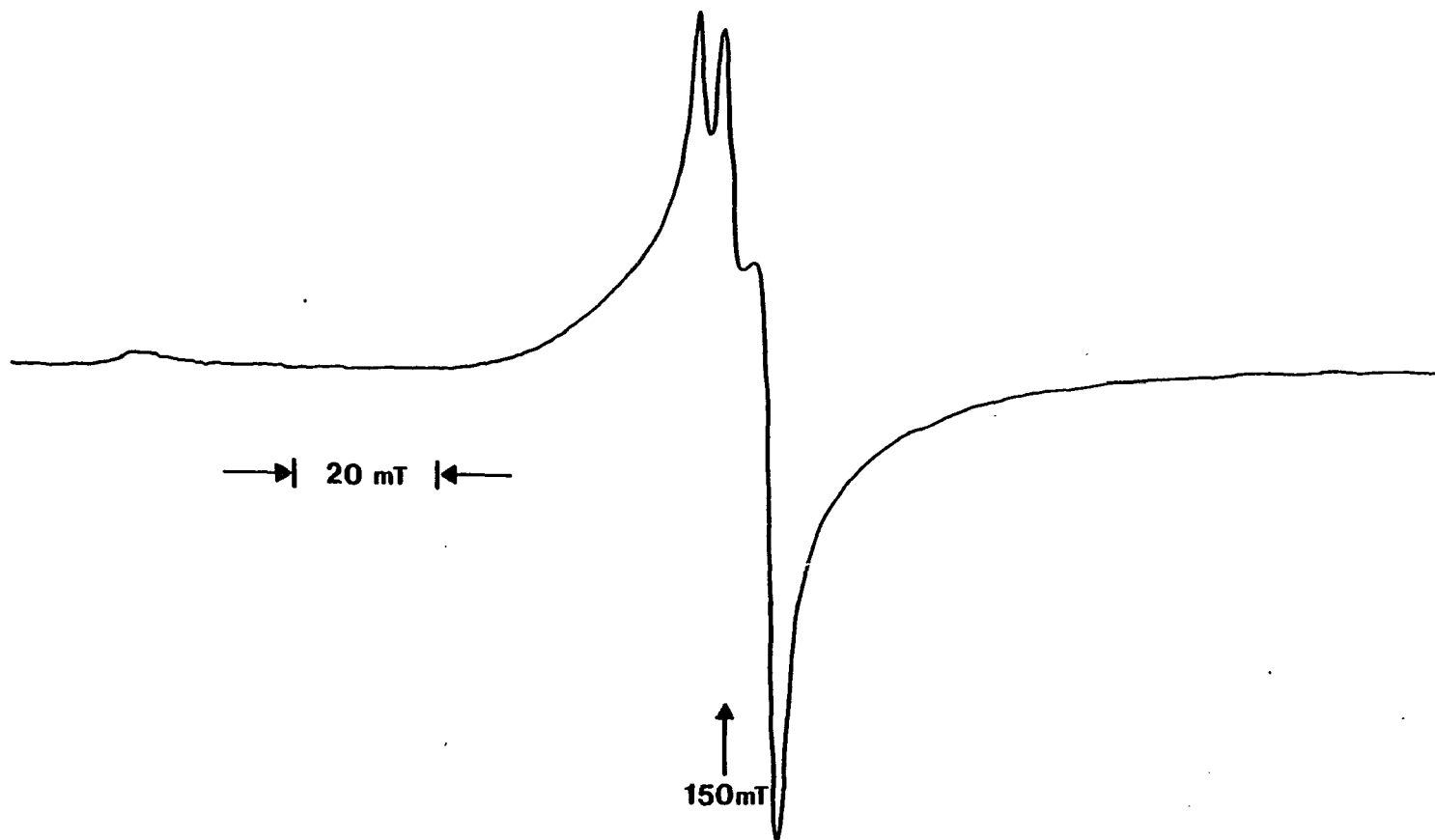


Figure 2.1. Frozen solution 77K X-band iron EPR spectrum of diferric human serum transferrin. Instrument settings: power = 20 mw, modulation amplitude = 10 G, sweep rate = 2000 G/16 min, time constant = 0.3 sec.

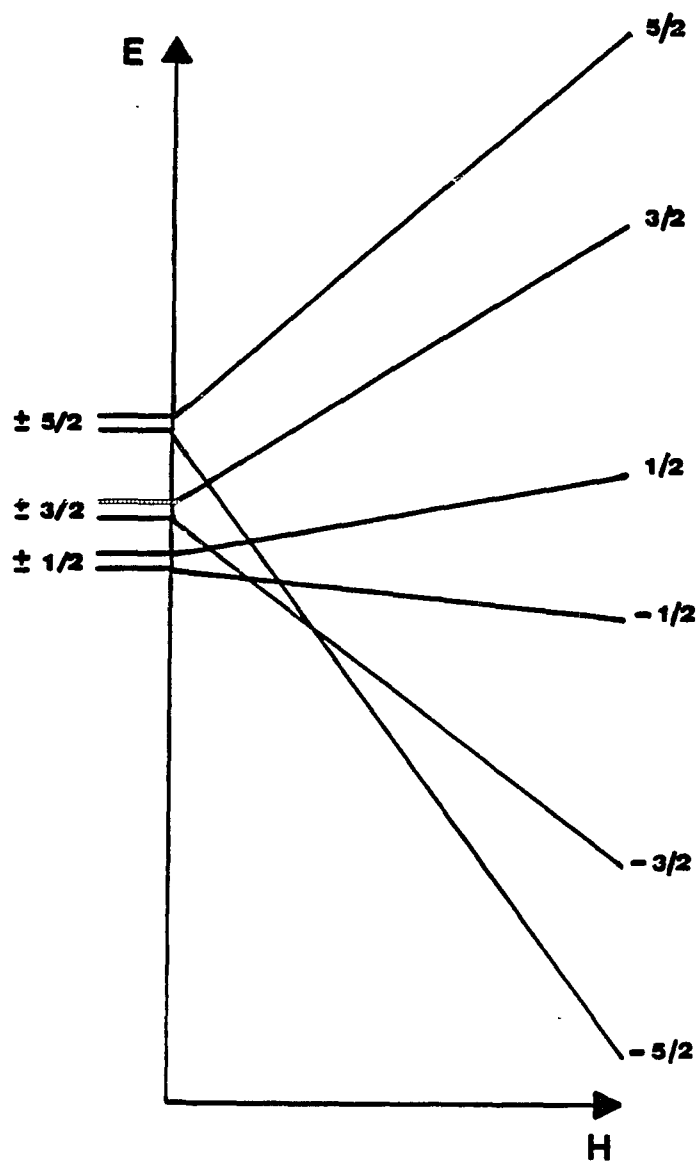


Figure 2.2. Iron III energy level diagram. Sixfold degeneracy removed by zero field. Position of spin states differ depending on frequency. The  $g = 4.3$  transition at X-band is between  $+3/2$  and  $-3/2$  states.



band frequency correspond to those spin states separated by an energy difference of 9.2 GHz: the selection rule for allowed transitions in a strong magnetic field,  $m_s = \pm 1$ , is not always obeyed. The characteristic X-band signal at  $g' = 4.3$ , referred to above for iron transferrins, is the transition between the  $-3/2$  and  $+3/2$  spin states (52).

Perturbations on the iron EPR spectra of transferrin and ovotransferrin due to perchlorate were first noted by Price and Gibson (55). This anion was subsequently shown to perturb the EPR spectra of Cu(II), Gd(III), and VO(II) transferrins, indicating that the changes were a property of the protein (56). Chloride was also shown to perturb the EPR spectrum of VO(II)-transferrin (56). In light of these observations a detailed study of anion-induced changes in the iron EPR spectrum of transferrin was undertaken with the goal of determining the origin of the changes. It is established in this chapter that inorganic anions bind specifically to transferrin. The stoichiometries and binding constants are presented.

### Experimental Procedure

Commercial preparations of iron-free human serum transferrin of stated 99% purity were purchased from Behring Diagnostics Corporation and used without further purification. The concentrations of apotransferrin were determined spectrophotometrically at 280 nm using  $E_{1\%}^{280}$  of 11.4 (3) and a molecular weight of 78,000 (57): this converts to a molar extinction coefficient of

$8.89 \times 10^{-4} \text{ M}^{-1} \text{ cm}^{-1}$ . Stock solutions of aqueous ferrous ammonium sulfate  $\text{Fe(II)(NH}_4)_2(\text{SO}_4)_2$  were prepared in 0.01 M HCl. At this pH, oxidation of Fe(II) is retarded. The protein was brought to near 100% saturation by the addition of two equivalents of 0.1 M Fe(II) to apotransferrin samples in 0.1 M HEPES (N-2-hydroxyethyl-piperazine-N-2'-ethanesulfonic acid)/NaOH, 0.01 M  $\text{HCO}_3^-$ , pH 7.5. Normally a 10-fold excess of bicarbonate was added to insure stoichiometric binding of the iron to the protein. A salmon pink color characteristic of diferric transferrin slowly developed. The solutions were in contact with air at 4 degrees centigrade for a minimum of 24 hours or until no further increase in absorption at 465 nm was observed.

1.0 M stock solutions of the sodium salts of all anions were prepared volumetrically. Sodium pyrophosphate and sodium dodecylsulfate were dissolved by warming and then slowly cooling the supersaturated solutions to room temperature and using them immediately thereafter. Buffers and salt solutions were rendered metal free by shaking over Chelex-100. Glassware was cleansed of metals by soaking in 1:1  $\text{H}_2\text{SO}_4$ - $\text{HNO}_3$  followed by rinsing in doubly distilled deionized water. All solutions were prepared in doubly distilled water and buffered at pH 7.5 in 0.1 M HEPES buffer (Sigma Chemical Corp.). Distilled deionized water was obtained from a Barnstead still and subsequently passed through a Barnstead D0803 ion exchange column.

C-terminal monoferric transferrin was prepared by adding one equivalent of Fe(II) to apotransferrin at pH 6.0 followed

by air oxidation of the iron. The solution was allowed to stand until no further increase in the  $A^{465}$  was observed. The purity of the C-terminal monoferric transferrin was verified by urea/polyacrylamide-gel electrophoresis (48). N-terminal monoferric transferrin was prepared by the method of Williams (58). Apo-transferrin was dissolved in 0.1 M HEPES/NaOH, 0.01 M  $\text{HCO}_3^-$ , and pH 7.5 such that the concentration was 20 mg/ml (total volume 4 ml). Enough iron, as ferrous ammonium sulfate was introduced to saturate the protein. The solution was allowed to stand for 24 hours at which time the percent saturation was checked at 465 nm. The protein was then diluted to 4 mg/ml with a 0.1 M HEPES, 0.5 M NaCl, 1 mM  $\text{Na}_4\text{P}_2\text{O}_7$ , pH 7.5 solution. Enough desferrioxamine (CIBA Pharmaceuticals) was added to complex 50% of the iron. The amount of iron being removed from transferrin was followed at 465 nm. When the reaction had reached completion as evidenced by no further change in absorbance, the protein was dialyzed against 2 one-liter volumes of 0.1 M Tris, pH 7.5 followed by dialysis against one 100-ml volume of 0.1 M HEPES, pH 7.5. Finally, N-terminal monoferric transferrin was concentrated on an Amicon model 3 ultrafiltration apparatus fitted with a PM 10 (MW cutoff = 10,000) membrane under 20 psi of nitrogen. Urea/polyacrylamide-gel electrophoresis showed the presence of only N-terminal monoferric and a small amount of apotransferrin.

Urea/polyacrylamide-gel electrophoresis was accomplished as follows. After thoroughly cleaning the glass plates with

95% ethanol to prevent gel sticking, a thin layer of Vaseline was applied to the spacer bars. The plates were assembled and warmed briefly in an oven at 100° C to shorten set-up time and stop any leaks that might occur. The gel was prepared by dissolving 3.25 g acrylamide, 160 mg bisacrylamide and 60 mg ammonium persulfate in 2.5 ml stock buffer (242 g Trizma Base, 12 g disodium EDTA, and 12.36 g boric acid/liter of buffer at pH 8.5) and 47.5 ml of 6.3 M deionized urea. Urea was deionized on a Biorad AG501-X8CD mixed bed anion-cation exchange resin, 20-50 mesh, immediately before use. A solution of 30  $\mu$ l of NNN'N'-tetramethylethylenediamine (TEMED) was added to the gel solution as an initiator. The gel was poured immediately thereafter and the comb inserted. After standing for one hour under fluorescent light, the comb was removed and the gel was ready to use.

Typically 10-50  $\mu$ l of samples (1 mg/ml) in 10% glycerol-90% tank buffer (5% stock buffer) colored with bromphenol blue were applied. The glycerol aids in layering the sample in the slot. Urea that had leached out of the gel was removed with a Pasteur pipet just prior to sample application. Samples were electrophoresed at 120 V (constant voltage) for 20 hours with an LKB 2103 power supply unit. The initial current readings were about 60 mA but fell during the course of the run to around 30 mA. Staining solution was 0.25 % Coomassie Blue R250 in methanol/acetic acid/water (5:1:5). The gel was stained for 10 minutes and then destained for 1/2 hour with two changes of destain solution (100 ml methanol, 150 ml glacial acetic acid to 2 liters with water) followed by destaining overnight in a third change.

EPR spectra were measured at X-band frequency on a Varian E-4 or E-9 spectrometer interfaced with a Minc-11 laboratory computer (Digital Equipment Corporation). Samples were placed in calibrated tubes (approximately 4 mm o.d., 3 mm i.d.) for spectra recorded at 98° K. Titrations of the protein with the various anions were carried out by delivering a calculated volume of 1 M titrant in 0.1 M HEPES/NaOH, pH 7.5 into 0.4 ml of buffered 1 mM diferric transferrin. Approximately 300  $\mu$ l of the sample was withdrawn and frozen in a quartz tube by immersion in liquid nitrogen. Temperature of the sample was measured with a copper-constantan thermocouple immersed in the frozen solution and maintained at 98° K by employing a Varian V-4257 variable temperature cavity insert on the spectrometer. Spectra were recorded, digitized, and stored on floppy disc after each addition of titrant.

### Results

Figure 2.3 shows the effect of chloride on the iron EPR spectrum of diferric human serum transferrin. Both the  $g'=4.3$  and the  $g'=9.7$  signals are changed. A broad shoulder is evident on the low field side of the characteristic doublet at  $g'=4.3$ . This feature increases in amplitude as the concentration of chloride is increased. This increase as well as that in the  $g'=9.7$  signal is enhanced in the computer subtracted difference spectra of Figure 2.4. In addition to chloride, this effect is observed for the sodium salts of perchlorate, ATP, pyrophosphate, dodecylsulfate, and thiocyanate. The feature of interest in the thiocyanate spectrum appears at a slightly lower field value than

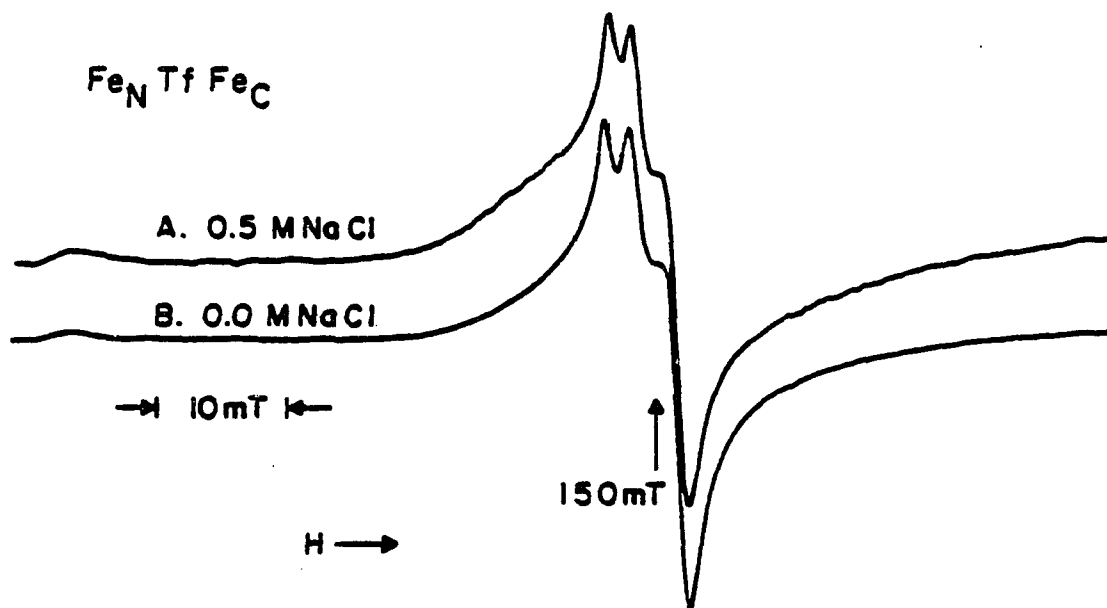


Figure 2.3. Effect of chloride ion on the X-band EPR spectrum of diferric transferrin. (A) 0.5 M NaCl, (b) no NaCl. Conditions: 1 mM protein, 0.1 M HEPES, 0.01 M NaHCO<sub>3</sub>, pH 7.4, 98 K. Instrument Settings: power = 20 mw, modulation amplitude = 10 G, sweep rate = 2000 G/16 min, time const = 0.3 sec.

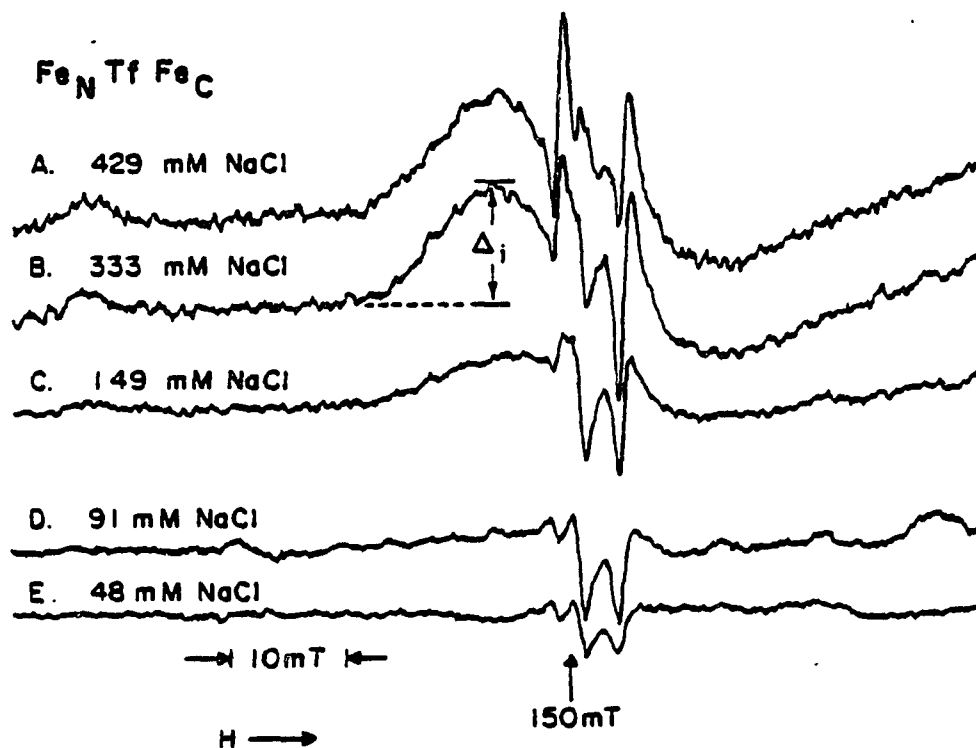


Figure 2.4. Computer subtracted EPR difference spectrum as a function of chloride concentration. Spectrum B subtracted from spectrum A of Figure 2.3. The difference spectrum parameter  $\Delta_i$  is indicated. Conditions as in Figure 2.3.

that of the other salts (Figure 2.5). The sodium salts of tetrafluoroborate, orthophosphate, bicarbonate, sulfate and adenosinemonophosphate, tested at 0.5 M concentration and pH 7.5, showed little effect.

The fact that some sodium salts are ineffective in bringing about a significant change in the EPR spectrum precludes the possibility that sodium is involved or that the effect is due to variation in ionic strength. Moreover, absorbance measurements of the iron-transferrin complex at 465 nm indicate that, except for pyrophosphate, none of the anions is removing iron from the protein, eliminating the possibility that small Fe(III)-anion complexes are contributing to the EPR difference spectrum. Also, solutions of 0.5 M ATP, chloride, perchlorate or thiocyanate containing 1 mM Fe(III) at pH 7.5 in the absence of protein do not exhibit  $g'=4.3$  signals. Solutions of pyrophosphate and iron under the same conditions do exhibit a featureless signal at  $g'=4.3$  (Figure 2.6) that may contribute up to 5% to the observed difference spectrum. The possibility that the difference spectrum arises from non-specifically bound iron was also ruled out by eluting diferric transferrin on Sephadex G75, a procedure known to remove such iron (59). The EPR spectrum responded to perchlorate in the same way both before and after elution. In protein preparations in which Fe(III)-NTA in the ratio of 1:2 was used instead of Fe(II) to saturate the protein with iron, no anion effect was observed.

The EPR first derivative peak-to-peak amplitude of the



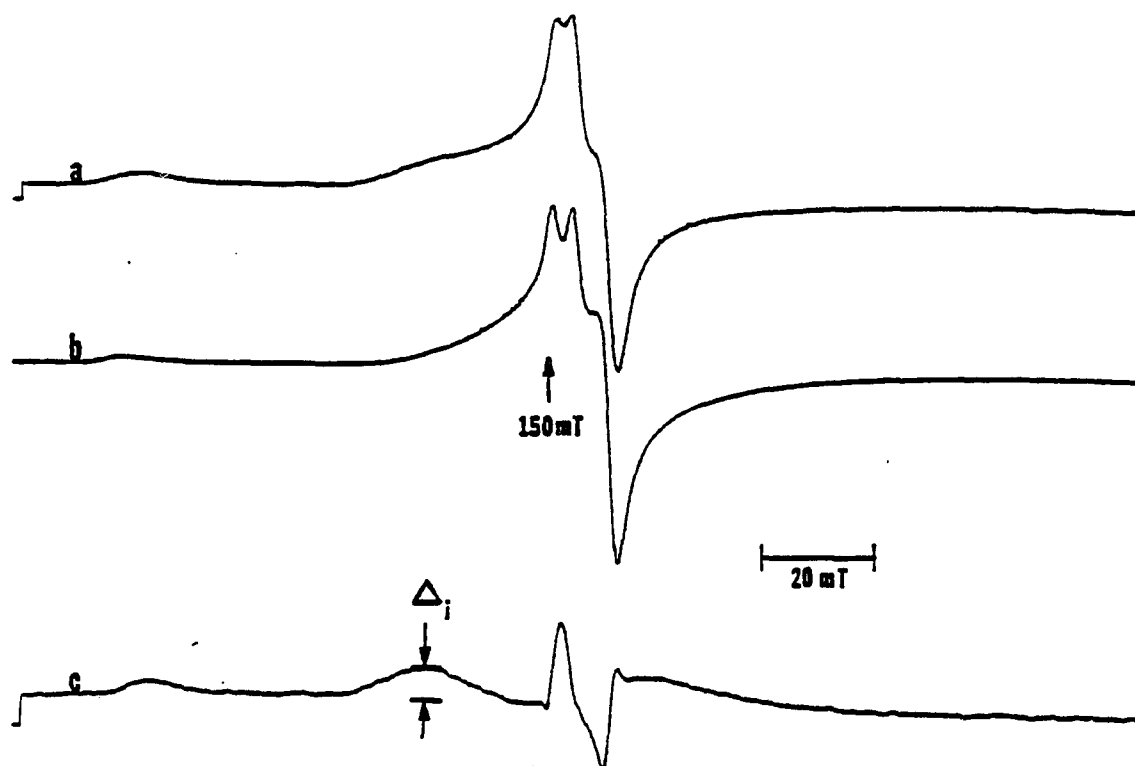


Figure 2.5. Effect of thiocyanate on 77 X-band Fe(III) EPR spectrum of 1mM diferric transferrin in 0.1 M HEPES, 0.01 M  $\text{NaHCO}_3$  pH 7.4. a) Transferrin with 0.5 M SCN; b) Transferrin, no SCN; c) computer subtracted difference spectrum (a-b).  $\Delta_i$  is the extinction of the feature of interest under these conditions.

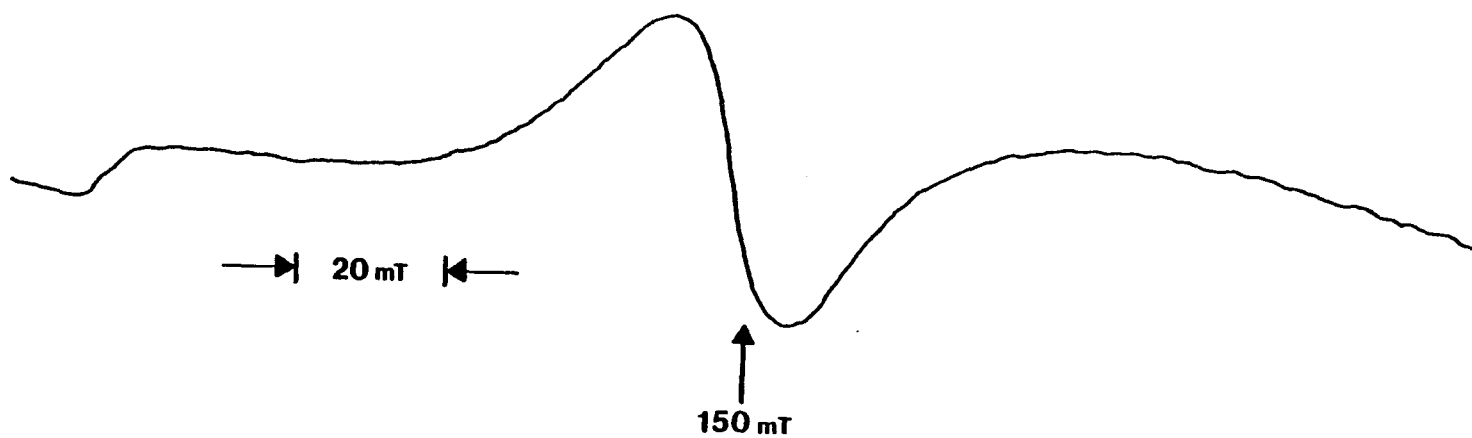


Figure 2.6. Frozen solution 77K iron EPR spectrum of 1 mM iron (III) and 0.01 M pyrophosphate at pH 7.5. Instrument settings as in Figure 2.3.

Fe(III) signal at 150 mT decreases with the addition of salts, e.g., NaCl and NaClO<sub>4</sub>, but the integrated intensity remains fairly constant. At 0.5 M chloride, the amplitude corrected for dilution is reduced by approximately 40% while the intensity obtained from double integration of the spectrum between field values of 50 mT and 250 mT is reduced by only 10%. Price and Gibson have observed a reduction in amplitude with perchlorate as well (55). Other amplitude reductions are presented in Table 2.1. The small reduction in integrated intensity with increasing salt concentration could be due to a slight change in dielectric properties of the sample or to some EPR intensity outside the range of the limits of integration. The reproducibility of the double integral between samples did not warrant extending the limits further.

Power saturation studies of diferric transferrin samples with 0.5 M chloride and with no chloride reveal that for microwave power settings between 0.01 and 30 mW no saturation is occurring (Figure 2.7). Furthermore, as shown in Figure 2.8, the perturbations on the iron EPR spectrum due to chloride are evident at very low power settings well below the saturation limit. The EPR spectrum is also independent of the method of freezing the sample: slow immersion in liquid nitrogen or quick freezing in n-pentane slush.

All Fe(III) spectra as a function of salt were either computer scaled to the same peak-to-peak amplitude of the  $g'=4.3$  signal or to the same integrated intensity prior to subtrac-

Table 2.1

## % Reduction of EPR Signal Amplitude

Anion <sup>a</sup>	Reduction <sup>b</sup>
$\text{HP}_2\text{O}_7^{3-}$	60%
$\text{Cl}^-$	54%
$\text{ClO}_4^-$	52%
$\text{ATP}^{3-}$	48%
$\text{SCN}^-$	30%
$\text{HPO}_4^{2-}$	20%
$\text{F}^-$	17%
$\text{SO}_4^{2-}$	10%
$\text{BF}_4^-$	10%

- a) Conditions: 1 mM protein in 0.1 M HEPES/NaOH buffer, pH 7.4. Spectra measured at 98 K with an anion concentration of 0.5 M
- b) Reduction is the amount (in percent) that the peak-to-peak amplitude of the iron EPR signal of diferric transferrin is reduced attending addition of the above anions.

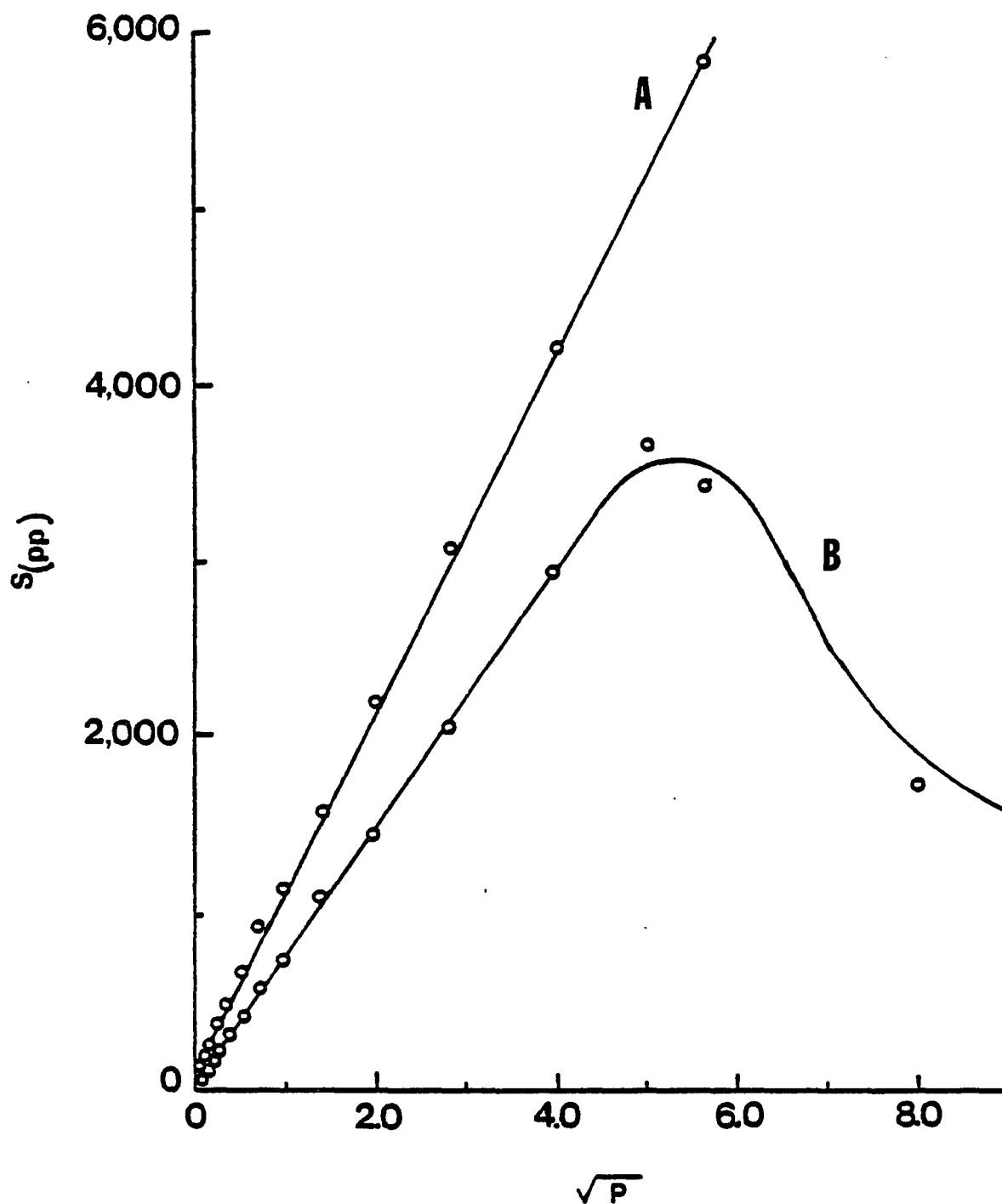


Figure 2.7. Effect of microwave power on the iron EPR peak-to-peak signal amplitude of diferric transferrin. A: 1mM diferric transferrin at pH 7.5. Straight line indicates that signal is responding with the square root of power. B: 1mM diferric transferrin in 0.5 M NaCl. Beyond 20 mW, curvature is exhibited indicating that the sample is being power saturated. Signal expressed in arbitrary units as S/G.

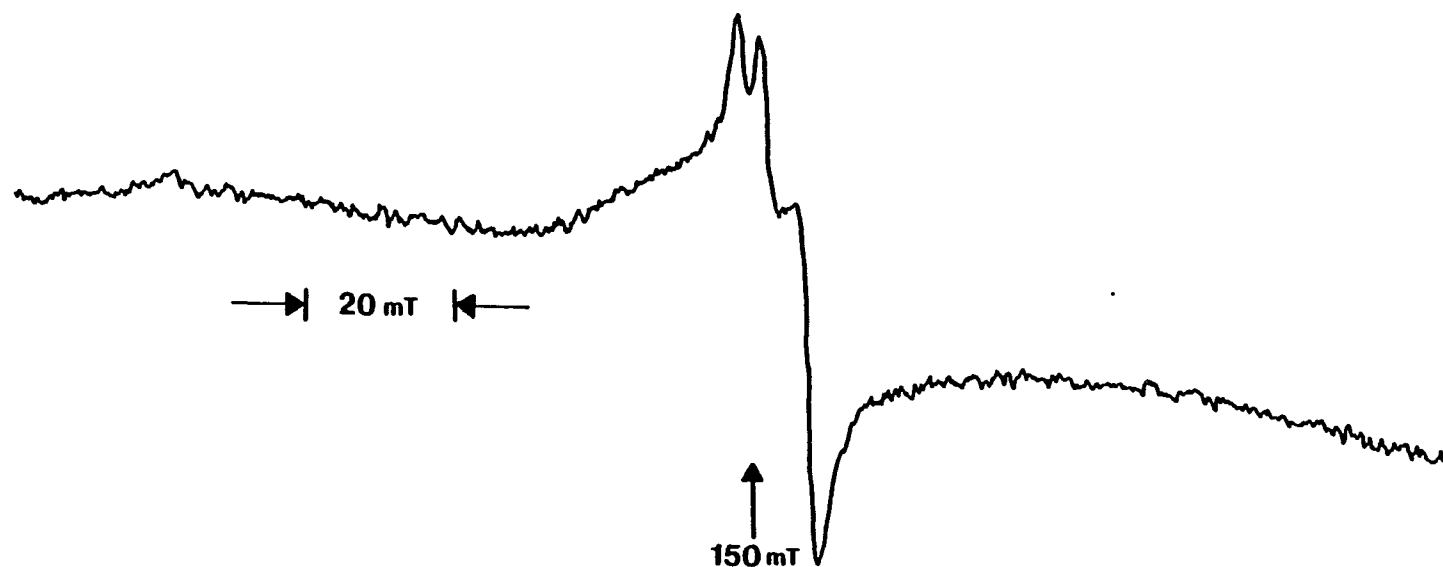


Figure 2.8. Frozen solution 77K X-band EPR spectrum of diferric transferrin in 0.1 M HEPES, 0.01 M  $\text{NaHCO}_3$ , 0.5 M NaCl, pH 7.4. Instrument settings as in Figure 2.3 except that the power is only 1 mw. The feature of interest is evident even at this low power setting.

tion. Because the analysis of the data in terms of anion binding to the protein involves taking the ratio of the amplitudes of the difference spectra, the stoichiometries and binding constants obtained are not very sensitive to the method of scaling and are the same for both methods within experimental error (Table 2.2).

The value of  $\Delta_i$  in the difference spectrum as a function of salt concentration for three different anions is shown in Figures 2.9 and 2.10. The curves display saturation behavior, indicative of a binding process. To a first approximation, the binding of these anions to an iron containing domain of the protein can be represented by the following simplified equilibrium



where domain' represents an anion-protein complex in which the electronic environment of the metal center is altered, giving rise to a new EPR spectrum. The apparent overall association constant, K, is given by

$$K = [\text{domain}']/[\text{domain}][A]^n = R/(1-R) [A]^n \quad (2.1)$$

where  $R (= \Delta_i/\Delta_{\max})$  is the degree of saturation of the anion binding sites.

$\Delta_i$  and  $\Delta_{\max}$  are determined from the graphs in Figures 2.9 and 2.10. Equation 2.1 is equivalent to the Hill equation and predicts that a plot of  $-\log(R/1-R)$  vs  $-\log[A]$  will yield a straight line with a slope of n and an intercept of  $-\log K$ . Straight

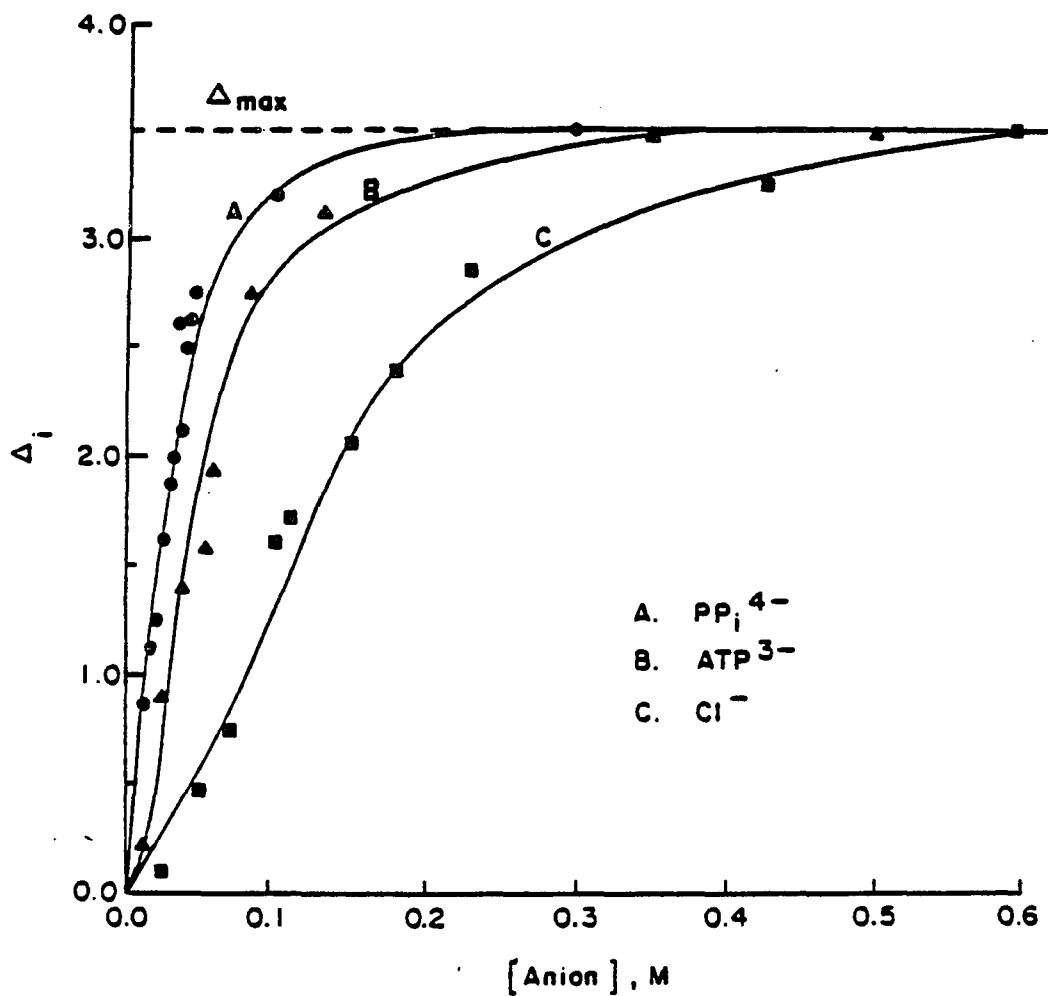


Figure 2.9. Difference spectrum parameter  $\Delta_1$  in arbitrary units as a function of anion concentration for different anions. The maximum value  $\Delta_{max}$  at saturating levels of anion is indicated. Conditions as in Figure 2.3.



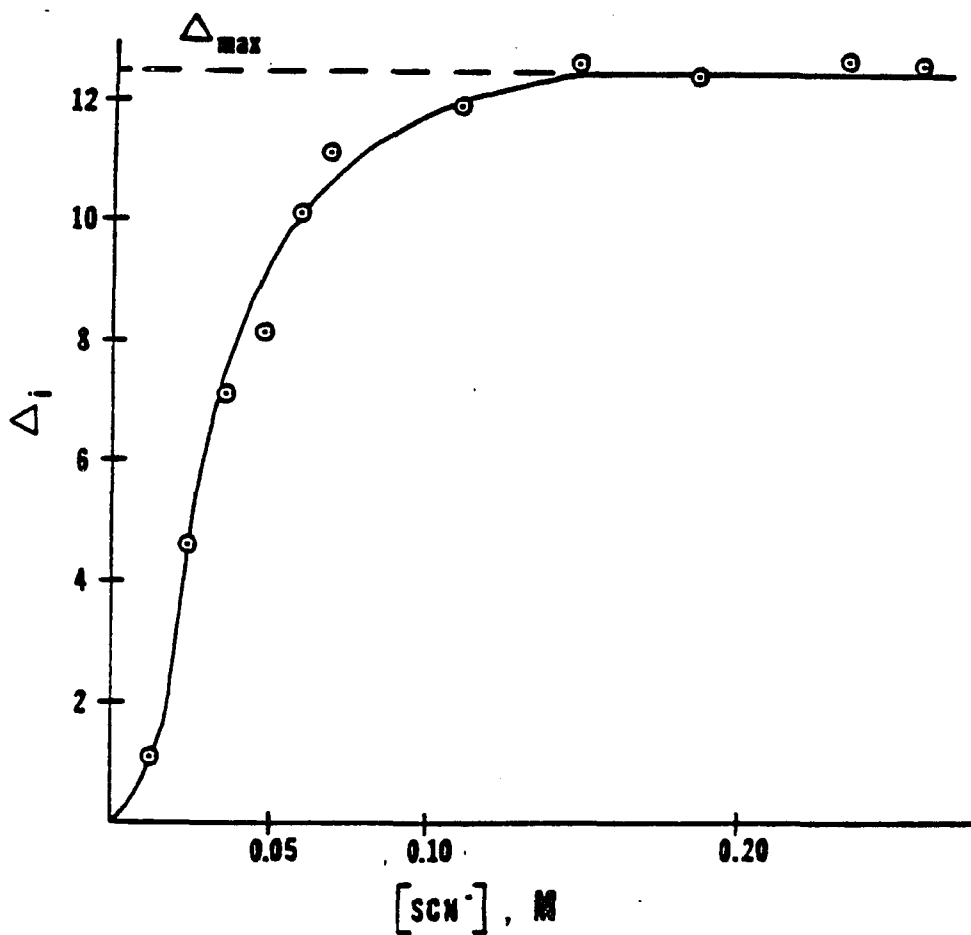


Figure 2.10. EPR titration of 1 mM diferric transferrin in 0.1 M HEPES, 0.01 M NaHCO<sub>3</sub>, pH 7.4 with 1.0 M NaSCN, pH 7.4.  $\Delta_i$  is measured from the computer subtracted difference spectra obtained after each addition of titrant.  $\Delta_{\max}$  is the limiting value of  $\Delta_i$ .

Table 2.2

Binding Data for Anions with Human Transferrin<sup>a</sup>

Anion	Protein	$n^b$	$\log K^c$	$K^d$	$r^e$
$SCN^-^f$	FeTfFe <sup>g</sup>	2.39(.34)	3.56(.09)	3630	0.9949
$ClO_4^-$	FeTfFe	2.34(.31)	2.90(.06)	795	0.9969
$HP_2O_7^{3-}$	FeTfFe	1.85(.37)	2.86(.07)	725	0.9695
$ATP^{3-}$	FeTfFe	1.99(.36)	2.62(.12)	420	0.9886
$Cl^-^h$	FeTfFe	2.15(.15)	1.97(.05)	93	0.9969
$Cl^-$	FeTf <sup>i</sup>	2.02(.41)	2.75(.24)	562	0.9456
$Cl^-$	TfFe <sup>j</sup>	2.13(.27)	2.11(.08)	128	0.9906
$HPO_4^{2-}$	FeTfFe	—	—	$\leq 2$	—
$AMP^{2-}$	FeTfFe	—	—	$\leq 2$	—
$SO_4^{2-}$	FeTfFe	—	—	$\leq 2$	—
$F^-$	FeTfFe	—	—	$\leq 2$	—
$BF_4^-$	FeTfFe	—	—	$\leq 2$	—

<sup>a</sup>Conditions: 1mM protein in 0.1 M HEPES/NaOH buffer, pH 7.4. Spectra measured at 98K and scaled to the same peak-to-peak amplitude of the  $g' = 4.3$  signal before subtraction. The difference spectrum parameter  $\Delta_1$  measured from the broad spectral feature at 140 mT.

<sup>b</sup>Hill coefficient with the 95% confidence interval from the linear regression given in parentheses.

<sup>c</sup> $\log_{10}$  of the overall apparent association constant  $K$  for the binding of  $n$  anions. 95% confidence interval in parentheses. Because the measurement is performed on a frozen solution, the temperature corresponding to the value of  $K$  is unknown.

<sup>d</sup>The experimental reproducibility of these values is about ten percent.

<sup>e</sup>Correlation coefficient of the linear regression

<sup>f</sup>Analysis of the  $g' = 9.7$  line at 70 mT with  $\Delta_1$  measured at this field and spectra scaled to the same peak-to-peak amplitude at  $g' = 4.3$  gives the following results:  $n = 2.31(.35)$ ;  $\log K = 3.47(.09)$ ; and  $r = 0.994$ .

<sup>g</sup>diferric Transferrin

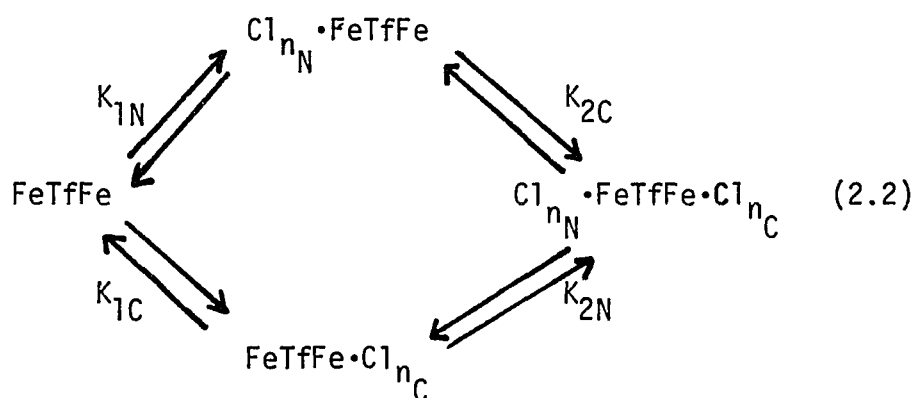
<sup>h</sup>Analysis of the  $g' = 4.3$  signal with the spectra scaled to the same integrated intensity before subtraction gives the following results:  $n = 2.32(.33)$ ;  $\log K = 1.95(.11)$ ; and  $r = 0.9905$  where  $\Delta_1$  is measured from the broad feature at 140 mT; and  $n = 2.22(.23)$ ;  $\log K = 1.88(.07)$ ; and  $r = 0.9932$  where  $\Delta_1$  is measured from the sharp feature at 158.5 mT.

<sup>i</sup>N-terminal monoferric

<sup>j</sup>C-terminal monoferric

line plots are obtained for all of the anions which perturb the EPR spectrum (Figures 2.11 and 2.12). The values of the Hill coefficient  $n$  are generally 2.0 within the 95% confidence interval for all the effective anions (Table 2.2). The overall apparent association constants are also summarized in Table 2.2. Similar results are obtained if the analysis is performed on the  $g'=9.7$  signal instead (c.f.  $\text{SCN}^-$  in Table 2.2).

Since transferrin has two EPR active Fe(III) centers, the precise meanings of the values of  $n$  and  $K$  obtained from the plots in Figures 2.11 and 2.12 are not clear. An obvious question is whether one or both metal binding domains are influenced by the binding of anions. It is not possible to tell from the above treatment whether the values of  $n \approx 2$  (Table 2.2) reflects the binding of two anions in each of the two domains ( $n_N=2$ ,  $n_C=2$ ), two in only one domain ( $n_N=2$ ,  $n_C=0$ ), one in each domain ( $n_N=1$ ,  $n_C=1$ ), or some other combination. To examine these possibilities, a more elaborate model of anion binding to diferric transferrin was developed. The overall binding scheme is given by



where

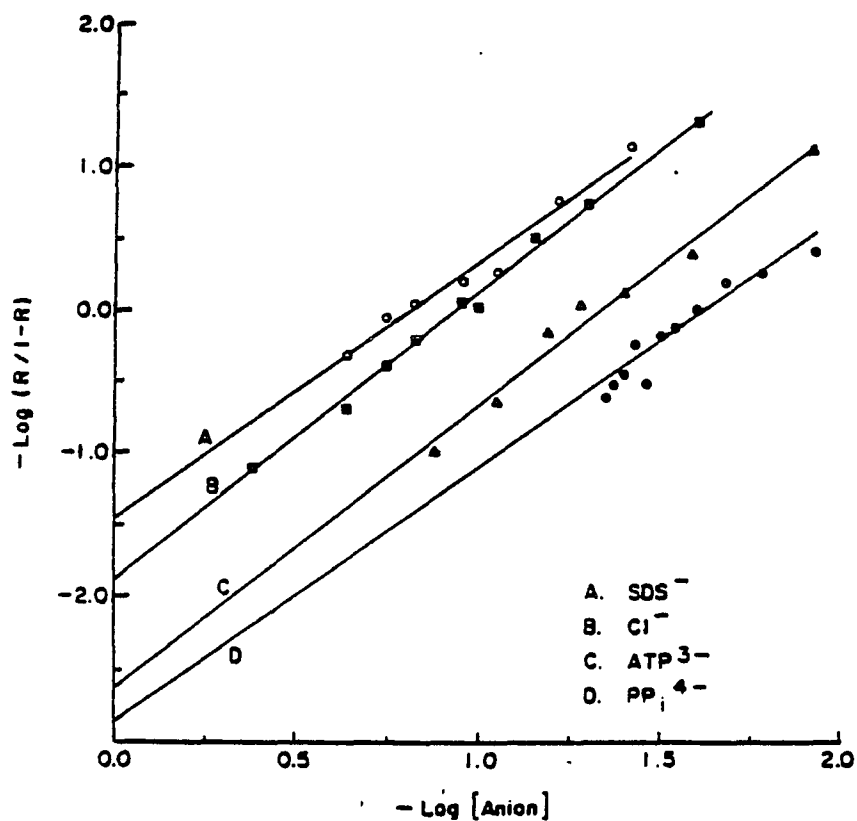


Figure 2.11. Hill plots of the data in Figure 2.9 for several anions. The slope is the Hill coefficient  $n$  and the intercept of the ordinate is  $-\log K$ . Values from the linear regression are presented in Table 2.2.

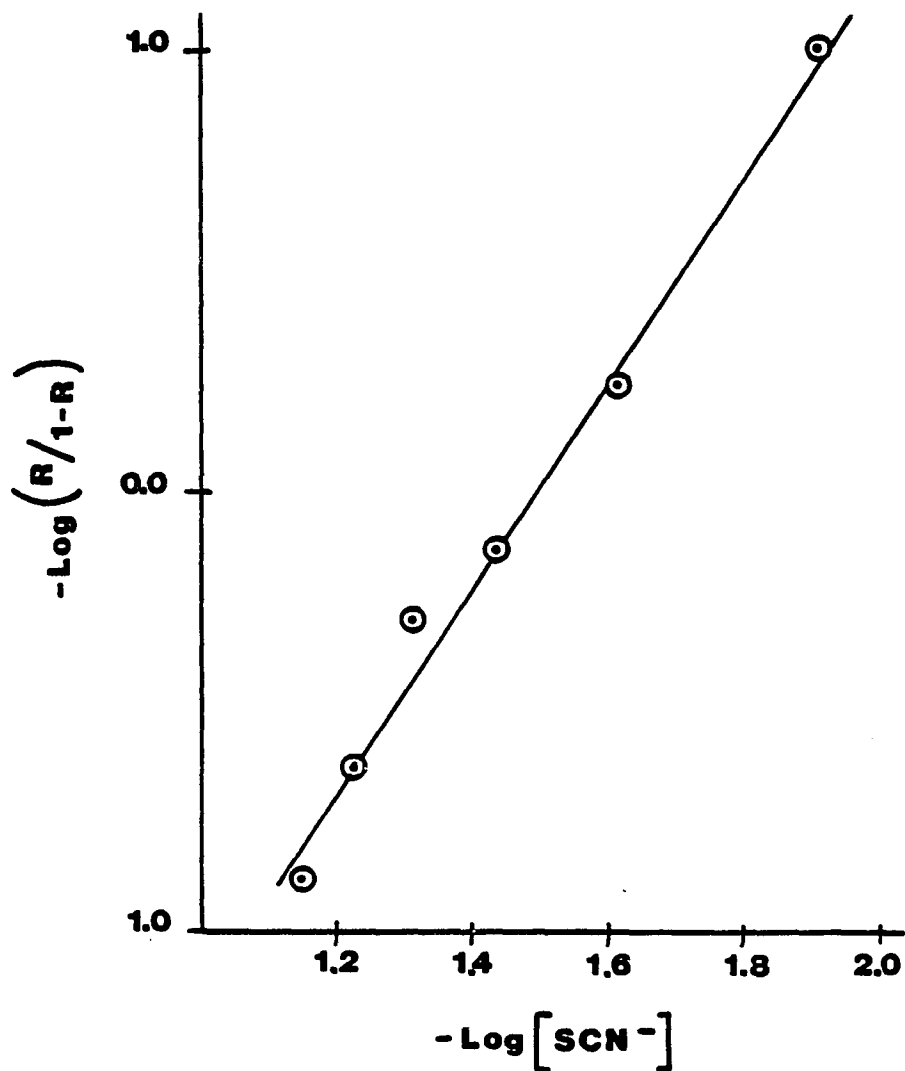


Figure 2.12. Log plot of the titration of 1 mM diferric transferrin in 0.1 M HEPES, 0.01 M  $\text{NaHCO}_3$ , pH 7.4 with 1.0 M  $\text{NaSCN}$ , pH 7.4. The slope is  $n$ , the number of  $\text{SCN}^-$  anions bound per EPR Chromophore, and the intercept is  $-\log K$ .  $n = 2.39 \pm 0.342$ ,  $-\log K = 3.56 \pm 0.087$ , correlation coefficient = 0.995.

$$K_{1N} = \frac{[Cl_{n_N} \cdot FeTfFe]}{[FeTfFe][Cl]^{n_N}} \quad (2.3)$$

$[Cl_{n_N} \cdot FeTfFe]$  is the analytical concentration of the diferric species with  $n_N$  moles of chloride bound in the N-terminal domain. The other concentrations are defined similarly. The K values are conditional overall stability constants for the binding of  $n_N$  and  $n_C$  chloride ions in the N- and C-terminal domains, respectively. This scheme also allows for positive ( $K_{2N}/K_{1N} = K_{2C}/K_{1C} > 1$ ) or negative ( $K_{2N}/K_{1N} = K_{2C}/K_{1C} < 1$ ) cooperativity between domains in chloride binding. A similar scheme for the binding of iron to transferrin has been presented in detail elsewhere (43,48).

When chloride is added to diferric transferrin, a distribution of anion-containing species will be formed, each of which will contribute to the observed difference spectrum parameter  $\Delta_i$ . The calculated value,  $\Delta_{calc}$ , is given by

$$\Delta_{calc} = \Delta_N X_N + \Delta_C X_C + \Delta_{N,C} X_{N,C} \quad (2.4)$$

where  $X_N$ ,  $X_C$ , and  $X_{N,C}$  are the mole fractions of the transferrin species  $Cl_{n_N} \cdot FeTfFe$ ,  $FeTfFe \cdot Cl_{n_C}$ , and  $Cl_{n_N} \cdot FeTfFe \cdot Cl_{n_C}$ , respectively. The values of  $\Delta_N$ ,  $\Delta_C$ , and  $\Delta_{N,C}$  are the respective "extinctions" in the EPR difference spectrum of each of these species.

$\Delta_{N,C}$  is taken as the value of  $\Delta_{max}$  obtained when diferric transferrin is titrated with chloride (Figure 2.9). The values of  $\Delta_N$  and  $\Delta_C$  were chosen as  $\Delta_N = \Delta_C = \Delta_{N,C}/2$ , corresponding to chloride inducing the same maximum spectral change in both domains, and  $\Delta_N = \Delta_{N,C}$  with  $\Delta_C = 0$ , corresponding to a change in one

domain only. Here it is assumed that the spectra of the two domains are additive.

Cooperativity between domains enters equation 2.4 through the values of  $X_N$ ,  $X_C$ , and  $X_{N,C}$ . The expressions for the mole fractions derived by a procedure analogous to that outlined for iron binding to transferrin (48) are given by

$$X_N = \frac{1}{1 + 1/K_{1N}[Cl]^{n_N} + \frac{K_{1C}[Cl]^{n_C}}{K_{1N}[Cl]^{n_N}} + K_{2C}[Cl]^{n_C}} \quad (2.5)$$

$$X_C = \frac{1}{1 + 1/K_{1C}[Cl]^{n_C} + \frac{K_{1N}[Cl]^{n_N}}{K_{1C}[Cl]^{n_C}} + K_{2N}[Cl]^{n_N}} \quad (2.6)$$

$$X_{N,C} = \frac{1}{1 + \frac{K_{2C}[Cl]^{n_C} + K_{2N}[Cl]^{n_N}}{K_{2C}K_{2N}[Cl]^{n_C}[Cl]^{n_N}} + 1/K_{2C}K_{2N}[Cl]^{n_C}[Cl]^{n_N}} \quad (2.7)$$

where the constants are subject to the constraint  $K_{2N}/K_{1N} = K_{2C}/K_{1C}$  imposed by the cyclic equilibrium 2.2.

Equations 2.4 through 2.7 were used to compute  $\Delta_{calc}$  at the experimental concentrations of chloride. From this,  $\log(R/1-R)$  where  $R = \Delta_{calc}/\Delta_{max}$ , was evaluated and compared with the experimentally obtained quantity. Initially, a set of equilibrium constants and integer values of  $n_N$  and  $n_C$  were assumed. A non-linear regression analysis employing a simplex optimization procedure was performed in which the values of the  $K_i$  were varied to provide a least squares fit to the  $\log(R/1-R)$  data for the given choice of  $n_N$  and  $n_C$ . It was believed that through this

procedure a simulation of the experimental curve of Figure 2.9 for the correct values of  $n_N$  and  $n_C$ , would be obtained. The results of this analysis for different values of  $n_N$  and  $n_C$ , with and without cooperativity between domains in chloride binding, are presented in Table 2.3.

All models in Table 2.3 provide straight line plots of  $-\log(R/1-R)$  vs  $-\log[Cl]$ , but several of them can be discarded as providing unsatisfactory simulations of the experimental curve. The slope of the line in case I is only 1 (compared to an experimentally obtained value of 2) and the negative binding constants obtained in case KK indicate that (for this case) an attempt to fit the experimental curve with an inappropriate model is being made. Of the remaining models, the last three listed in Table 2.3 provide satisfactory fits to the experimental data (c.f. model  $S_y$  values with the experimental value). The calculated values of  $n$  and  $\log K$  for all three models are also close to the experimental values. A comparison of cases III and IV reveals that only a slight improvement in fit is obtained when cooperativity between domains is introduced (case IV). It is concluded that if chloride binds in both domains of transferrin it does so essentially independently. Therefore, only cases III and V need be considered further.

To determine which of the two satisfactory cases (III or V) of Table 2.3 applies to diferric transferrin, N- and C-terminal monoferric transferrins were prepared and each titrated with chloride. The EPR spectra of the monoferric species with and without chloride shown in Figure 2.13 indicate that the effect



Table 2.3  
Results of Model Calculations for Chloride Binding to Human Serum Transferrin<sup>a</sup>

Case	$n_N$	$n_C$	Cooperativity	$K_{1N}$	$K_{1C}$	$K_{2N}$	$K_{2C}$	$n_{calc}^b$	$(\log K)_{calc}^c$	$r^d$	$S_y^e$
I	1	1	no	7.71	7.71	---	---	1.02	0.967	.9960	.455
II	1	1	yes	-10.44	8.44	10.87	-8.79	2.08	1.91	.9982	.0654
III	2	2	no	64.95	68.39	---	---	2.00	1.85	.9992	.095
IV	2	2	yes	52.61	52.63	73.06	73.08	2.13	1.95	.9995	.069
V	2	0	---	67.23	---	---	---	2.00	1.84	.9999	.088
Experimental			---	---	---	---	---	$2.15 \pm .15^f$	$1.97 \pm .05^f$	.9969	.066 <sup>g</sup>

a) Calculations based on equations (5) through (8) with  $\Delta_N = \Delta_C = \frac{\Delta_{N+C}}{2} = 1.75$ .  $K_i$  values are subject to the constraint

$$\frac{K_{2N}}{K_{1N}} = \frac{K_{2C}}{K_{1C}} \text{ imposed by the cyclic equilibrium.}$$

b) Calculated from the linear regression of  $\log (\theta/1-\theta)_{calc}$  vs.  $\log [Cl]_{expt}$ .

c) Calculated from the intercept of the regression line in footnote b.

d) Correlation coefficient of the regression in footnote b.  $r$  is a measure of the linearity of the line predicted by the model and does not reflect the fit of the model to the data.

e) The residual is defined as  $S_y = [(Y_{calc} - Y_{obs})^2 / n' - p]^{1/2}$  where  $Y_{calc} = \log(\theta/1-\theta)_{calc}$ ,  $Y_{obs} = \log(\theta/1-\theta)_{obs}$ ,  $n'$  (=9) is the number of experimental points and  $p$  (=2 or 3) is the number of independent parameters in the equation.  $S_y$  is a measure of the goodness of the fit of the model to the data.

f) Experimental values, Table I.

g) The residual of the experimental data is defined by  $S_y = [(Y_{obs} - Y)^2 / n' - 2]^{1/2}$  where  $Y$  is the calculated value of  $-\log(\theta/1-\theta)$  from the linear regression line at each value of  $-\log[Cl]_{expt}$ .

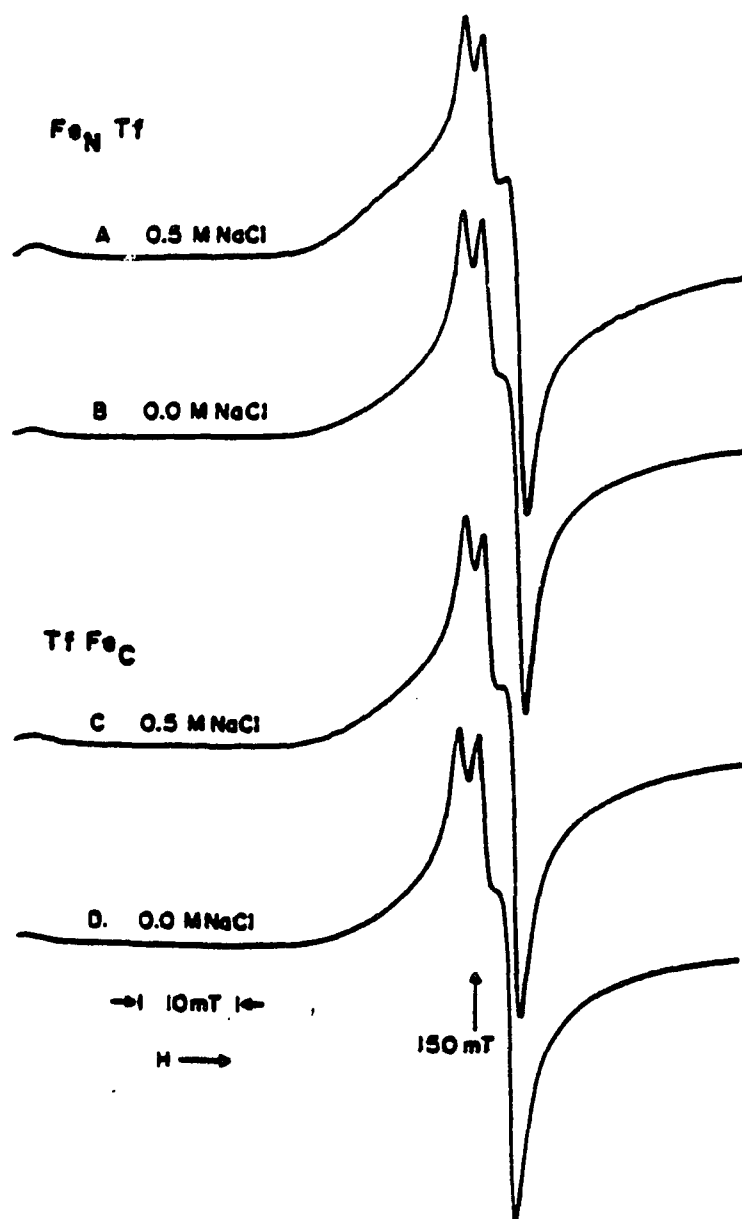


Figure 2.13. Effect of chloride on the X-band EPR spectra of the monoferric transferrins. (A) N-terminal monoferric with 0.5 M NaCl, (B) N-terminal monoferric without NaCl, (C) C-terminal monoferric with 0.5 M NaCl, (D) C-terminal monoferric without NaCl. Conditions and instrument settings as in Figure 2.3.

on the spectrum occurs in both halves of the protein but is greater in the N-terminal domain than in the C-terminal domain, e.g.  $\Delta_C \approx \Delta_N/2$  when referenced to the same peak-to-peak amplitude for both monoferrics.

The Hill plots for chloride binding are presented in Figures 2.14 and 2.15. The chloride binding data for the monoferric transferrins are also summarized in Table 2.2. The results indicate that two chloride ions bind to both the N-terminal and C-terminal monoferric species. By inference, four anions bind to diferric transferrin. The value of K for the C-terminal monoferric is about the same as observed for the diferric protein while the value of K for the N-terminal monoferric is somewhat higher.

The effects of perchlorate on the iron EPR spectrum of diferric transferrin observed in this study are similar to those reported by Price and Gibson (55). Their early work demonstrated that perchlorate produced opposite effects on the EPR spectra of human serum transferrin and ovotransferrin. This has also been observed in the present study when perchlorate is used; however, both proteins respond to chloride in the same manner (c.f. Figures 2.3 and 2.16). A logarithmic plot of the data from a titration of ovotransferrin with chloride (Figure 2.17) likewise yields a straight line with  $n=2.00 \pm 0.36$ ,  $\log K = 1.29 \pm 0.08$ , (correlation coefficient = 0.986), indicating that chloride also binds to ovotransferrin but more weakly than to serum transferrin.

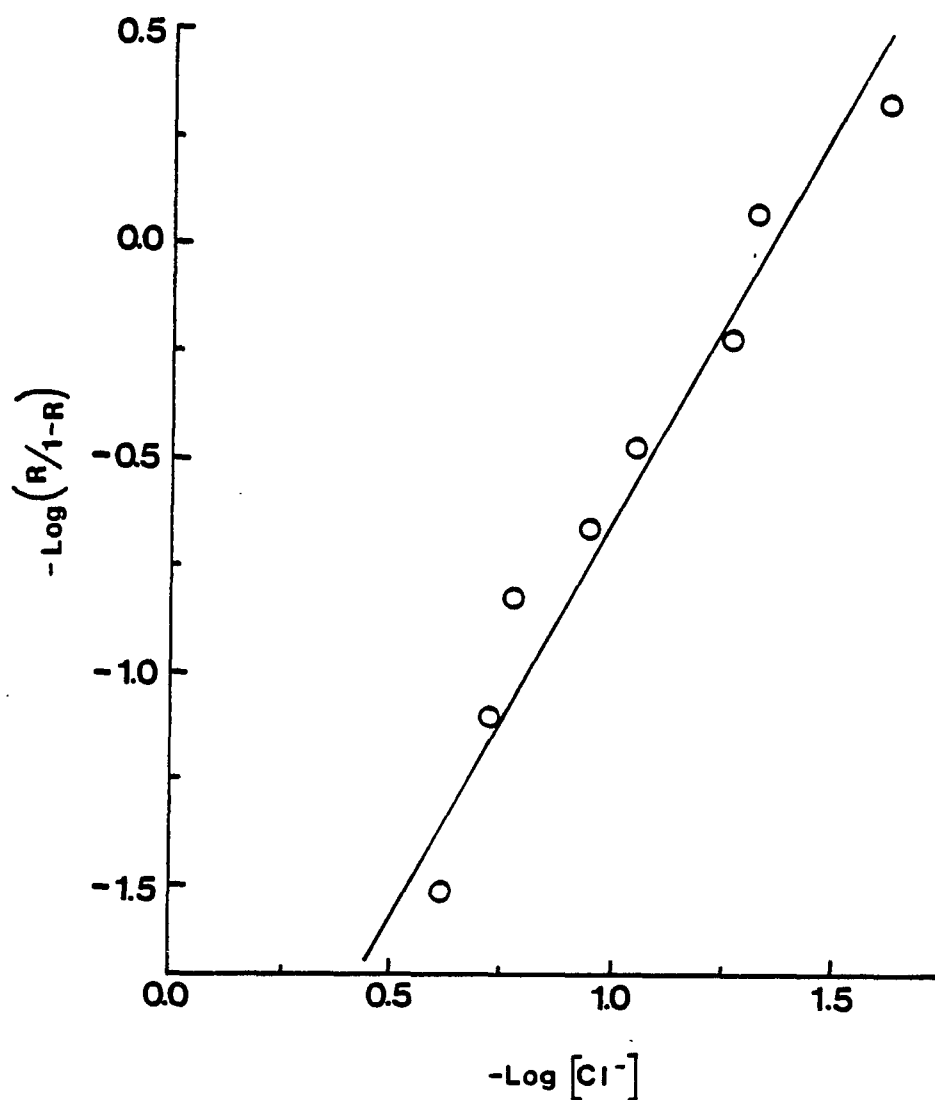


Figure 2.14. Hill plot of data acquired during titration of 1 mM N-terminal monoferric transferrin in 0.1 M HEPES, 0.01 M  $\text{NaHCO}_3$ , at pH 7.5 with 1.0 M NaCl.  $n = 2.02 \pm 0.41$ ,  $-\log k = 2.75 \pm 0.24$ , correlation coefficient = 0.9456.

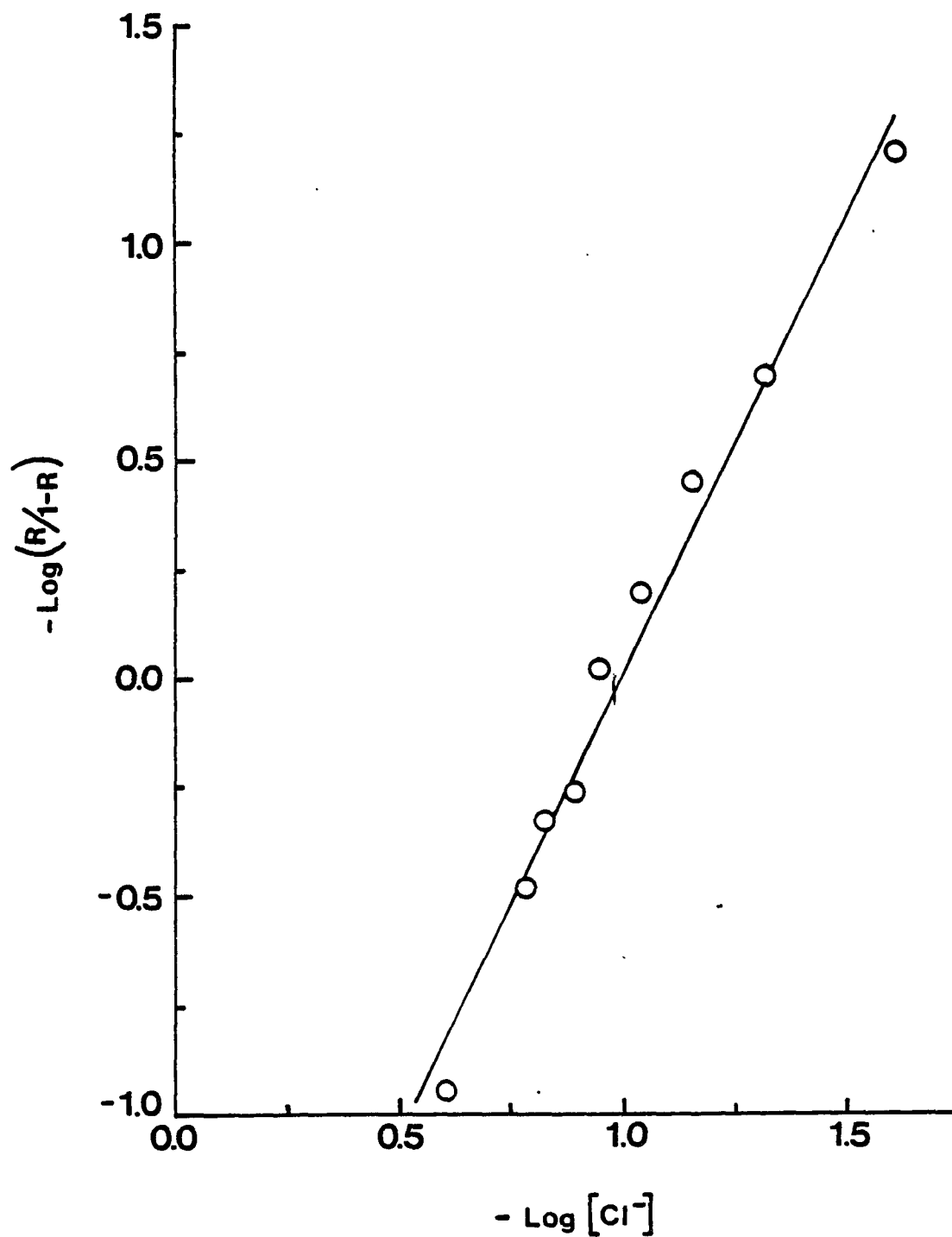


Figure 2.15. Hill plot of results obtained during titration of 1 mM C-terminal monoferric transferrin in 0.1 M HEPES, 0.01 M  $\text{NaHCO}_3$  at pH 7.5 with 1.0 M NaCl.  $n = 2.13 \pm 0.27$ ,  $-\log K = 2.11 \pm 0.08$ , correlation coefficient = 0.9906.

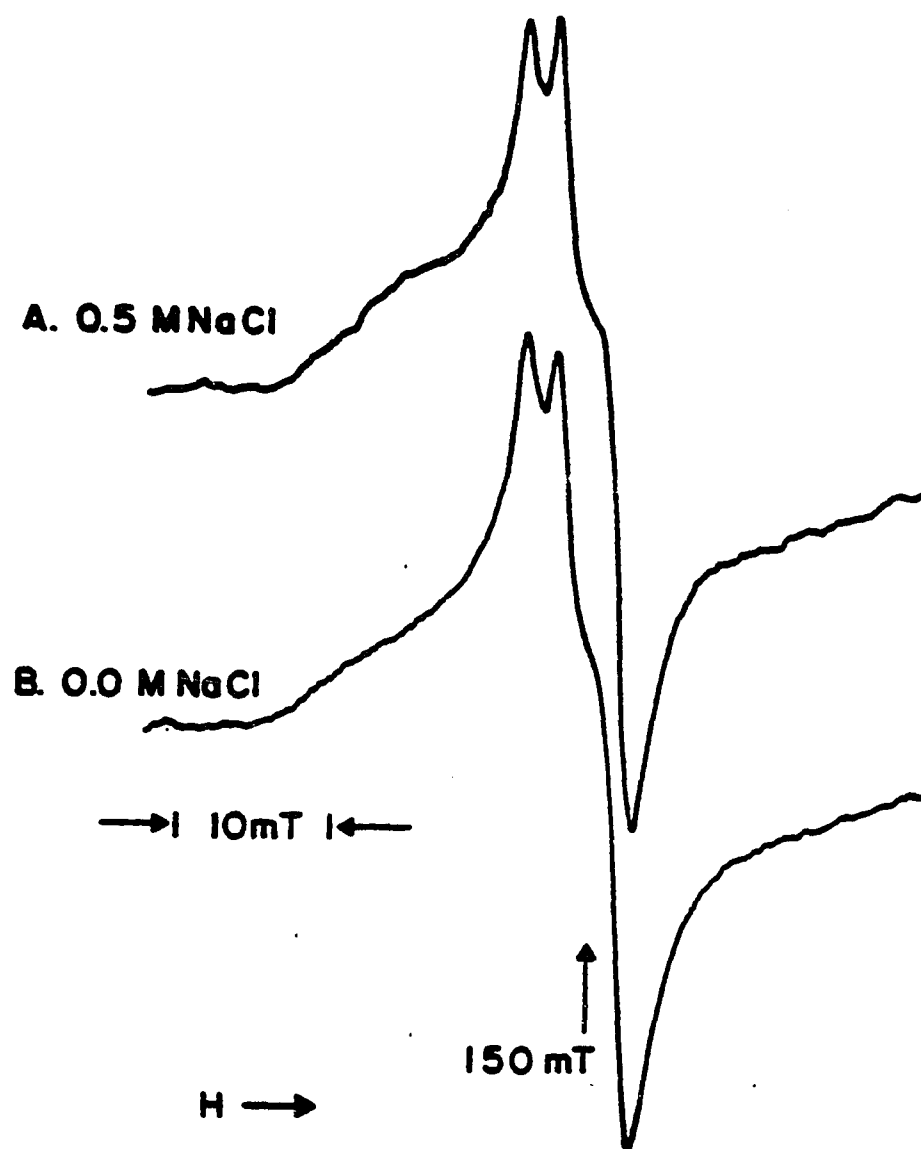


Figure 2.16. Effect of chloride on the X-band EPR spectrum of diferric ovotransferrin. (A) 0.5 M NaCl, (B) no NaCl. Conditions and instrument settings as in Figure 2.3.

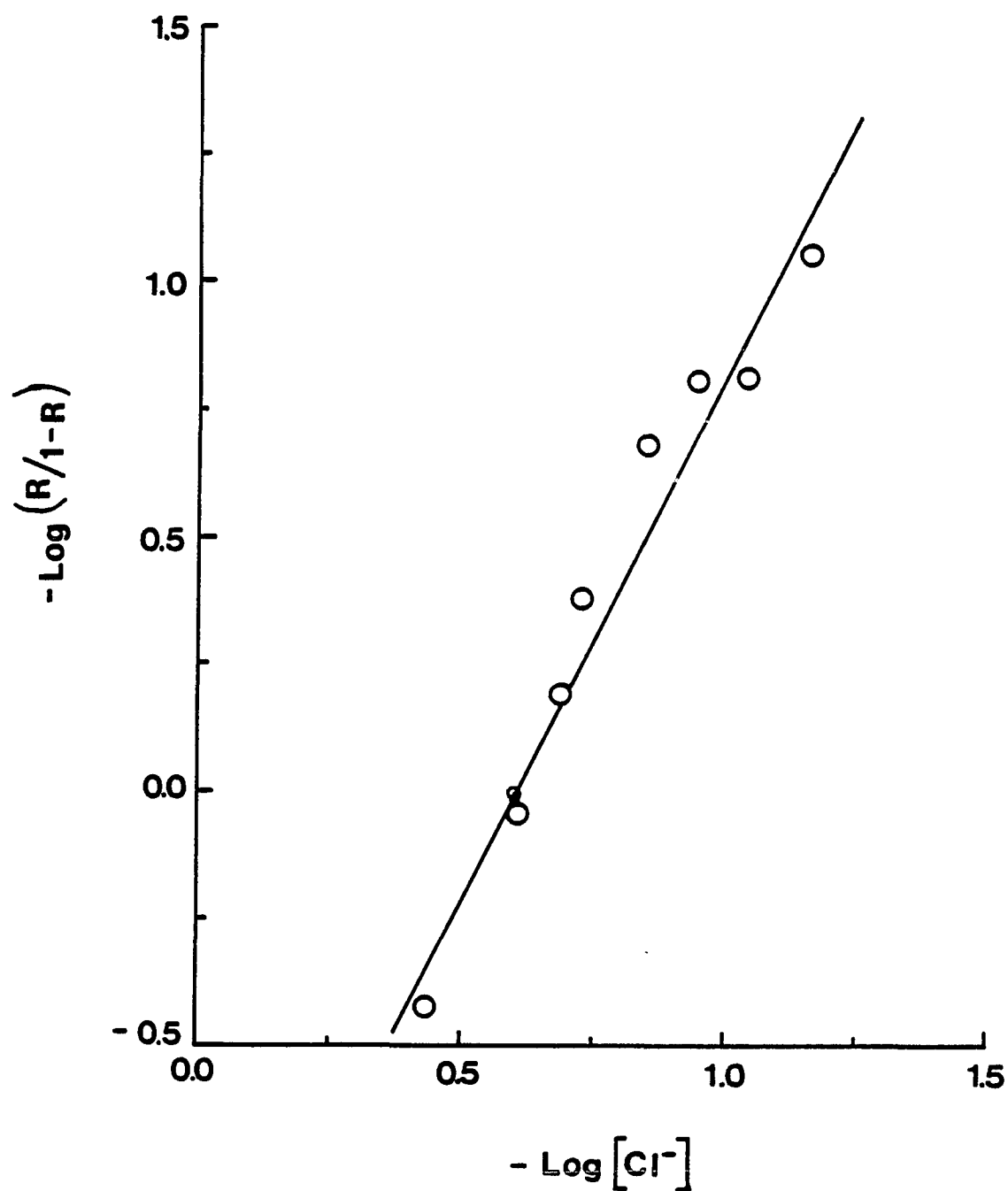


Figure 2.17. Hill plot of data obtained during titration of 1 mM diferric ovotransferrin in 0.1 M HEPES, 0.01 M  $\text{NaHCO}_3$  at pH 7.5 with 1.0 M NaCl.  $n = 2.00 \pm 0.36$ ,  $-\log K = 1.29 \pm 0.08$ , correlation coefficient = 0.9860.

### Discussion

Based on the observations reported here, human serum transferrin has binding sites for non-synergistic anions which affect the metal centers of the protein. Titration of the monoferric transferrins indicates that there are two sites in each domain of the protein in accord with the predicted results for case III of our computer modeling study. Previous investigations also lend support to this conclusion. For example, perchlorate has been shown to affect both the N- and C-terminal metal binding fragments of ovotransferrin; and chloride is known to affect the kinetics of iron release from both domains in diferric transferrin (47,48,60). Moreover, the EPR spectra of both sites of divanadyl human transferrin are changed by perchlorate (61).

The existence of these anion binding sites raises the question as to their location on the protein. In diferric transferrin it is unlikely that the anions bind to a significant extent at the sites occupied by the synergistic anion since none of them facilitates iron binding in the absence of bicarbonate. The observation that all of the anions alter the EPR spectrum in a similar manner seems to preclude the possibility that they are directly ligated to the metal. With various metal coordinated synergistic anions, different spectra are produced in both Fe(III) and VO(II) transferrins (35,62). Perchlorate is a relatively tightly held anion (see Table 2.2) but is known to be a poor ligand for metal ions, while fluoride, which has little



or no effect on the EPR spectrum (vide supra), is a good ligand for Fe(III). It is more likely that these anions bind to positively charged amino acids or possibly to amide dipoles of the protein.

The origin of the changes observed in the EPR spectra is not clear. It is unlikely that a major structural modification occurs at the metal site attending anion binding since the perturbations are small. A more reasonable explanation is that anion binding causes an allosteric effect on the metal centers as a result of a conformational change in the protein. There is ample evidence in the literature that transferrin exists in more than one conformation (9,12,63). EPR spectral changes in Gd(III), Cu(II), and VO(II) transferrins have also been observed attending the addition of perchlorate and chloride, indicating that the anion sites may be preserved in all of these metal derivatives of the protein (27,56).

The effect of anions on the conformational states of proteins often follow the lyotropic series  $F^- < SO_4^{2-} < HPO_4^{2-} < CH_3CO_2^- < Cl^- < Br^- < NO_3^- < I^- < ClO_4^- < SCN^-$  (64). This series is approximately the same sequence for the affinity of anions for positively charged sites on proteins. Inspection of Table 2.2 reveals that the strength of interaction for the anions reported here also follows this series.

It may also be significant that ATP and pyrophosphate which bind to the protein (Table 2.2) are very efficient catalysts for mediating the removal of iron from transferrin to desferrioxamine in vitro (50,51). The kinetics of this process show

saturation behavior with respect to the anion, a result consistent with, but not proof of, anion binding to the protein. Furthermore, the diphosphate structure appears to be important. Neither AMP nor orthophosphate functions as efficient catalysts of iron removal nor does either bind appreciably to the anion sites observed here.

It is interesting that solutions of the diferric protein which have been prepared from Fe(III)-nitrilotriacetate do not show the effect of anions on the EPR spectrum. Price and Gibson have observed that the presence of NTA in solutions of transferrin negates the response of the EPR spectrum to perchlorate (55). NTA is also known to bind tenaciously to transferrin and can only be removed by dialysis or gel permeation chromatography in the presence of perchlorate (40).

The calculations indicate that cooperativity between domains in anion binding is negligible: however, the Hill plots for diferric and monoferric transferrins (Figure 2.11 and Table 2.2) show that within each domain two anions bind with strong positive cooperativity. The strong positive cooperativity in anion binding is unexpected since normally the binding of a second ligand is more difficult than the first. This implies that, in the protein, the interaction of the first anion causes structural changes that facilitate binding of the second anion. Such a change would be consistent with an allosteric mechanism discussed above. Strong positive cooperativity in binding of nonstereospecific anions to other proteins is not known. In this regard, transferrin appears to be unique.

Chasteen and Williams have recently shown that two functional groups undergo proton dissociation with strong positive cooperativity in the monoferric transferrins to bring about a change in the binding affinities of the two iron sites (48). The phenomena of cooperativity of anion binding and of proton dissociation may be related in some way.

The results presented here do not demonstrate that the observed anion sites are directly involved in the kinetics of iron removal from transferrin. However the parallels between the kinetics of iron removal and the strength of anion binding to transferrin raise this question (47,49-51). In addition, the unusual property of positive cooperativity exhibited in both anion binding and proton dissociation by transferrin poses new questions about this important protein. Further studies are clearly necessary to understand fully the role that anions play in the structure of transferrin, the thermodynamics of iron binding, and in the mechanism of iron removal.

### CHAPTER III

#### THERMODYNAMICS OF IRON BINDING TO TRANSFERRIN

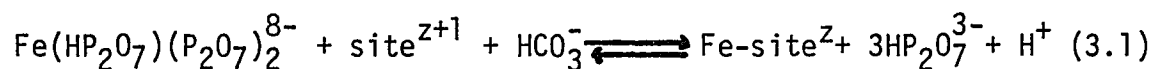
A major and yet unsolved problem in iron metabolism is how the metal is transferred from transferrin to iron requiring cells such as reticulocytes. The precise location of iron release from transferrin is not known, but it has been proposed that, after binding to a receptor site on the surface of the cell, the protein is internalized via endocytosis. Once in the cytoplasm, iron is removed and the apoprotein returns to the extracellular medium (67,68). Alternatively, it has been suggested that iron is liberated at the cell surface prior to endocytosis (71).

Recent studies on cultured rat fibroblasts suggest that the endocytotic vacuoles containing transferrin bound to its receptor fuse with the acidic lysosome where, because of the low pH, iron is released from the protein (69,70). The molecular mechanism of iron removal from transferrin is an area of some dispute. In order to lower the binding affinity of transferrin for Fe(III), it may be necessary to protonate the ligands of the iron binding site and/or dissociate completely the synergistic anion from the primary anion site (12). It has been proposed that bicarbonate release is a prerequisite for iron release from transferrin. Reduction of Fe(III) to Fe(II) is another possible means of removing iron in vivo (72-74).

Another possibility is that chelation and ligand exchange provide the free energy necessary for removal of iron from the protein. Phosphorus-containing nucleotides and polyphosphates which are present in the cytosol of reticulocytes are of particular interest because they are potential chelators of iron. Several of these agents (ATP, pyrophosphate, ADP, 2,3-diphosphoglycerate, etc.) have been shown to facilitate release of iron from transferrin in vitro and most are relatively abundant (e.g., ATP  $\approx$  2 mM) in immature and mature red blood cells (50,51,75). In addition to catalyzing the release of iron from transferrin, pyrophosphate and other polyphosphates are effective mediators of iron uptake by rat fibroblasts and ferritin (67,77,78). Furthermore, most of these mediators of iron removal (small chelates capable of delivering iron to or removing iron from the protein) also seem to facilitate exchange of transferrin-bound bicarbonate with ambient bicarbonate, suggesting that they may labilize iron by disrupting the primary anion binding site (75, 76).

This chapter is dedicated to establishing whether, under conditions within the cytosol where pyrophosphate would be in great excess over transferrin, Fe(III) binding to pyrophosphate might be thermodynamically favored. Several earlier kinetic studies have demonstrated that the mediator pyrophosphate is a much more efficient catalyst than other polyphosphates (such as ATP or 2,3-diphosphoglycerate) at facilitating the removal of Fe(III) from transferrin in vitro and depositing it in des-

ferrioxamine B, a chelator drug with a higher affinity for iron than the protein (50,51). However, no information is available on the stoichiometry and equilibrium constant for the competition reaction between apotransferrin and pyrophosphate for Fe(III) under equilibrium conditions in the absence of desferrioxamine B. Such knowledge would be valuable in interpreting kinetic data as well as providing a means of assessing the feasibility of iron removal from the protein by pyrophosphate in vivo. In this chapter it is shown that the equilibrium distribution of iron(III) between transferrin and pyrophosphate is pH- and bicarbonate-dependent and follows the equation



where Fe-site represents iron bound at one of the specific iron binding sites on the protein. The change in charge from Z to Z+1 takes into account the fact that the protein gains a negative charge when Fe(III) binds. The equilibrium constant has been determined.

A first order dependence on bicarbonate concentration in the equilibrium binding of iron to transferrin is demonstrated for the first time. This experiment proves that bicarbonate does not bind appreciably to transferrin in the absence of iron. In the past, the proportionality between iron and bicarbonate binding has always been assumed based on the early work of Warner and Weber which showed that one mole of  $\text{CO}_2$  was liberated per iron released when conalbumin solutions were acidified (66).

### Experimental Procedure

The preparation of solutions, apotransferrin, monoferric transferrins and diferric transferrin were as previously described in Chapter II.

The percent Fe saturation of transferrin was studied as a function of pH and pyrophosphate concentration by monitoring changes in absorbance at 465 nm on a dual beam Carey 219 spectrophotometer. Two equivalents of freshly prepared 0.01 M ferrous ammonium sulfate were added to one milliliter of 0.5 mM apotransferrin. The salmon pink color characteristic of specifically bound iron slowly developed over the 24-hour equilibration period. 200  $\mu$ l of the protein solution was mixed with 1800  $\mu$ l of 0.05 M HEPES/0.05 M EPPS/0.01 M  $\text{NaHCO}_3$ , pH 7.8 buffer in a 1 cm quartz cuvette giving approximately 50  $\mu$ M diferric transferrin. The pH was adjusted to 7.5 with 1.0 N HCl and the amount of iron bound to transferrin determined at 465 nm using a molar absorptivity of  $2500 \text{ M}^{-1} \text{ cm}^{-1} \text{ Fe}^{-1}$  (9).

The competitive effect of pyrophosphate concentration on iron binding to transferrin was studied by titrating diferric transferrin with a 0.1 M pyrophosphate/50  $\mu$ M diferric transferrin/0.01 M  $\text{HCO}_3^-$ , 0.1 HEPES, pH 7.5 solution. Titrations were carried out by delivering a calculated volume of titrant into a 1-cm quartz cuvette containing two milliliters of 50  $\mu$ M diferric transferrin/0.01 M  $\text{HCO}_3^-$ /0.1 M HEPES at pH 7.5. The pH of the solution was measured after each addition of titrant and found to be invariant within  $\pm 0.02$  pH units throughout the experiment.

Sufficient time was allowed after each addition for the system to re-equilibrate. Achievement of equilibrium after each injection was determined spectrophotometrically at 465 nm by allowing the pyrophosphate to react until no further decrease in absorbance was observed. Typically 30 to 60 minutes was required. This procedure was continued until subsequent additions did not change the absorbance of the solution further.

A similar titration was conducted to study the effect of bicarbonate on the competitive equilibrium. The procedure was analogous to that described above. In this experiment a freshly prepared 0.5 M  $\text{HCO}_3^-$ /50  $\mu\text{M}$  diferric transferrin/0.04 M pyrophosphate, pH 7.5 solution was titrated into a stoppered cuvette containing two milliliters of 50  $\mu\text{M}$  diferric transferrin/0.04 M pyrophosphate/0.1 M HEPES at pH 7.5. Only ambient levels of bicarbonate due to dissolved  $\text{CO}_2$  were initially present in the diferric transferrin solution.

The effect of pH was also investigated by titrating three milliliters of 50  $\mu\text{M}$  diferric transferrin/0.04 M pyrophosphate/0.01 M  $\text{HCO}_3^-$ /0.05 M HEPES/0.05 EPPS, pH 7.2 solution with standard 1.0 N NaOH. The pH and  $A^{465}$  were measured after each addition of base. Approximately twelve 5  $\mu\text{l}$  additions were made over the pH range 7.2 to 9.2. A 50  $\mu\text{l}$  sample of protein solution was withdrawn from the cuvette after each addition of NaOH and subjected to urea/polyacrylamide-gel electrophoresis. The procedure for electrophoresis has been previously described in Chapter II.

In another experiment, approximately 300  $\mu\text{l}$  was withdrawn



from the cuvette, placed in a quartz EPR tube, and the frozen solution EPR spectrum measured. A broad poorly resolved spectrum similar to that of iron transferrin with an effective  $g$  value of 4.3 was obtained (Figure 3.1); however, ultrafiltration of the sample in a Amicon model 3 ultrafiltration cell equipped with a PM 10 (MW cutoff = 10,000) membrane revealed this spectrum to be a superimposition of two  $g'=4.3$  rhombic iron signals (Figures 3.2 and 3.3): one due to an iron(III)-pyrophosphate complex and the other due to transferrin bound iron.

The effect of pH was studied in both directions, i.e., raising the pH from 7.2 to 9.2 and then slowly lowering the pH back to 7.2 with 1.0 N HCl. Absorbance measurements were taken after each addition of acid. Identical plots of percent saturation vs pH were obtained, indicating that the system was at true equilibrium.

The number of protons released when Fe(III) complexes to pyrophosphate was determined by pH restoration measurements. 0.01 M Fe(II) was prepared in both deoxygenated water and in 0.01 M HCl. By using the method of Fitzgerald and Chasteen (79), the pH of the iron solution was adjusted to 7.5 or to 9.0 under a blanket of moist nitrogen gas. Once the desired pH was obtained, aliquots of Fe(II) were added to ten milliliters of a pH 7.5 or 9.0 0.01 M pyrophosphate solution exposed to the air. In more concentrated pyrophosphate solutions insoluble white precipitates were obtained. Following a 30-minute equilibration period for each increment of iron added, the pyrophosphate solution

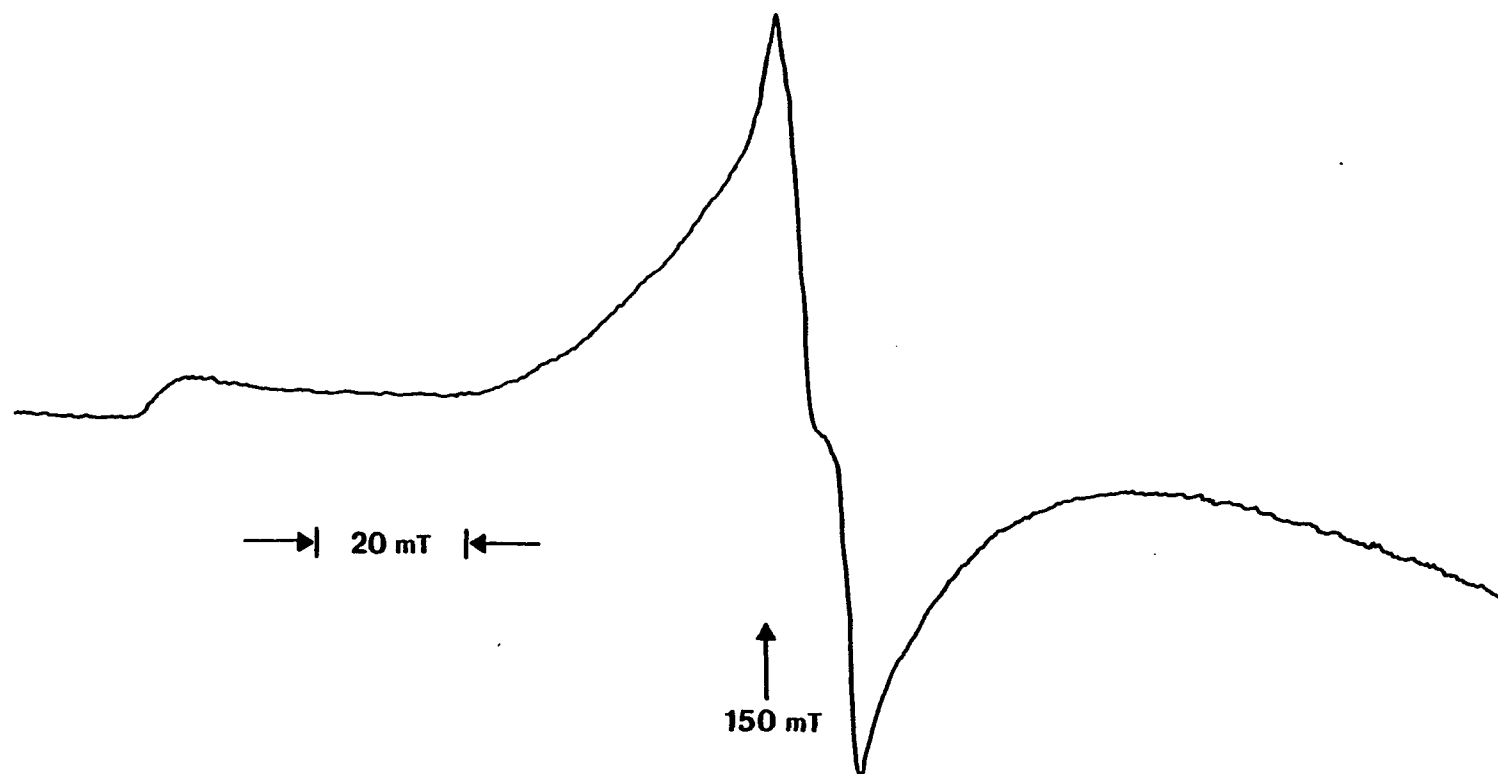
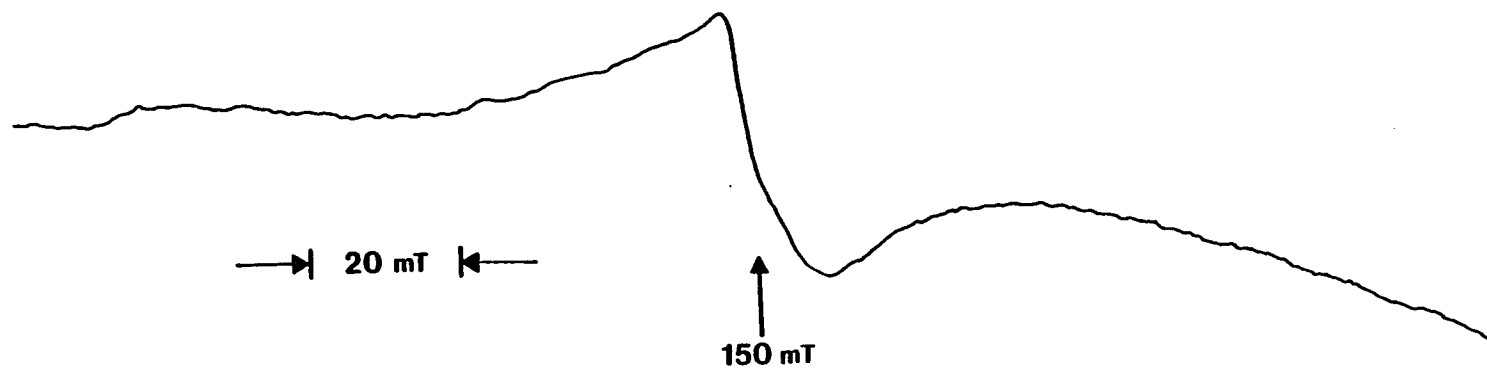


Figure 3.1. Frozen solution 77K X-band EPR spectrum of a solution of pyrophosphate, transferrin and iron (III). Conditions: 50  $\mu$ M di-ferric transferrin, 0.04 M pyrophosphate, 0.05 M HEPES, 0.05M EPPES, pH 8.5. Instrument settings: power = 20 mw, modulation amplitude = 10 G, sweep rate = 2000 G/16 min, time constant = 0.3 sec.



52

Figure 3.2. Frozen solution 77K X-band EPR spectrum of eluent obtained when the solution in Figure 3.1 was subjected to ultrafiltration. Spectrum is due to an iron:pyrophosphate complex. Instrument settings as in Figure 3.1.

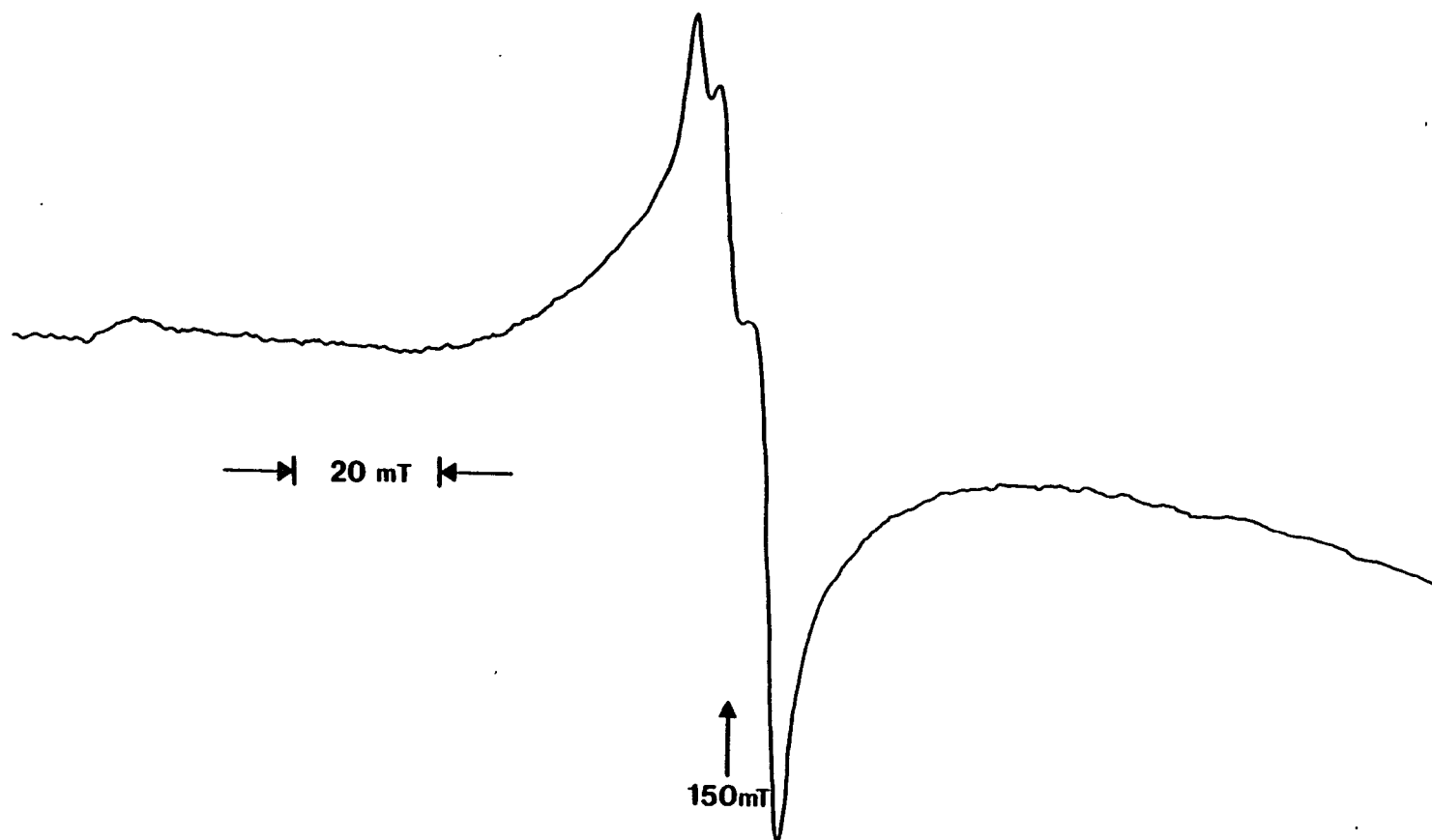


Figure 3.3. Frozen solution X-band EPR spectrum of the retentate obtained when the solution in Figure 3.1 was subjected to ultrafiltration. Instrument settings as in Figure 3.1.

was titrated back to the original pH with standardized 1.0 N NaOH. Duplicate runs with pyrophosphate:Fe ratios of 40:1, 10:1, 5:1, and 2.5:1 were performed. Finally, to insure that no oxidation of Fe(II) to Fe(III) was occurring prior to its addition to the pyrophosphate solution, duplicate runs of the same pyrophosphate:Fe ratios were performed with solid ferrous ammonium sulfate crystals. These experiments were also performed with the pyrophosphate solution at pH 7.5 and pH 9.0.

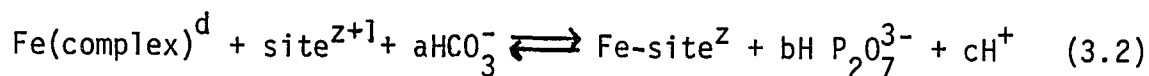
Experiments were also conducted in a medium designed to mimic closely the ionic environment of serum. 300  $\mu$ l of 50 mg/ml diferric transferrin was mixed with 2700  $\mu$ l of a physiological saline buffer solution (0.12 M NaCl, 0.5 mM KCl, 1 mM  $\text{MgSO}_4$ , 1 mM  $\text{CaCl}_2$ , and 20 mM  $\text{NaHCO}_3$ , pH 7.8) in a three milliliter anaerobic quartz cell (1 cm pathlength). The cell was tightly stoppered with a serum cap and flushed for approximately 1 hour with a moist stream of 95%  $\text{O}_2$ , 5%  $\text{CO}_2$  specialty gas. This atmosphere has the  $\text{O}_2/\text{CO}_2$  tension of blood and provided a means of fixing the concentration of bicarbonate accurately and of buffering the solution easily. Aliquots of 0.1 M pyrophosphate and 5 mg/ml diferric transferrin in physiological saline buffer that had been purged with the gas mixture were titrated into the cuvette and the resulting changes in iron binding monitored. A slight positive pressure of gas was left in the cell during the equilibration period. The pH was checked after each measurement. The average value was 7.242 and was found not to vary more than  $\pm 0.025$  pH units. A duplicate experiment was performed on a

solution containing 0.025 M  $\text{HCO}_3^-$ . The pH of this solution averaged 7.432.

The pH was measured on an Orion model 901 pH meter equipped with a radiometer GK2321C calomel-glass combination electrode. The temperature of all studies was 37° C. All chemicals were reagent grade and prepared in doubly distilled deionized water. Preparation and handling of glassware and chemicals have been described in Chapter II.

### Results

When pyrophosphate is added to solutions of diferric transferrin, a decrease in absorbance at 465 nm is observed. The loss of specifically bound Fe(III) is dependent on pH and bicarbonate concentration and is consistent with the equilibrium reaction



Various logarithmic forms of equation 3.3 for the equilibrium constant Q were analyzed to determine the values of the coefficients a, b, and c.

$$Q = \frac{[\text{Fe-site}][\text{HP}_2\text{O}_7^{3-}]^b[\text{H}^+]^c}{[\text{Fe}(\text{complex})^d][\text{site}^z][\text{HCO}_3^-]^a} \quad (3.3)$$

Bicarbonate, pyrophosphate, and pH were varied independently and the effect that each of these variables exerted on the amount of iron bound to transferrin was measured. [Fe-site] is measured

from the absorbance at 465 nm. The value of  $[\text{Fe}(\text{complex})]$  (=  $[\text{site}]$ ) is calculated from mass balance;  $[\text{H}^+]$  is determined from the pH of the solution; and  $[\text{HCO}_3^-]$  is equal to the concentration added. The concentration of  $\text{HP}_2\text{O}_7^{3-}$  is given by

$$[\text{HP}_2\text{O}_7^{3-}] = \frac{[\text{PP}_i]}{\frac{K_a}{[\text{H}^+]} + 1} \quad (3.4)$$

where  $[\text{PP}_i]$  is the analytical concentration of pyrophosphate.  $K_a = 6.3 \times 10^{-9}$  is the fourth proton dissociation constant for pyrophosphate. In the pH range 7.2 to 9.2 employed here,  $\text{HP}_2\text{O}_7^{3-}$  and  $\text{P}_2\text{O}_7^{4-}$  are the only species of pyrophosphate present in appreciable amounts.

#### Determination of b

Figure 3.4 shows the dependence of the percent iron saturation of transferrin as a function of pyrophosphate concentration. The observed decrease in absorbance at 465 nm with increasing pyrophosphate concentration clearly demonstrates pyrophosphate's ability to compete with transferrin for iron at pH 7.5. To insure that iron was indeed being removed from transferrin and that a colorless ternary  $\text{Fe-Tf-PP}_i$  complex was not being formed in solution, the reaction mixture was separated by urea/polyacrylamide-gel electrophoresis. Only a single band corresponding to apotransferrin was observed at pH 7.5 in the presence of 0.04 M pyrophosphate.

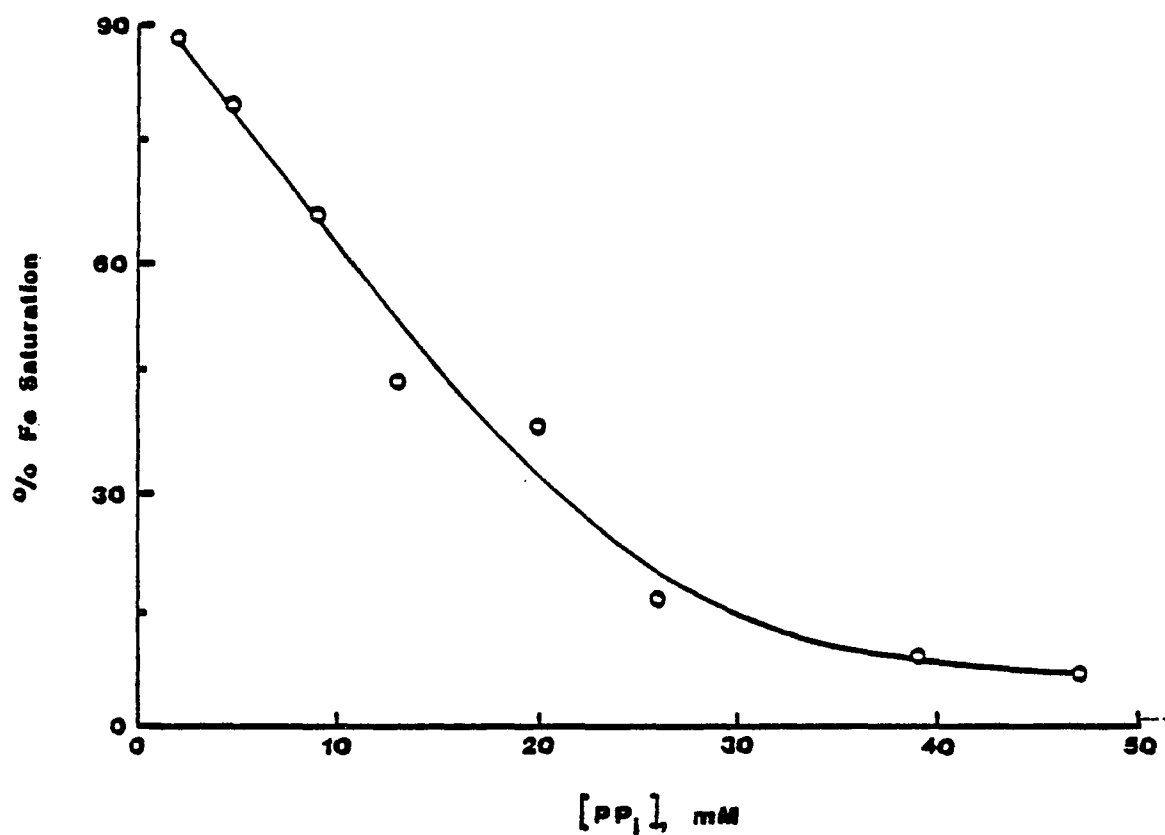


Figure 3.4. Dependence of the percent iron saturation of transferrin as a function of pyrophosphate concentration. Conditions: 56  $\mu$ M diferric transferrin, 1.3 mM  $\text{NaHCO}_3$ , 0.01 M HEPES at pH 7.5 and 37° C.



This same solution did exhibit a slight absorbance at 465 nm when referenced to a 0.1 M HEPES buffer solution. However, when referenced to an apotransferrin/buffer solution, the absorbance decreased to a baseline value. Accordingly, in determining the percent saturation all absorbances measured vs buffer as the reference were corrected by subtracting from them the final absorbance measured at the end of the pyrophosphate titration. This correction amounts to approximately 15% of the absorbance at 465 nm of diferric transferrin.

These results were used in determining  $b$ , the number of pyrophosphates in equation 3.3. A plot of  $\log B$ , where  $B = [\text{Fe}(\text{complex})][\text{site}]/[\text{Fe-site}]$ , vs  $\log[\text{PP}_i]$  at constant pH and bicarbonate concentration should yield a straight line with a slope equal to  $b$ . A log-log plot in which the pyrophosphate concentration is varied at pH 7.5 and a bicarbonate concentration of 0.01 M is presented in Figure 3.5. A straight line with a slope of  $3.02 \pm 0.29$  (correlation coefficient 0.9925) is obtained indicating that a 3:1 pyrophosphate:iron complex is formed.

Earlier studies of iron pyrophosphate complexes have concluded that in excess pyrophosphate a 2:1 pyrophosphate:iron complex is formed having an association constant  $= 10^{5.55}$  (80,81). It is difficult, however, to compare our results with the literature values because of the different reaction conditions. The present study was conducted at a constant pH of 7.5, whereas earlier conclusions were obtained by titrating a basic solution of pyrophosphate at an original pH of 9.5 with Fe(III) and

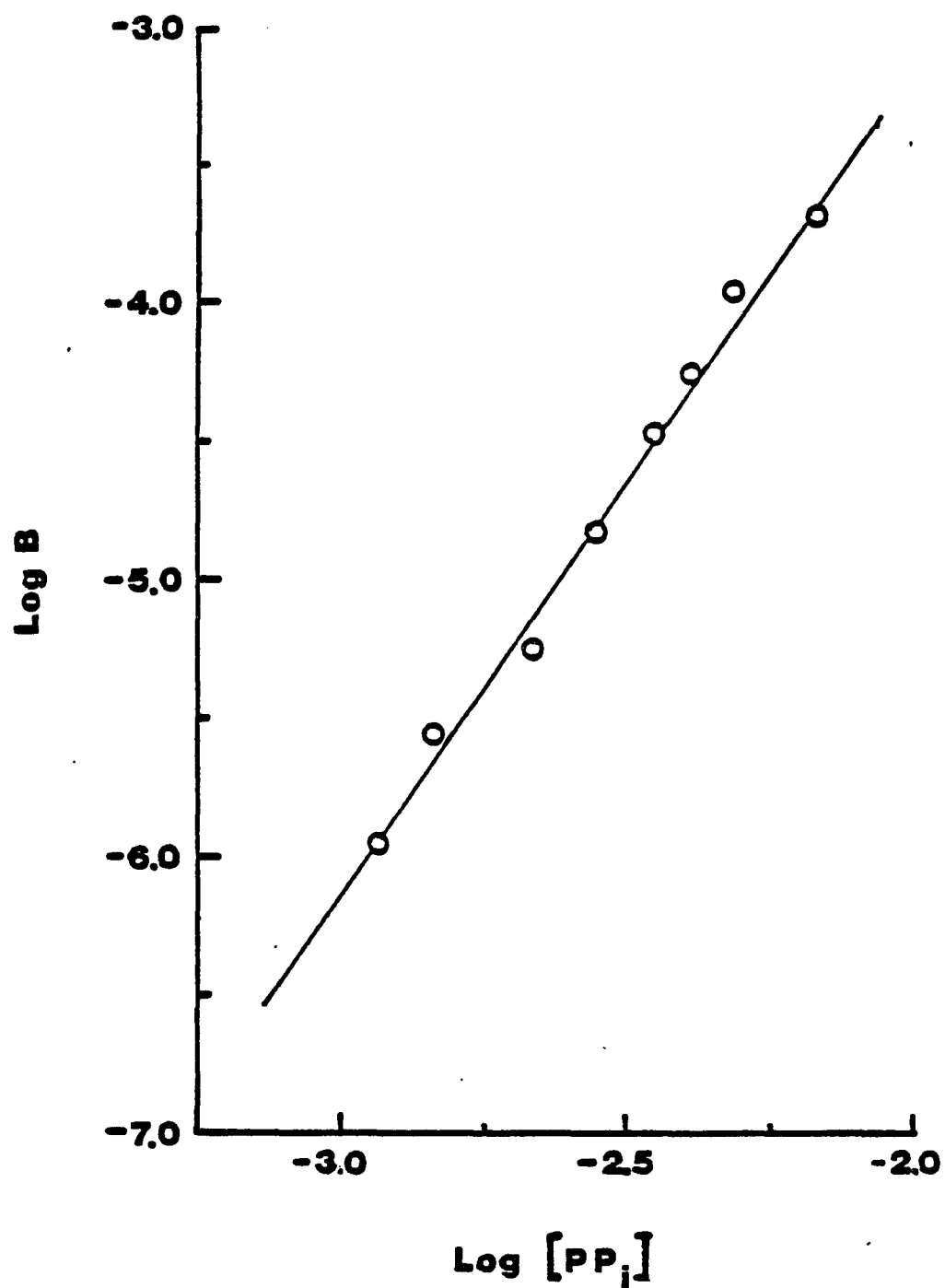


Figure 3.5. Log-log plot of data shown in Figure 3.4.  $B = [\text{Fe}(\text{complex})][\text{site}]/[\text{Fe-site}]$ . Slope of the line is equal to  $b$ , the number of pyrophosphates involved in equation 3.2.  $b = 3.02 \pm 0.29$ , correlation coefficient = 0.9925.

monitoring the change in pH. No corrections for the amount of free acid inherent in Fe(III) solutions were applied to the latter analyses. Moreover, although an iron complex with a log K of 5.55 might exist in acid solution,  $K_{sp}$  data indicate that the same complex exposed to a pH of 7.5 would hydrolyze and precipitate.

Recent kinetic studies conducted by Bates and coworkers provide further evidence for the formation of a 3:1 pyrophosphate: iron complex at pH 7.5 (82). The ability of pyrophosphate to deliver iron to transferrin reaches a maximum rate at a  $PP_i$ : Fe ratio of 3:1. Below this stoichiometry hydrolysis of iron presumably occurs retarding the kinetics of the reaction.

#### Determination of c

The pH dependence of the percent Fe saturation of transferrin in the presence of 0.04 M pyrophosphate is presented in Figure 3.6. A Henderson-Hasselbach plot of the data gives an apparent pK of approximately 8 for the titration curve. Figure 3.7 shows the data cast into another log-log plot where Log C, with C equal to  $[Fe(\text{complex})][\text{site}][HCO_3^-]/[Fe\text{-site}][HP_2O_7^{3-}]$ , is plotted against pH. Over the pH range 7.2 to 8.5 a straight line is obtained with a slope equal to  $1.14 \pm 0.14$ . From these results, the value of c, the coefficient of  $H^+$  in the equilibrium, is taken to be one. (The values of the equilibrium constants are changing over this pH range, vide infra, but not sufficiently enough to affect the determination of the coefficient c).

Results of urea/polyacrylamide-gel electrophoresis (Figure

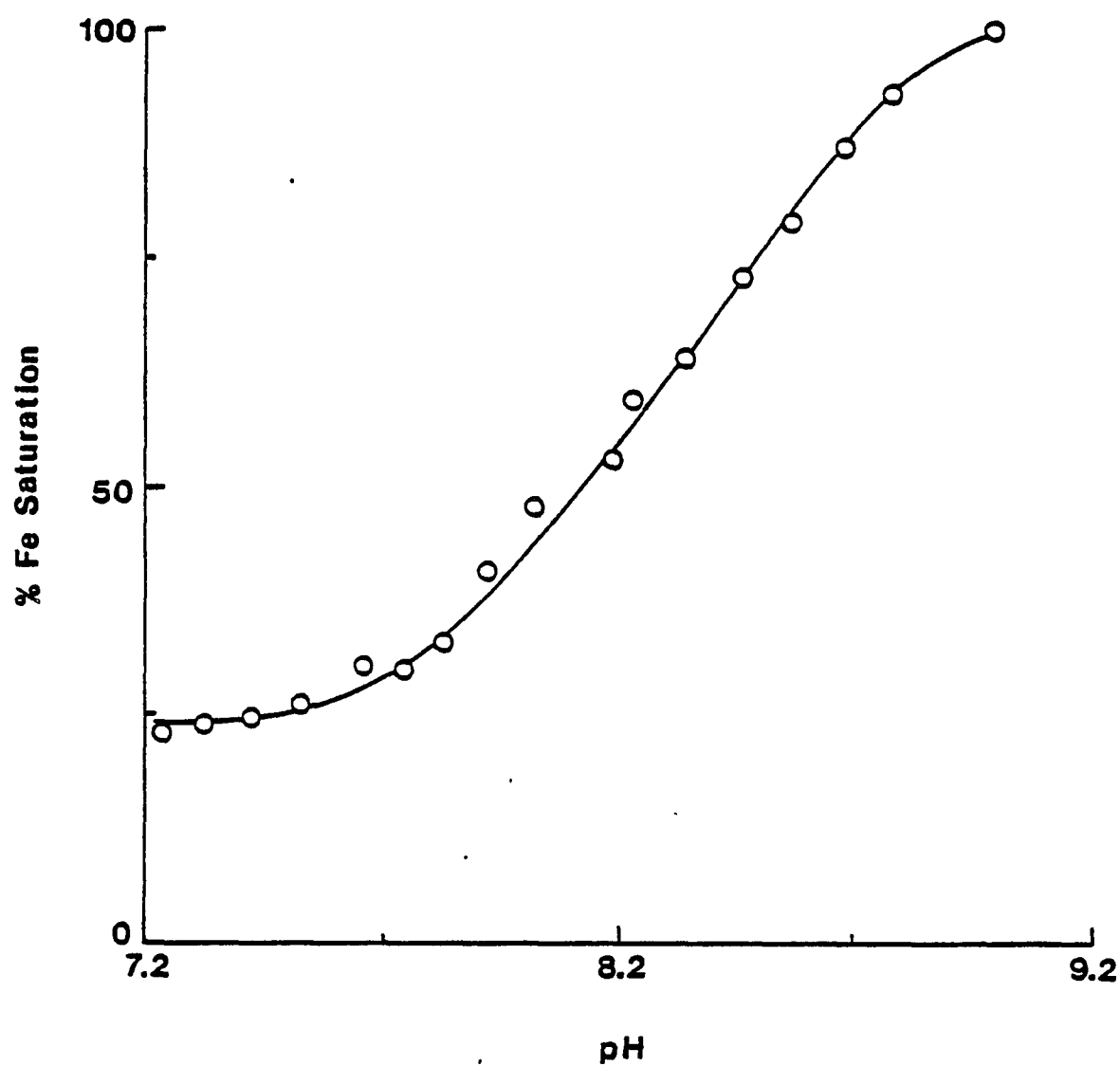


Figure 3.6. Dependence of the percent iron saturation of transferrin as a function of pH at a fixed pyrophosphate and bicarbonate concentration of 40 mM and 10 mM respectively. Protein concentration = 50  $\mu$ M, temperature = 37° C.

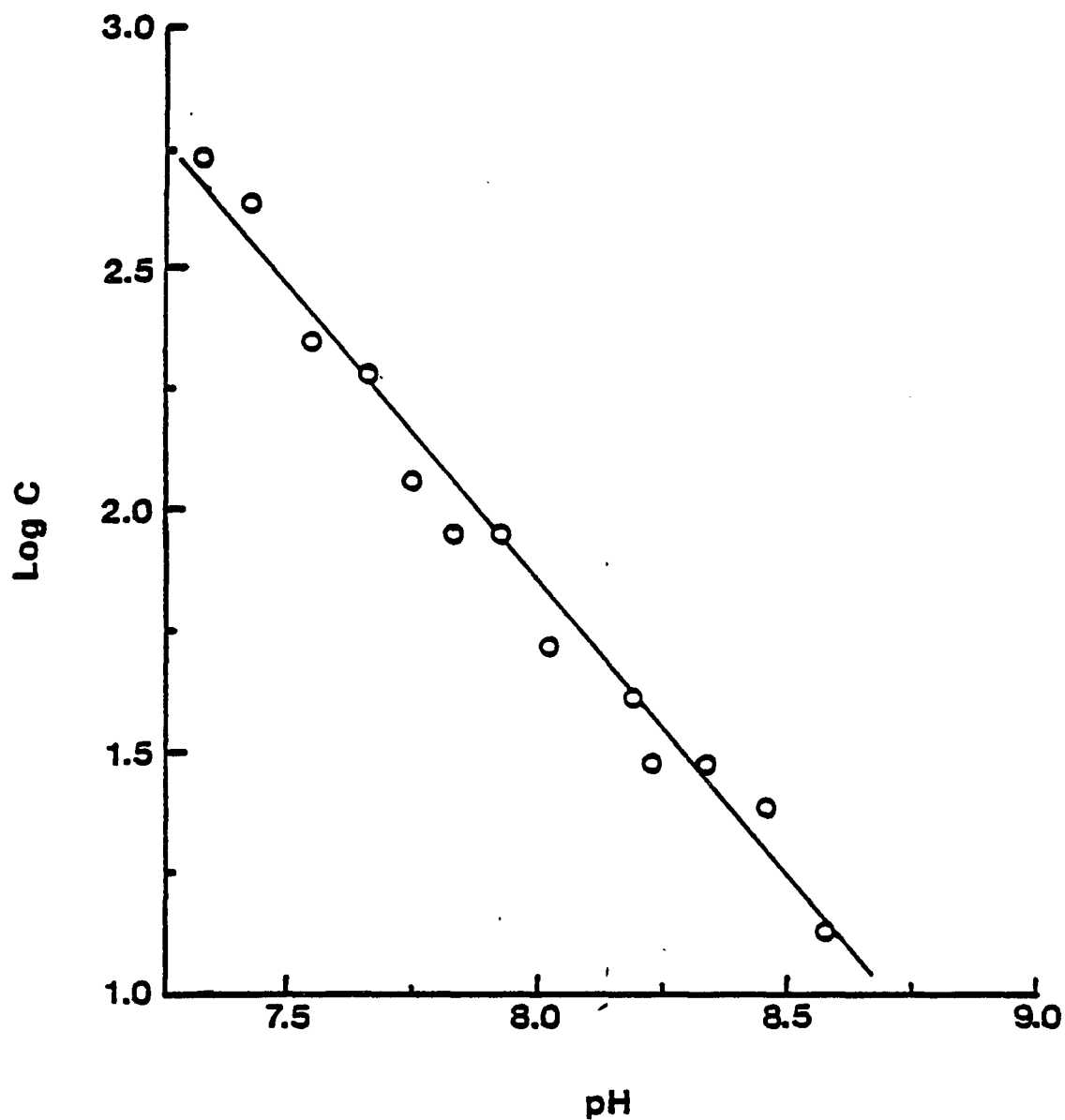


Figure 3.7. Log-log plot of data from Figure 3.6.  $C = [\text{Fe}(\text{complex})][\text{HCO}_3^-][\text{site}]/[\text{Fe-site}][\text{HP}_2\text{O}_7^{3-}]^3$ . The slope of the line is equal to  $c$ , the number of protons involved in equation 3.2.  $c = 1.14 \pm 0.14$ , correlation coefficient = 0.9875.

3.8) conducted on transferrin samples withdrawn during the pH titration indicate that, with increasing pH, there is an increase in the relative stability of iron binding in the N-terminal domain over that in the C-terminal domain, a result consistent with previous studies (48). At low pH values and less than 100% saturation, iron is bound in the C-terminal half of the molecule, becoming preferentially bound in the N-terminal half as the pH is raised.

#### Determination of a

In order to observe the effect of bicarbonate on the competitive equilibrium, the percent iron saturation of the protein in the presence of pyrophosphate was studied as a function of added bicarbonate. It is important to establish that bicarbonate is directly involved in the binding of iron to transferrin. Some question has remained as to whether bicarbonate binds appreciably to the protein prior to iron binding. If bicarbonate binds strongly to apotransferrin, the percent saturation should be independent of the concentration of added bicarbonate provided a stoichiometric amount is present originally. As demonstrated in Figure 3.9, the percent saturation of transferrin is clearly a function of added bicarbonate. An increase in transferrin-bound iron is observed with increasing bicarbonate concentration at pH 7.5. Casting this data into another log-log plot (Figure 3.10) yields a straight line with a slope of  $0.982 \pm 0.24$ , indicating that one bicarbonate is involved per iron sequestered by the protein. The direct involvement of bicarbonate in the

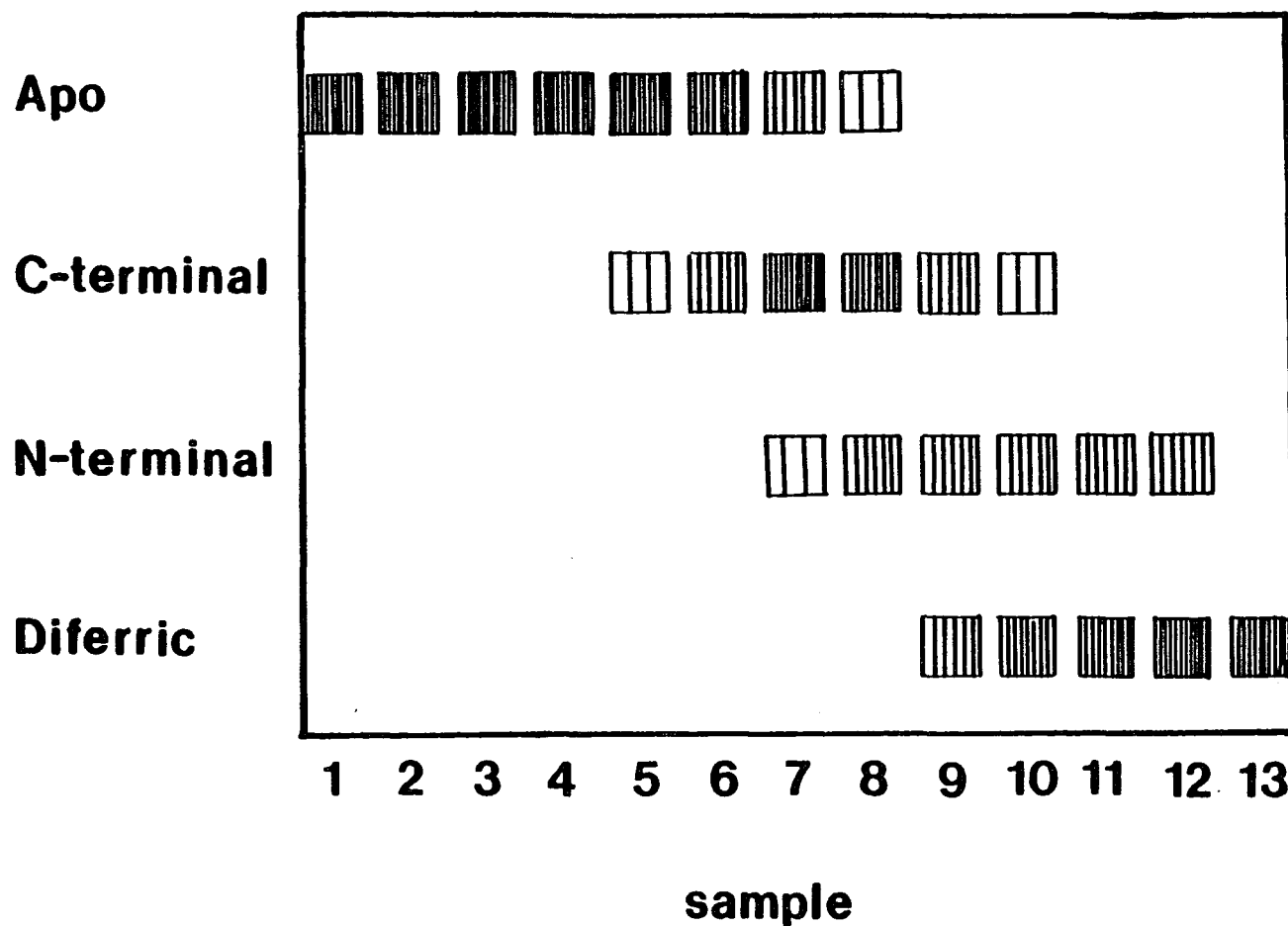


Figure 3.8. Results of urea/polyacrylamide-gel electrophoresis conducted on transferrin samples withdrawn during the pH titration shown in Figure 3.6. Darker areas represent heaviest concentration of protein species. Sample #, pH: 1, 7.15; 2, 7.32; 3, 7.50; 4, 7.70; 5, 7.90; 6, 8.12; 7, 8.31; 8, 8.53; 9, 8.74; 10, 9.14; 11, 9.34; 12, 9.56; 13, diferric transferrin.

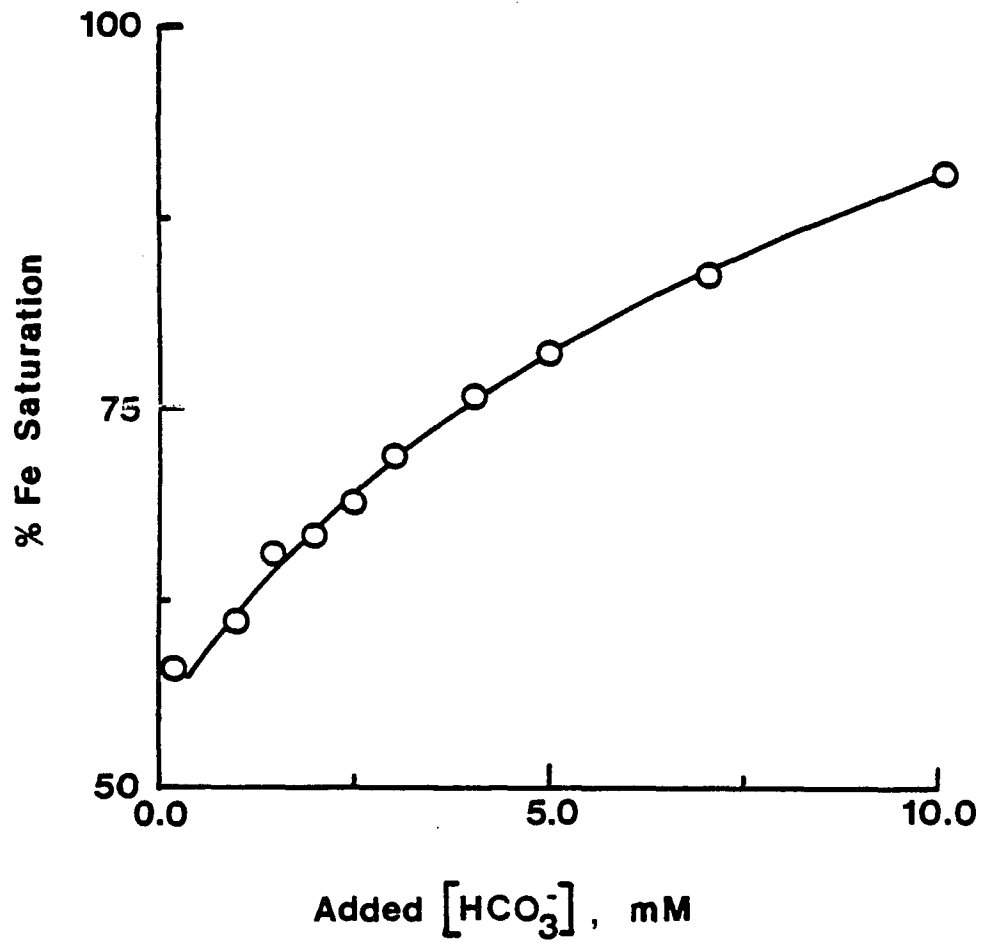


Figure 3.9. Dependence of the percent iron saturation of transferrin as a function of added bicarbonate at pH 7.5 and a pyrophosphate concentration of 5 mM. Protein concentration = 50  $\mu\text{M}$  at 37° C. Buffer is 0.1 M HEPES.



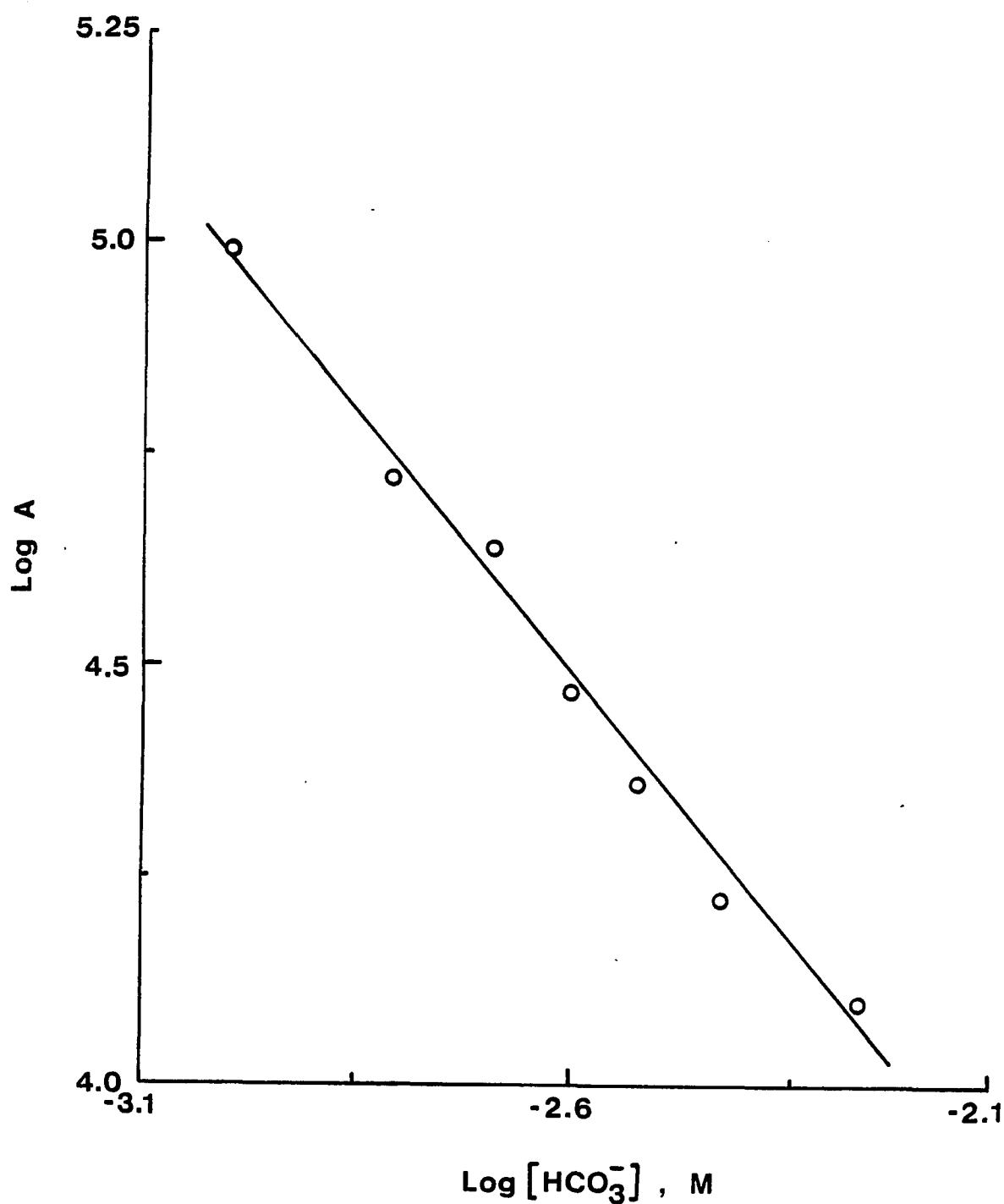
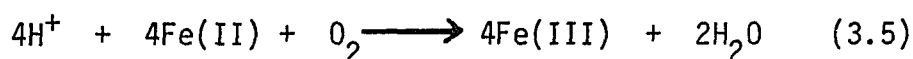


Figure 3.10. Log-log plot of data from Figure 3.9.  $\text{Log } A = [\text{Fe-site}][\text{HP}_2\text{O}_7^{3-}]^3/[\text{Fe}(\text{complex})][\text{site}]$ . Slope of the line is equal to  $a$ , the number of bicarbonates involved in equation 3.2.  $a = 0.982 \pm 0.24$ , correlation coefficient = 0.994.

competitive equilibrium demonstrates that bicarbonate does not bind significantly to the specific anion site in the absence of iron.

From the values of  $a=1$ ,  $b=3$ , and  $c=1$  and charge balance, the charge  $d$  of the Fe-pyrophosphate complex must be equal to 8-. This value was checked by titrating 0.01 M pyrophosphate at pH 7.5 with Fe(II) and measuring, by pH restoration, the number of protons released (or consumed). When Fe(II) is oxidized to Fe(III) one proton per iron is consumed, viz.

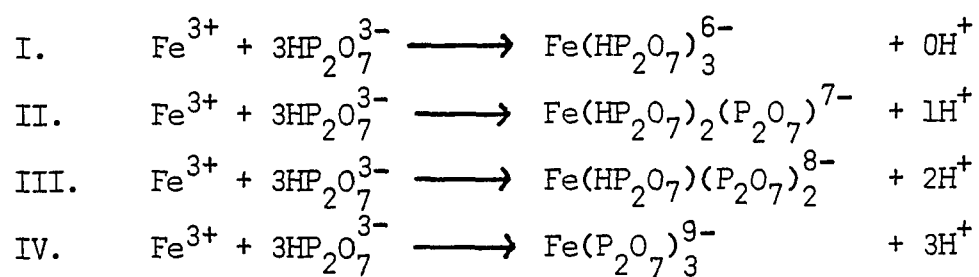


Upon complexation to three pyrophosphates, however, a variety of possibilities could occur depending on the state of protonation of the pyrophosphate ligands. These possibilities are summarized in Table 3.1. Which of the four possibilities is occurring was determined by measuring the change in the number of protons in solution for the overall reaction (i.e., equation 3.5 + either I, II, III, or IV of Table 3.1).

Addition of Fe(ii) to pyrophosphate at pH 7.5 caused a reduction in pH for Fe:PP ratios of 1:20, 1:10, 1:5, and 1:2.5. 1.0 N standard NaOH was used to restore the solution to the original pH. For all but the 1:2.5 case,  $1.02 \pm 0.18$  equivalents of base (per Fe(II)) were required. An insoluble white precipitate was observed in the latter case, which has been attributed to the fact that the pyrophosphate concentration was not sufficient to complex all the iron fully. Solutions with large iron:pyrophosphate ratios have been observed to polymerize, yielding in-

Table 3.1

Possible Reactions of Iron(III)  
and Pyrophosphate at pH 7.5



soluble material (67). Hydrolysis of the uncomplexed iron(III) or partial hydrolysis of an Fe(III)-pyrophosphate complex would produce the observed increase in the number of protons generated for the 1:2.5 ratio. The existence of  $\text{Fe}(\text{OH})_2(\text{P}_2\text{O}_7)^{3-}$  is known (80).

The only possibility of Table 3.1 and equation 3.5 that would generate the net of one proton produced for the other ratios is Case III. It is therefore concluded that the active species in solution is  $\text{Fe}(\text{HP}_2\text{O}_7)(\text{P}_2\text{O}_7)^{8-}$  in agreement with the value of  $d$  obtained from charge balance.

To insure that the iron-pyrophosphate complex contained Fe(III) and not appreciable Fe(II), 400  $\mu\text{l}$  aliquots were withdrawn and their 77° K frozen solution EPR spectra measured at X-band frequency. All samples produced spectra identical to that of Figure 3.3.

pH-Restoration experiments were also conducted at pH 9.0. At this pH fewer protons should be generated per iron since the predominant species in solution would now be  $\text{P}_2\text{O}_7^{4-}$ . This assumption is borne out in the results tabulated in Table 3.2. That the pH never increased upon addition of Fe(II) is probably due to some hydrolysis of Fe(III) at this high pH. Small amounts of precipitate which redissolved when the pH was restored to 9.0 were observed for all but the 20:1 sample. The resulting solutions were slightly yellow in color, unlike the pH 7.5 samples, which were colorless. Insoluble ferric pyrophosphate complexes are known to dissolve in excess alkaline  $\text{P}_2\text{O}_7^{4-}$ . The results can

Table 3.2

Titratable Protons released during Fe Complexation<sup>a</sup>

<u>Fe<sup>2+</sup> added/pyrophosphate</u>	<u>H<sup>+</sup> Released/Fe<sup>2+</sup> b</u>
20 <sup>c</sup>	1.02, 1.1
10 <sup>c</sup>	0.98, 0.96
5 <sup>c</sup>	0.95, 1.04
2.5 <sup>c</sup>	1.42, 1.35
20 <sup>d</sup>	0.41, 0.52
10 <sup>d</sup>	0.30, 0.35
5 <sup>d</sup>	0.65, 0.72
2.5 <sup>d</sup>	0.82, 0.74

a) Conditions: 50 ml of 10 mM pyrophosphate.

b) Primary data of two independent determinations.

c) pH = 7.5

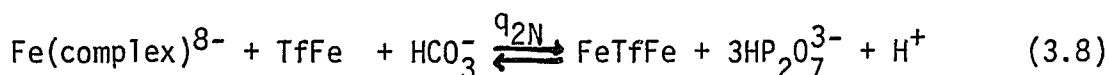
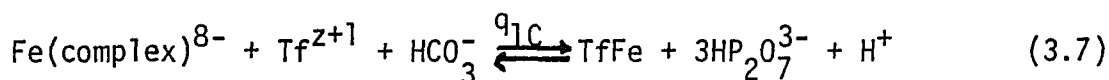
d) pH = 9.0

be explained neither by air oxidation of Fe(II) followed by simple hydrolysis of Fe(III) nor hydrolysis of uncomplexed Fe(II) to  $\text{Fe}(\text{OH})_2$ . A net of two protons would be generated in the former case whereas the presence of oxygen in the samples renders the latter case unlikely.  $\text{Fe}(\text{OH})_2$  is green-black in the presence of air; the observed precipitate is white (83).

#### Determination of Q

Figure 3.11 shows the percent iron saturation of transferrin in a physiological saline buffer solution as a function of pyrophosphate concentration at three different values of pH when referenced to apotransferrin in the same buffer. This data is plotted in Figure 3.12 as  $\log[\text{Fe}(\text{HP}_2\text{O}_7)(\text{P}_2\text{O}_7)_2^{8-}][\text{site}][\text{HCO}_3^-]/[\text{Fe-site}][\text{H}^+]$  vs  $\log[\text{HP}_2\text{O}_7^{3-}]$ . The value of the site equilibrium constant, Q, as determined from the intercept, is found to be  $1.12 \times 10^6$ .

The evaluation of the equilibrium constant Q in this manner is not sufficiently refined to distinguish between the two iron centers of the protein. Since transferrin is a two-sited protein, a distribution of iron containing species is actually formed in solution. Four equilibrium expressions for successive iron binding to transferrin must be written, viz.



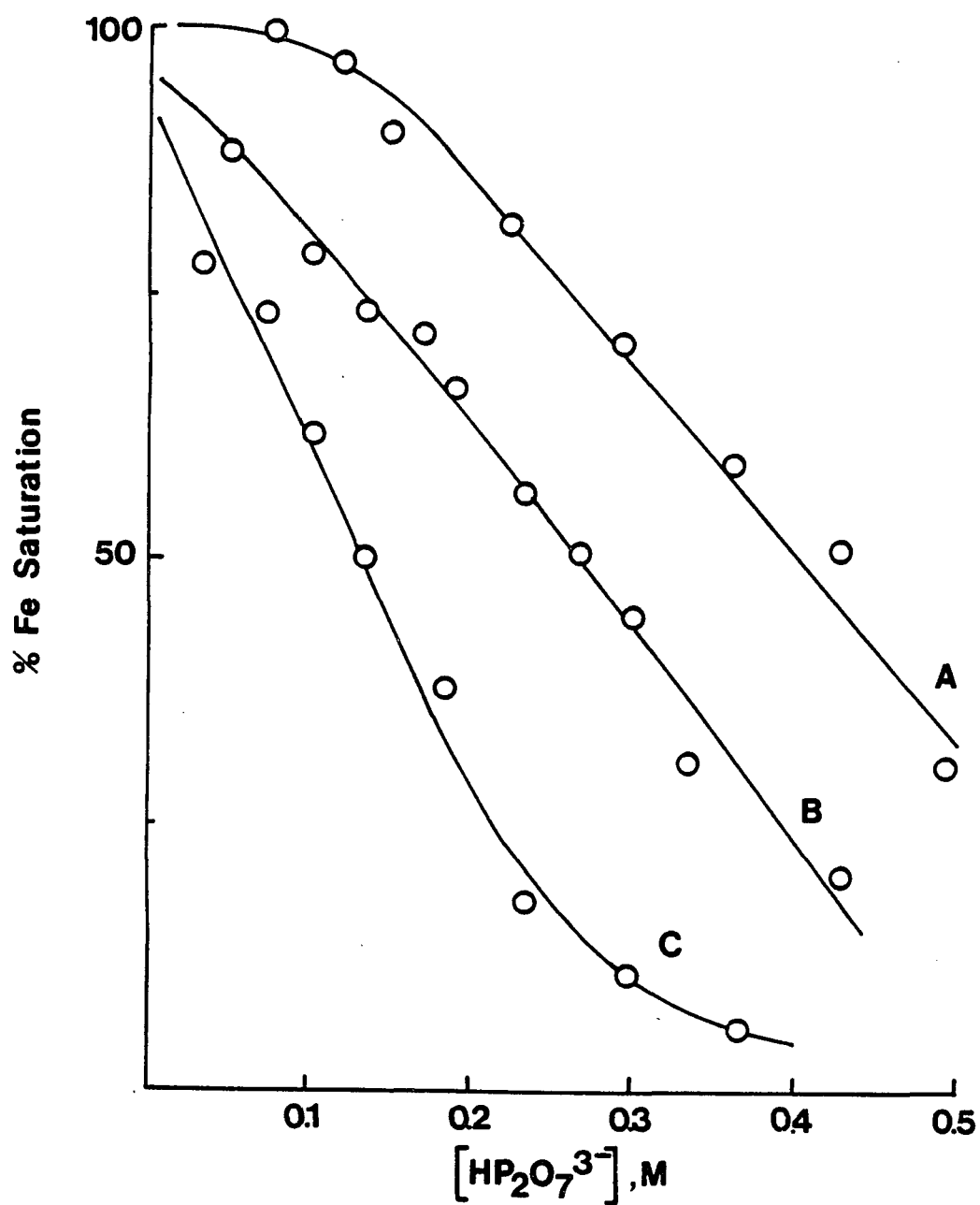


Figure 3.11. Dependence of the percent iron saturation of 5 mg/ml diferric transferrin in physiological saline buffer at pH 7.8 (A), 7.45 (B), and pH 7.23 (C). Temperature = 37 C. pH and bicarbonate concentrations regulated by 95% O<sub>2</sub>/5% CO<sub>2</sub> specialty gas.

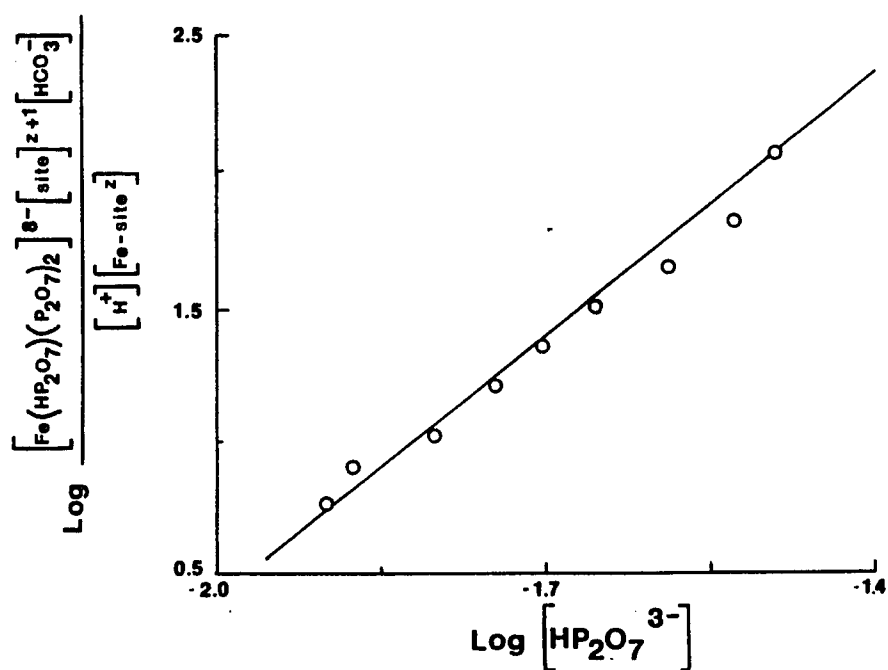
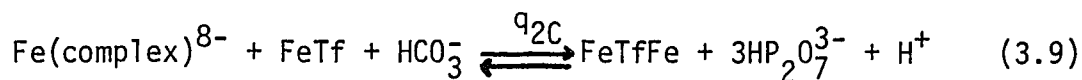


Figure 3.12. Log-log plot of data shown in Figure 3.11 (B). The intercept is equal to  $\log Q$ , an average site equilibrium constant for the competition reaction of equation 3.2.  $n = 2.96 \pm 0.23$ ,  $\log Q = 6.05 \pm 0.066$ , correlation coefficient = 0.989.





For the case where the two sites are equivalent and independent, one has  $Q = q_{1N} = q_{1C} = q_{2N} = q_{2C}$ , i.e., the four intrinsic site constants are equal. Because one cannot distinguish between C and N-terminal monoferric species in this analysis, we define two thermodynamic equilibrium constants,  $Q_1$  and  $Q_2$  for the binding of the first and second iron to transferrin, viz

$$Q_1 = \frac{[\text{FeTf} + \text{TfFe}][\text{HP}_2\text{O}_7^{3-}]^3[\text{H}^+]}{[\text{Fe}(\text{complex})][\text{site}][\text{HCO}_3^-]} \quad (3.10)$$

$$Q_2 = \frac{[\text{FeTfFe}][\text{HP}_2\text{O}_7^{3-}]^3[\text{H}^+]}{[\text{FeTf} + \text{TfFe}][\text{HCO}_3^-][\text{Fe}(\text{complex})]} \quad (3.11)$$

where  $[\text{FeTfFe}]$  and  $[\text{Tf}]$  are the concentrations of diferric transferrin and apotransferrin, respectively, and  $[\text{FeTf} + \text{TfFe}]$  is the sum of the monoferric transferrin concentrations. This treatment is analogous to that for the ionization of a diprotic acid.  $Q_1$  and  $Q_2$  are related to the intrinsic site constants of equations 3.6-3.9 by the relationships

$$Q_1 = q_{1N} + q_{1C} \quad (3.12)$$

$$Q_2^{-1} = q_{2N}^{-1} + q_{2C}^{-1} \quad (3.13)$$

If the binding of iron to transferrin is totally random, then  $Q_1 = 2Q$  and  $Q_2 = Q/2$  from which  $Q_2 = Q_1/4$ . It is customary to write  $Q_2 = R Q_1/4$ , where  $R$  is introduced to account for non-random binding. For a totally random binding  $R = 1$ ; the only difference between  $Q_1$  and  $Q_2$  is the statistical factor  $1/4$ . An  $R$  value much less than one indicates sequential binding of

iron to transferrin (negative cooperativity) while a value of  $R$  greater than one would suggest pairwise binding (positive cooperativity). To evaluate  $Q_1$  and  $Q_2$  and hence  $R$ , the following equations were employed. The total concentration of protein sites occupied by iron is given by

$$[\text{Fe-site}] = [\text{FeTf}] + [\text{TfFe}] + 2[\text{FeTfFe}] \quad (3.14)$$

and the concentration of unoccupied sites by

$$[\text{site}] = 2[\text{Tf}] + [\text{FeTf}] + [\text{TfFe}] \quad (3.15)$$

Combining equations 3.10, 3.11, 2.14, and 3.15 leads to the following formulation for the ratio of occupied and unoccupied sites in terms of the experimentally dictated values of hydrogenpyrophosphate, bicarbonate,  $\text{Fe}(\text{complex})$ , and pH. A further substitution of  $x = [\text{Fe}(\text{complex})]/[\text{HP}_2\text{O}_7^{3-}]^3$  has been made.

$$\frac{[\text{Fe-site}]}{[\text{site}]} = \left( \frac{1}{2 + \frac{Q_1 [\text{HCO}_3^-] x}{[\text{H}^+]}} \right) \left( \frac{Q_1 [\text{HCO}_3^-] x}{[\text{H}^+]} + \frac{2Q_1 Q_2 [\text{HCO}_3^-]^2 x^2}{[\text{H}^+]^2} \right) \quad (3.16)$$

The values of  $Q_1$  and  $Q_2$  were determined by a simplex optimization procedure similar to that described in Chapter II.

As is evident from the graphs in Figure 3.13 the calculated curve for  $[\text{Fe-site}]/[\text{site}]$  conforms well with the experimental points, indicating that we are not using an inappropriate model for our analysis. From this model we obtain the values for  $Q_1$  and  $Q_2$  listed in Table 3.3 for different values of pH. It is

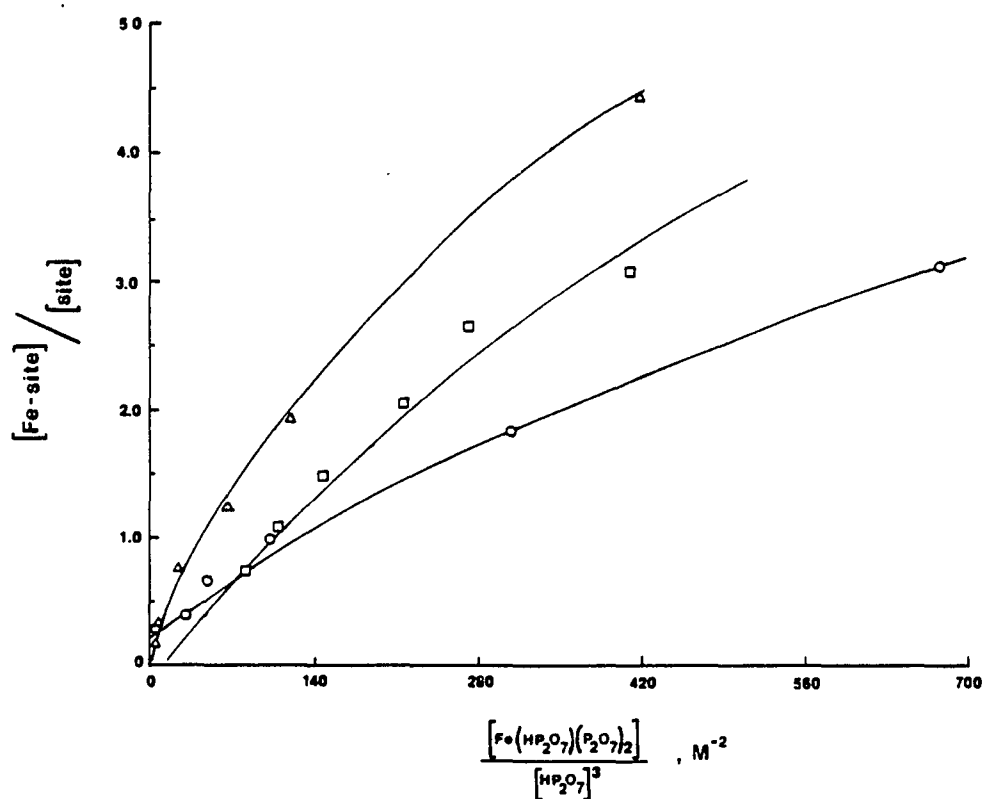


Figure 3.13. Results of nonlinear regression analysis of  $Q_1$  and  $Q_2$  at three different values of pH. Solid lines are calculated curves of experimental data (see results).  $\circ$  pH 7.23,  $\square$  pH 7.45,  $\triangle$  pH 7.80.

Table 3.3  
Summary of Equilibrium Constants  $Q_1$  and  $Q_2$

pH	$k_{1N}/k_{1C}^a$	$k_{2N}/k_{1N}^a$	Q	$Q_1$	$Q_2$	R	$R_{calc}^b$
7.23	.277	.717	$7.2 \times 10^{-7c}$	$2.2 \times 10^{-6}$	$2.3 \times 10^{-7}$	0.41	0.49
7.45	.933	.690	$1.1 \times 10^{-6c}$	$2.4 \times 10^{-6}$	$4.6 \times 10^{-7}$	0.75	0.53
7.80	1.22	1.18	$2.5 \times 10^{-6c}$	$4.4 \times 10^{-6}$	$1.4 \times 10^{-6}$	1.27	1.25

- a) From reference 48, interpolated to a chloride concentration of 0.15 M (see results).  
b) Calculated from  $k_{1N}:k_{1C}:k_{2N}:k_{2C}$  of reference 48.  
c) Q is related to  $Q_1$  and  $Q_2$  by the following equation

$$Q = \frac{Q_1 (2 + R Q_1 ([HCO_3^-]^2/[H+]^2 x^2))}{2 (2 + Q_1 ([HCO_3^-]/[H+] x))}$$

Note than when  $R = 1$ , the equation reduces to  $Q = Q_1/2$ , otherwise there is a concentration dependence that becomes significant when large deviations of R from one is observed

evident that over the pH range 7.2 to 7.8 the affinity of transferrin for the first and second iron changes. Furthermore, the binding of iron changes from negative to positive cooperativity in the physiological pH range with the equilibrium constant  $Q_2$  for the binding of the second iron to the protein largely influencing the value of  $R$ .  $Q_2$  increases by a factor of  $\approx 5$  over the pH range investigated while the value of  $Q_1$  remains fairly constant. This fact is also evident in Figure 3.13. As a check on the reliability of this study, a set of  $R$  values was calculated from previously published data for the relative values of the site binding constants ( $k_{1N}$ ,  $k_{1C}$ ,  $k_{2N}$ ,  $k_{2C}$ ) in the absence of pyrophosphate as obtained by urea/polyacrylamide-gel electrophoresis (48). When referring to values of reference 48, site binding constants for Fe(III) will be denoted by  $k$ . The site equilibrium constants presented here will be denoted by a  $q$ . The term  $k_{1N}/k_{1C}$  is the ratio of the site constants for the binding of the first iron in the N- and C-terminal domain of the protein, respectively, and is a measure of which site is favored by the first iron that binds. The cooperativity factor  $k_{2N}/k_{1N}$  is a measure of how readily the second iron on transferrin binds to the N-terminal site compared to the binding of the first iron to the N-terminal site.

Equations 3.13 and 3.14 relate the intrinsic site equilibrium constants,  $q_{1N}$ ,  $q_{1C}$ ,  $q_{2N}$ ,  $q_{2C}$  to  $Q_1$  and  $Q_2$ . Using the site preference factor  $k_{1N}/k_{1C}$  and the cooperativity factor  $k_{2N}/k_{1N}$  from the graphs in Figures 4 and 5 of reference 48, the

relative values of  $Q_1$  and  $Q_2$  were obtained and a set of  $R$  values were generated. It should be noted here that in the previous work, these ratios were quoted for chloride concentrations of either 0 or 0.5 M. Because chloride has a large effect on these relative values, it was necessary to correct them to a chloride concentration of 0.15 M, the levels used in this study.

Fortunately the effect of chloride concentration on  $k_{1N}/k_{1C}$  and  $k_{2N}/k_{1N}$  is linear over the range of 0 to 0.5 M. This allowed us to interpolate these ratios to the desired chloride concentration. For example, at pH 7.8, Chasteen and Williams report  $k_{1N}/k_{1C}$  of 0.48 and 1.603 with and without chloride, respectively. By multiplying the difference between these two values by the ratio of chloride concentrations one is comparing (i.e., 0.15 M/0.5 M) and adding this number to the site preference factor at 0 chloride, a good approximation of  $k_{1N}/k_{1C}$  at 0.15 M chloride results. A similar interpolation of the cooperativity factor was also necessary. From these two ratios,  $k_{1N}/k_{1C}$  and  $k_{2N}/k_{1N}$  ( $= k_{2C}/k_{1C}$ ) the relative values of  $k_{1N}:k_{1C}:k_{2N}:k_{2C}$  could be computed. A full listing of the site preference factors, cooperativity factors,  $Q_1$ ,  $Q_2$ , and  $R$  are presented in Table 3.3. Excellent agreement between our values and the literature values is achieved. Based on the comparable  $R$  values and the agreement between the urea gels of the two studies, we have calculated the thermodynamic site equilibrium constants of equations 3.6-3.9 for the stepwise binding of iron to transferrin in the presence of pyrophosphate (Table 3.4).

Table 3.4  
Stepwise Site Equilibrium Constants

<u>pH</u>	<u>q<sub>1N</sub>, M<sup>2</sup></u>	<u>q<sub>1C</sub>, M<sup>2</sup></u>	<u>q<sub>2N</sub>, M<sup>2</sup></u>	<u>q<sub>2C</sub>, M<sup>2</sup></u>
7.23	$4.8 \times 10^{-7}$	$1.7 \times 10^{-6}$	$3.4 \times 10^{-7}$	$1.2 \times 10^{-6}$
7.45	$1.2 \times 10^{-6}$	$1.2 \times 10^{-6}$	$7.8 \times 10^{-7}$	$8.3 \times 10^{-7}$
7.80	$2.4 \times 10^{-6}$	$2.0 \times 10^{-6}$	$2.9 \times 10^{-6}$	$2.4 \times 10^{-6}$

### Discussion

The results presented here clearly demonstrate pyrophosphate's ability to compete with transferrin for iron and that this competition is pH and bicarbonate-dependent. It has been well established that pyrophosphate is capable of stripping iron from transferrin (50, 51, 75, 77) but neither the detailed pH-dependence of the thermodynamics of the competition reaction nor the direct influence of bicarbonate on the equilibrium has been reported before.

According to our titration data, three pyrophosphates are required to remove one iron from the protein. The product of this reaction is a mixed pyrophosphate-iron complex  $\text{Fe}(\text{HP}_2\text{O}_7)(\text{P}_2\text{O}_7)_2^{8-}$ ; its composition has been established by charge balance and proton release experiments. Also liberated in this reaction is one bicarbonate ion. The direct involvement of bicarbonate in this equilibrium has been demonstrated, establishing that significant specific anion binding in the absence of iron does not occur.

When the pH of a transferrin, iron, and pyrophosphate solution is raised, an increase in iron binding to transferrin is observed. From the titration curve that is obtained it is apparent that a net of one proton is generated per iron bound below pH 8.5 and that the increase in the overall thermodynamic stability of the iron-transferrin complex with increasing pH is not large.



Our urea/polyacrylamide-gel electrophoresis experiments are in accord with those of Chasteen and Williams (48). Because of this agreement, we have used their ratios of  $k_{1N}:k_{1C}:k_{2N}:k_{2C}$  at several values of pH to calculate a set of R values to compare with those presented in this work and to obtain the stepwise equilibrium constants  $q_{1N}$ ,  $q_{1C}$ ,  $q_{2N}$ ,  $q_{2C}$  for the competition reaction between pyrophosphate and transferrin for iron. The site constants increase with increasing pH, the increase being larger for  $q_{1N}$  than  $q_{1C}$ . This is also consistent with the observation that  $k_{1N}/k_{1C}$  is larger at higher pH values (48).

Aisen et al. (43) have also measured the absolute values of the intrinsic thermodynamic site constants for iron binding to transferrin and reported similar results for R. It is not possible, however, to compare quantitatively the present values with those of Aisen et al. since the experiments were run at different temperatures and solute concentrations.

It is doubtful that the literature data on Fe-pyrophosphate complexes (83) is applicable to this study. Once the formation constant for the  $\text{Fe}(\text{HP}_2\text{O}_7)(\text{P}_2\text{O}_7)_2^{8-}$  complex observed here is known though, the equilibrium constant for the binding of iron to apotransferrin can be calculated from this data and an independent measure of the literature value obtained. From the  $K_{sp}$  for  $\text{Fe}(\text{OH})_3$  and the concentrations of pyrophosphate and  $\text{Fe}(\text{complex})$  used in the proton release experiments, a lower limit on the binding of  $\text{Fe}(\text{III})$  to apotransferrin can be calculated. From reference 21, the  $K_{sp}$  of iron hydroxide is  $2.5 \times 10^{-39}$ . At pH 7.5, the maximum free iron concentration is therefore  $7.9 \times 10^{-20}$  M, which translates

into a minimum association constant ( $K_{pp}$ ) of the Fe-pyrophosphate complex of  $3.93 \times 10^8$ . This number was calculated by substituting the concentrations of Fe(complex) and pyrophosphate used in the proton release studies previously described into the equation  $K_{pp} = [\text{Fe}(\text{complex})][\text{H}^+]^2 / [\text{Fe}(\text{III})][\text{HP}_2\text{O}_7^{3-}]^3$ . The product,  $Q_1 \times K_{pp} = 180$  reflects the minimum value for the association of iron to apotransferrin; this number is consistent with those reported by Aisen (43).

The values of  $Q_1$  and  $Q_2$  obtained here can be used to help establish whether iron binding to transferrin or to pyrophosphate is favored in the cell. Cellular concentrations of pyrophosphate are variable. In the cytosol concentrations of approximately 0.25 mM (84) are typical, while in mitochondria, where pyrophosphate is known to shuttle across the membrane, its concentration can reach 20 mM (85). Using these values, a bicarbonate concentration of 10 mM, and a pH of 7.5, equations 3.10 and 3.11 can be employed to calculate what concentration of transferrin is necessary to facilitate a 50% dissociation of iron from the protein. Setting the ratio of  $[\text{FeTfFe}]/[\text{Tf}] = 1$ , substituting for  $[\text{H}^+]$ ,  $[\text{HCO}_3^-]$ , and  $[\text{HP}_2\text{O}_7]$ , we solve for the value of  $[\text{Fe}(\text{complex})]$ , which is equivalent to the concentration of iron removed from transferrin. This value is the same as the concentration of protein for 50% iron saturation to occur.

We find that at 0.25 mM pyrophosphate the concentration of transferrin would have to be  $2.4 \times 10^{-11}$  M. Under the same conditions of bicarbonate and pH, the presence of 20 mM pyrophosphate requires a protein concentration of  $2.5 \times 10^{-5}$  M to achieve

the same results. Typical serum levels of transferrin are around  $10^{-5}$  M. The concentration within the cell is not known but would probably be lower. The importance of careful regulation of the bicarbonate concentration to this equilibrium can also be seen in these calculations. If a bicarbonate concentration of  $3.4 \times 10^{-5}$  M (ambient levels) is used (43), 50 percent of the iron will be removed at protein and pyrophosphate concentrations of 5  $\mu$ M and 0.5 mM respectively. The family of curves presented in Figure 3.14 was generated by calculating the percent iron saturation for any given protein and pyrophosphate concentration at pH 7.4 and a bicarbonate concentration of 20 mM.

The curves in Figure 3.14 allow one to predict what metabolic conditions would have to prevail before iron would be removed from transferrin and subsequently taken up by pyrophosphate. There is evidence that ferric-pyrophosphate complexes bind to the mitochondria membrane where iron is reduced by the respiratory chain to Fe(II). The ferrous ion is liberated and, through an energy-requiring reaction, is passed to the ferrochelatase inside the mitochondria to be inserted into heme (86,87). To our knowledge no information is available on the change in free energy attending the latter processes in iron metabolism.

The results of the present study indicate that pyrophosphate complexation of iron might be capable of providing the free energy necessary for iron removal from transferrin in vivo and that the feasibility of this process is extremely dependent on pyrophosphate concentration. However, extrapolation from findings

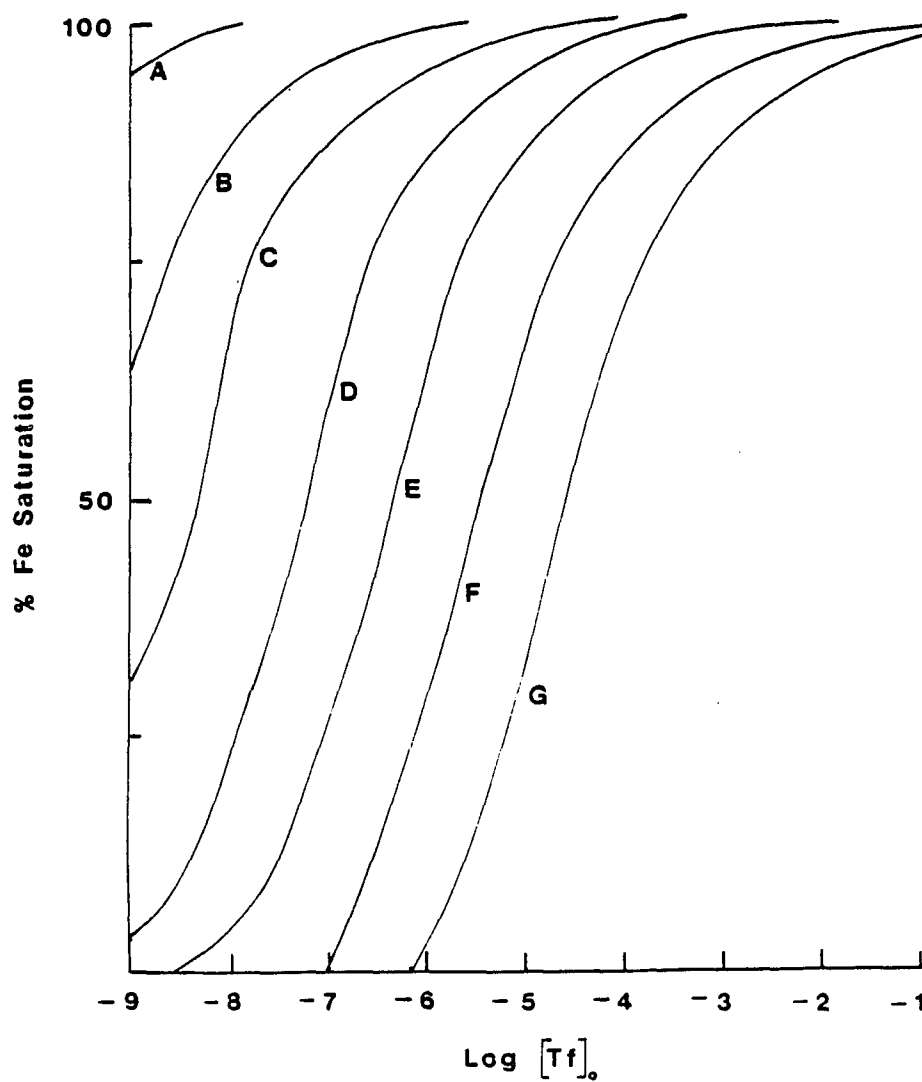


Figure 3.14. Family of curves allowing one to predict the percent iron saturation of transferrin when pyrophosphate and protein concentrations are known. Pyrophosphate concentration 0.1 mM (A), 0.5 mM (B), 1 mM (C), 2.5 mM (D), 5 mM (E), 10 mM (F), 20 mM (G). pH and bicarbonate concentration assumed to be 7.4 and 20 mM respectively.

in vitro to the situation in vivo is exceedingly difficult.

Other factors not included in the present study may prove important in establishing the means whereby iron is removed from transferrin and shuttled to sites of utilization, especially since it is known that iron mobilized by pyrophosphate is not quantitatively accumulated by mitochondria (77) and that the rate of uptake differs when pyrophosphate alone or when the chelator and a reductant are present (74). The suggestion that transferrin has access to low pH endocytotic vacuoles implicates yet another variable. Nonetheless, the results presented in this chapter clearly demonstrate the importance of small phosphorus containing chelators (especially pyrophosphate) in the chemistry of transferrin. Much has yet to be learned about the operation of this small-molecular weight polyphosphate pool in the cell and its significance to the cytosolic transport of iron.

## CHAPTER IV

### STUDY OF ATP AND PYROPHOSPHATE BINDING TO TRANSFERRIN BY $^{31}\text{P}$ NMR SPECTROSCOPY

EPR difference spectroscopy has established that inorganic anions bind with pairwise cooperativity to transferrin and affect the electronic environment of the metal centers. We believe the most likely site of this interaction to be positively charged amino acid residues on the protein. It is probable that anion binding sites close to the metal sites of transferrin are the ones primarily responsible for alterations in the iron binding properties of the protein. Paramagnetic relaxation enhancement of the anion NMR signals due to the Fe(III) enable one to focus on those limited number of sites close to the metal. This chapter reports a preliminary study of the interaction of the anions pyrophosphate and ATP with diferric transferrin by measuring the paramagnetic induced relaxation of the  $^{31}\text{P}$  nucleus as a function of temperature, protein concentration, and anion concentration.

#### Experimental

Diferric human serum transferrin was prepared as in Chapter II and III. All buffers, salts, and  $\text{D}_2\text{O}$  were shaken over Chelex 100 for a minimum of 24 hours prior to use. Diferric transferrin was ultrafiltrated in an Amicon Model 3 ultrafiltration cell equipped with a PM 10 (molecular weight cutoff = 10,000)

membrane with nine volumes of 0.09 M HEPES/0.01 M  $\text{NaHCO}_3$ , pH 7.5 buffer to elute any unbound Fe(III).

ATP of the highest purity was purchased from Sigma Chemical Corporation and its binding to transferrin studied at pH 7.5. Because pyrophosphate is capable of stripping iron from transferrin at pH 7.5, all NMR studies in which pyrophosphate was used were run at pH 9.0.

$T_1$  values of  $^{31}\text{P}$  nuclei were determined at 36.2 MHz on a JEOL FX-90Q NMR spectrometer by the inversion recovery ( $180^\circ$ -t- $90^\circ$ ) pulse sequence (84). The 90 degree pulse was determined by measuring a 180 degree pulse width (evidenced by a null FID and signal in the transformed spectrum) and dividing by two. Four pulse intervals were stacked in each determination of  $T_1$ ; no change in  $T_1$  within the relative standard deviation of  $\pm 2.2\%$  was observed when six t values were stacked. The precision in measuring the  $T_1$  values was checked by placing 2 ml of a 0.1 M ATP/10%  $\text{D}_2\text{O}$ , pH 7.5 solution into a 10 mm flat bottom NMR tube equipped with a vortex plug. Four replicate measurements of the  $T_1$  values of the  $\alpha$ ,  $\beta$ , and  $\gamma$  phosphorus nuclei of ATP were made. The relative standard deviation of these measurements was found to be 1.6%. The tube was removed from the probe prior to each trial. Concentration effects were studied by measuring  $T_1$  values of 0.02, 0.04, 0.08, and 0.30 M ATP solutions at pH 7.5 and 10%  $\text{D}_2\text{O}$ . No effect of concentration on the  $T_1$  of the free ATP was observed. Finally, the precision of the 90 degree pulse was determined by measuring peak intensities after each of four successive 90 degree pulses. The

relative standard deviation in peak intensities was found to be  $\pm 2.1\%$ .

Temperature of the probe was measured by placing a thermometer in a coaxial arrangement inside a 10 mm NMR tube, inserting it into the probe and spinning it for five minutes. All spectra were measured at  $27 \pm 2^\circ \text{C}$ . Temperature was determined periodically throughout the NMR titrations.

Measurements of  $^{31}\text{P}$  relaxation times as a function of anion concentration for diamagnetic  $\text{Co(III)transferrin}$  (38, 85) and paramagnetic iron transferrin protein complexes allowed the paramagnetic contributions to the relaxation rate,  $T_{1p}$ , to be determined. The data was plotted according to the Dahlquist-Raftery equation (86) which has been modified to take into account cooperativity of anion binding, viz.

$$\frac{1}{T_{1p}} = \left( \frac{1}{T_{1app}} \right) \frac{n \cdot K \cdot [\text{anion}]_0^{n-1} [\text{Fe(III)}]_0}{1 + K \cdot [\text{anion}]_0^n} \quad (4.1)$$

where  $[\text{Fe(III)}]_0$  and  $[\text{anion}]_0$  are the total concentration of iron sites and anion respectively.  $K$  is the overall association constant for the cooperative binding of  $n$  anions per  $\text{Fe(III)}$  site.  $T_{1app}$  is the apparent relaxation time of the bound anion and is given by

$$\frac{1}{T_{1app}} = \frac{1}{t_M + T_{1M}} \quad (4.2)$$



$t_M$  and  $T_{1M}$  are the residence time and the NMR relaxation time of the bound anion, respectively. It is assumed in these equations that exchange is rapid on the NMR time scale, that is  $1/t_M \gg \Delta\omega$ , where  $\Delta\omega$  is the frequency difference between bound and free anion. This assumption can be confirmed by studying the effects of temperature on the  $T_1$  values (84).

The paramagnetic contribution to the 31-P relaxation rate of ATP and  $\text{HP}_2\text{O}_7^{3-}$  was obtained from the following equation.

$$\frac{1}{T_{1p}} = \left(\frac{1}{T_1}\right)_{\text{obs}} - \left(\frac{1}{T_1}\right)_o \quad (4.3)$$

where  $(1/T_1)_{\text{obs}}$  is the relaxation rate obtained in the presence of diferric transferrin.  $(1/T_1)_o$  is defined similarly, except that in this case no iron is present.

For NMR titrations at fixed anion concentrations, 2 ml of approximately 0.1 M phosphorus anion (either ATP or pyrophosphate) in 10%  $\text{D}_2\text{O}$ , 0.1 M HEPES buffer at pH 7.5 or pH 9.0 was titrated with 50  $\mu\text{l}$  aliquots of diferric transferrin in 0.1 M ATP, 10%  $\text{D}_2\text{O}$ , 0.1 M HEPES, 0.01 M  $\text{HCO}_3^-$ , pH 7.5. The  $T_1$  values were measured after each addition of titrant. The pH and  $A^{465}$  were checked after each titration to insure that no change in pH had occurred and that iron had not been removed from the protein. Titrations were conducted in 10 mm flat bottom NMR tubes sealed with a vortex plug. Similar titrations were accomplished

at fixed protein concentration and varying concentrations of anion.

## Results

### 31-P Spectroscopy of ATP Binding to Transferrin

Figure 4.1 shows the 31-P NMR spectrum of ATP. At pH 7.5 and 10 mM  $\text{HCO}_3^-$ , significant enhancement of the  $\alpha$ ,  $\beta$ , and  $\gamma$  phosphorus nuclei of ATP is observed in the presence of diferric transferrin. In the absence of diferric transferrin,  $T_1$  values of 5.24, 4.12, and 5.71 s are obtained for the  $\alpha$ ,  $\beta$ , and  $\gamma$  phosphorus nuclei, respectively compared to 2.08, 3.25, and 2.02 s in the presence of  $9.9 \times 10^{-5}$  M diferric transferrin. No change in  $T_1$  was observed with solutions of diamagnetic dicobalt-transferrin or apotransferrin and ATP. The concentration of ATP likewise did not affect the measured  $T_1$  values; the concentration effects were measured in a cobalt-transferrin solution.

A linear relationship between  $1/T_{1p}$  and diferric transferrin concentration with the concentration of ATP fixed at 0.30 M is obtained (Figures 4.2, 4.3, and 4.4). Since ATP exhibits multiplets in its NMR spectrum, we were faced with the problem of selecting which peak to use in determining the value of  $T_1$ . Because no significant difference was observed between peaks of the various multiplets, the value of  $T_1$  was taken as the average of the  $T_1$  for each line in the respective multiplet. All data points are also the average of two independent determinations of  $T_1$ . That the observed relaxation enhancement is not due to some

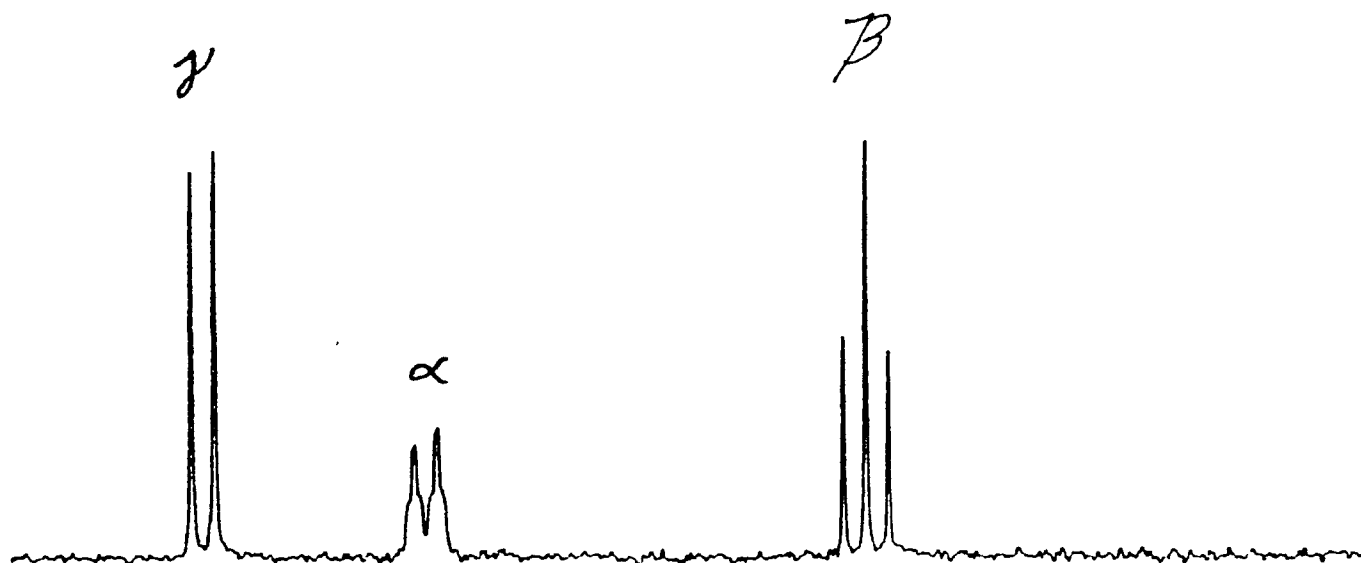


Figure 4.1.  $^{31}\text{P}$  NMR spectrum of 0.3M ATP in 10%  $\text{D}_2\text{O}$ .  $\alpha$ ,  $\beta$ , and  $\gamma$  peaks are labeled. Conditions: 0.30 M  $\text{ATP}^{2-}$  in 0.09 M HEPES, 10%  $\text{D}_2\text{O}$  at pH 7.5 and  $27^\circ\text{C}$ . Spectral width = 2500 Hz, one  $90^\circ$  pulse.

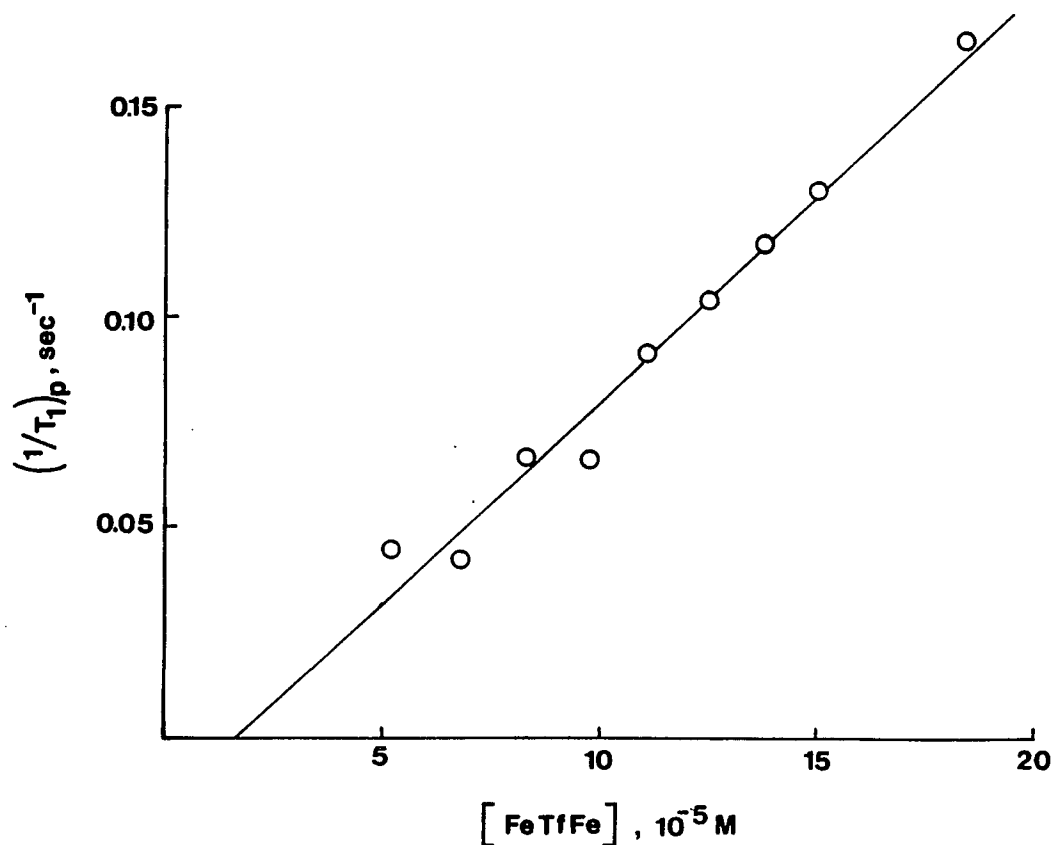


Figure 4.2. Plot of  $(1/T_1)_p$  vs  $[\text{FeTfFe}]$ . Data is for the paramagnetic enhancement of the alpha phosphorus of ATP. Conditions: 2 ml of 0.30 M ATP in 0.09 M HEPES, 10%  $\text{D}_2\text{O}$  at pH 7.5 titrated with 0.5 mM diferric transferrin in 0.09 M HEPES, 0.01 M  $\text{NaHCO}_3$ , 10%  $\text{D}_2\text{O}$ , 0.30 M ATP, pH 7.5.

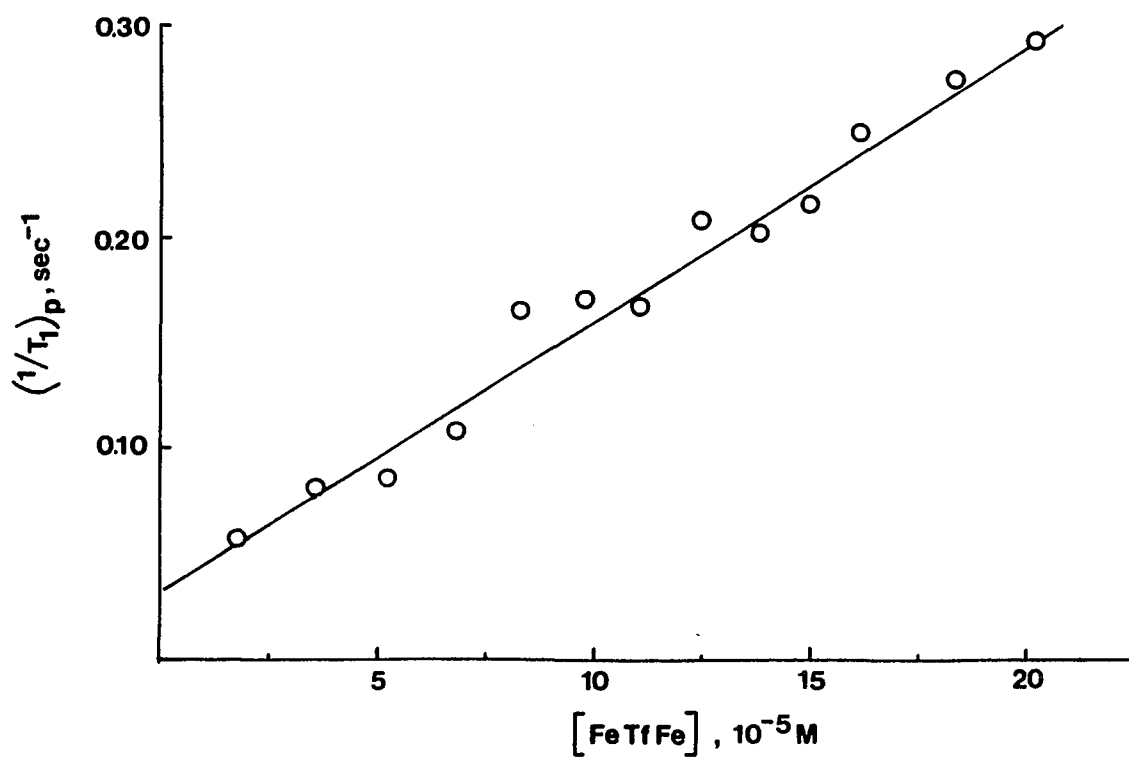


Figure 4.3. Plot of  $(1/T_1)_p$  vs  $[\text{FeTfFe}]$ . Data is for the paramagnetic enhancement of the beta phosphorus of ATP. Conditions as in Figure 4.2.

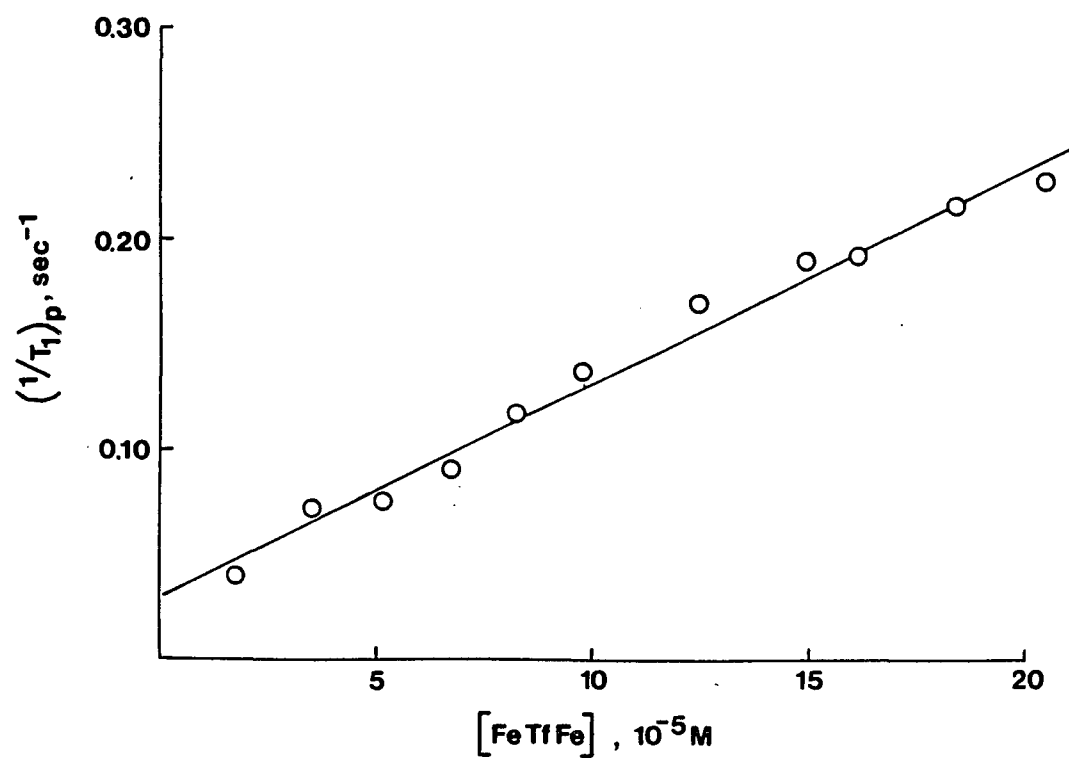


Figure 4.4. Plot of  $(1/T_1)_p$  vs  $[\text{FeTfFe}]$ . Data is for the paramagnetic enhancement of the gamma phosphorus of ATP. Conditions as in Figure 4.2.

Fe(III) that had been removed from the protein was verified by measuring the  $T_1$  of the ultrafiltrate obtained by passing the protein solution through an Amicon Model 3 ultrafiltration cell equipped with a PM 10 membrane. Values of  $T_1$  of 5.76, 4.21, and 5.92 s were obtained for the  $\alpha$ ,  $\beta$ , and  $\gamma$  nuclei, respectively, which are comparable to the values for ATP alone (vide supra).

Figures 4.5-4.7 are plots of  $1/T_{1p}$  vs ATP concentration for a fixed protein concentration of 50  $\mu$ M. The data has been fit to two different equations, the usual Dahlquist-Raftery equation (represented by the dashed line) where the binding of different anions is assumed to be independent, and a modified Dahlquist-Raftery equation in which two anions bind cooperatively per metal site (represented by the solid line). Both lines are the calculated lines obtained from a nonlinear regression analysis of both equations. The values of  $1/T_{1app}$  and  $K$ , the association constant, obtained by this method are presented in Table 4.1. Also presented in this table is the value of the residual,  $S_y$ , for each calculated line. An improvement in fit is obtained when cooperativity is taken into account. Furthermore, the systematic trend in the residuals of the individual points is eliminated. Inappropriate models will yield a trend in the residuals. Based on these results it appears that cooperativity in ATP binding to transferrin is observed at pH 7.5. Cooperative binding of ATP to transferrin has also been observed by EPR difference spectroscopy.

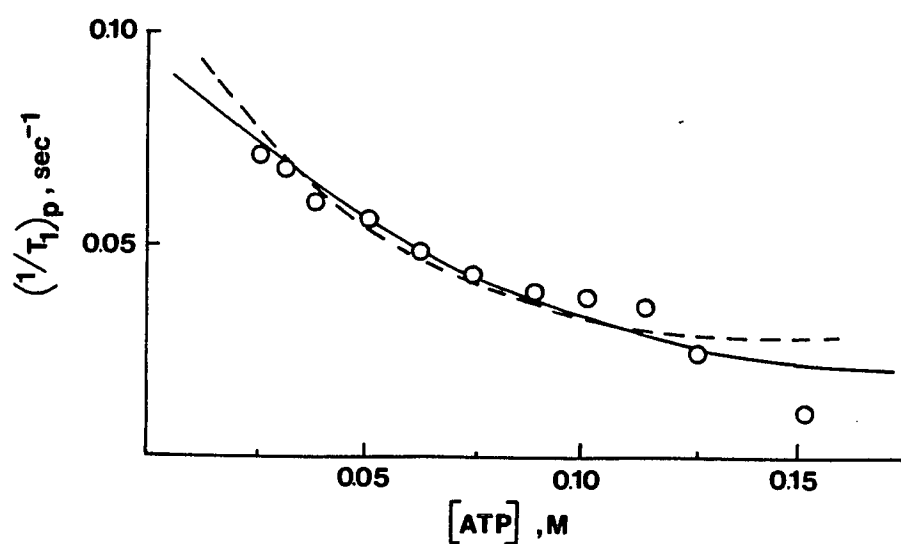


Figure 4.5. Plot of  $(1/T_1)_p$  vs  $[ATP]$  from the titration of 50  $\mu\text{M}$  diferric transferrin with 0.36 M ATP, pH 7.5. The dashed and solid lines are the theoretical lines obtained by a nonlinear regression analysis of the Dahlquist-Raftery equation (equation 4.1) for  $n = 1$  and  $n = 2$ , respectively. Data is for the alpha phosphorus of ATP.



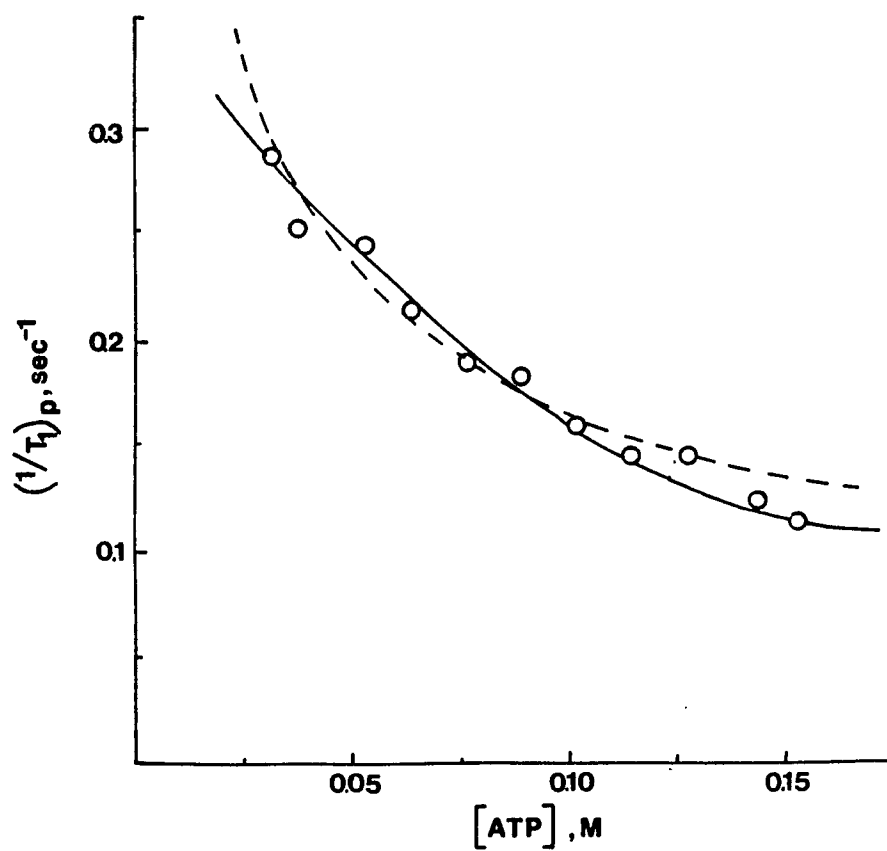


Figure 4.6. Plot of  $(1/T_1)_p$  vs  $[\text{ATP}]$  obtained from titration of 50  $\mu\text{M}$  diferric transferrin with 0.36 M ATP, pH 7.5. Data is for the beta phosphorus nucleus of ATP. See Figure 4.5 and results for explanation of dashed and solid lines.

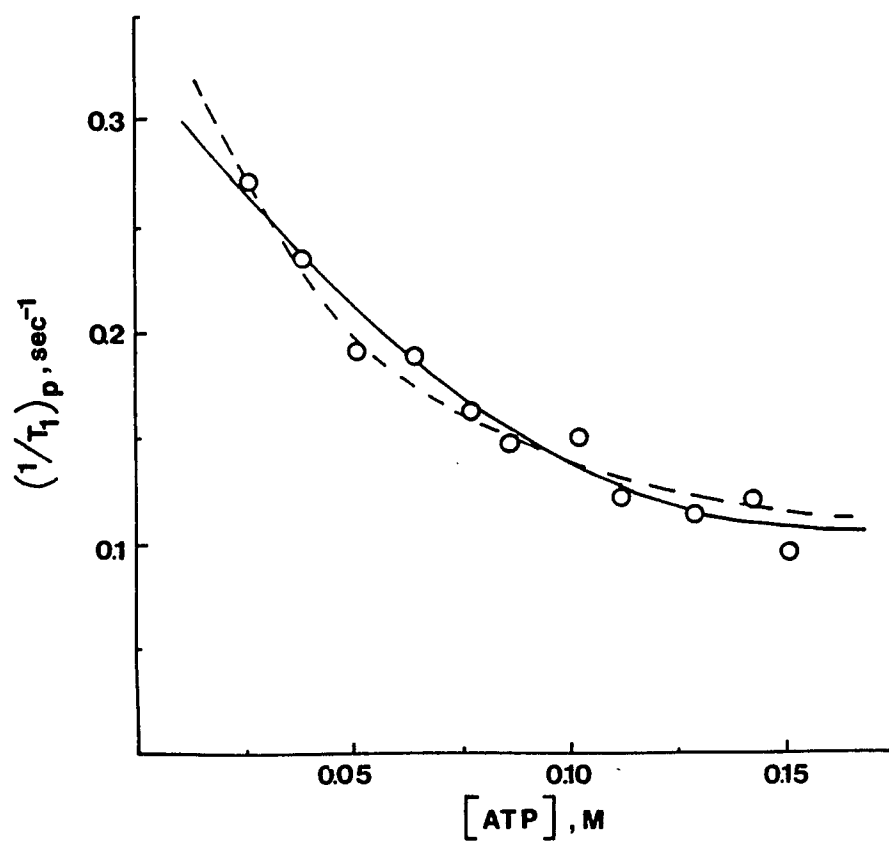


Figure 4.7. Plot of  $(1/T_1)_p$  vs  $[ATP]$  obtained from titration of 50  $\mu\text{M}$  diferric transferrin with 0.36 M ATP, pH 7.5. Data is for the gamma phosphorus of ATP. See Figure 4.5 and results for explanation of dashed and solid lines.

Table 4.1  
Summary of Binding Data of ATP  
to Transferrin<sup>a</sup>

peak	$1/T_{1app}, \text{sec}^{-1}$	K	$S_y$
$\alpha$	9.10	$1.6 \times 10^3$	$5 \times 10^{-3}$
$\beta$	26.7	$1.4 \times 10^3$	$8 \times 10^{-3}$
$\gamma$	33.2	$9.8 \times 10^2$	$9 \times 10^{-3}$
$\alpha$	23.7	$4.2 \times 10^2$	$2 \times 10^{-2}$
$\beta$	111	$2.8 \times 10^2$	$3 \times 10^{-2}$
$\gamma$	128	$2.8 \times 10^2$	$2 \times 10^{-2}$

- a) Conditions:  $9.5 \times 10^{-5}$  M diferric transferrin in 0.09 M  
HEPES, 0.01 M  $\text{NaHCO}_3$  at pH 7.5. Temperature =  $27 \pm 2$  °C.  
b) With cooperativity  
c) Without cooperativity

by EPR difference spectroscopy.

To verify that two ATP molecules are binding per metal site, a solution of diferric transferrin in buffer at pH 7.5 was titrated with aliquots of 0.1 M NTA which is known to bind tenaciously to transferrin. We have observed that when NTA is present in solution with ATP, there is no enhancement in the  $^{31}\text{P}$ -P relaxation rate of the ATP nuclei. Figure 4.8 shows the change in  $1/T_{1p}$  as a function of NTA concentration. As NTA is continually added, the relaxation rates of all three phosphorous nuclei decrease, indicating that NTA is competing effectively for anion binding sites on the protein. This change in  $1/T_{1p}$  continues until a ratio of approximately 4:1, NTA:transferrin, is achieved. It is important to note that the limiting values are very close to the values obtained in the absence of diferric transferrin.

When iron as Fe(II) is added stoichiometrically to a solution of apotransferrin and ATP, a change in the  $^{31}\text{P}$ -P relaxation rate is observed until a ratio of 2:1, Fe:protein, is reached (Figure 4.9). Beyond this point, the slope of the line changes indicating that, if the metal sites are being loaded sequentially, ATP is interacting with both metal sites to the same extent.

#### $^{31}\text{P}$ NMR Spectroscopy of Pyrophosphate Binding to Transferrin

When pyrophosphate is added to 56  $\mu\text{M}$  diferric transferrin at pH 9.0, significant enhancement in the relaxation rate is observed. In the absence of diferric transferrin we find  $T_1$

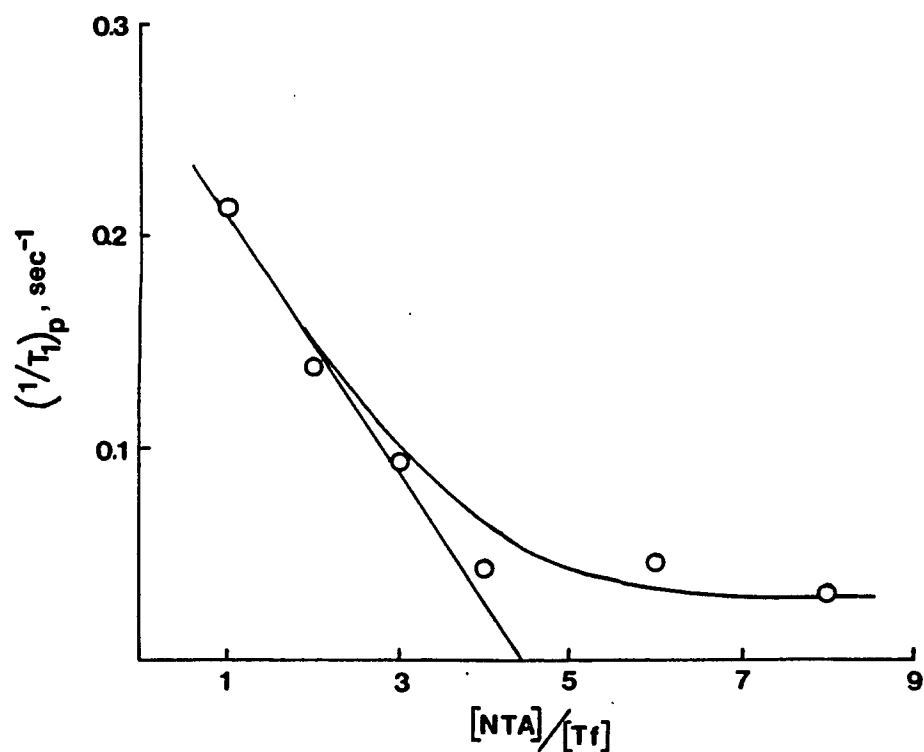


Figure 4.8. Plot of  $(1/T_1)_p$  vs  $[NTA]/[Tf]$  obtained from titration of 20  $\mu\text{M}$  diferric transferrin in 0.25 M ATP, 0.09 M HEPES, 0.01 M  $\text{NaHCO}_3$ , 10%  $\text{D}_2\text{O}$  at pH 7.5 with 0.1 M NTA at pH 7.5.

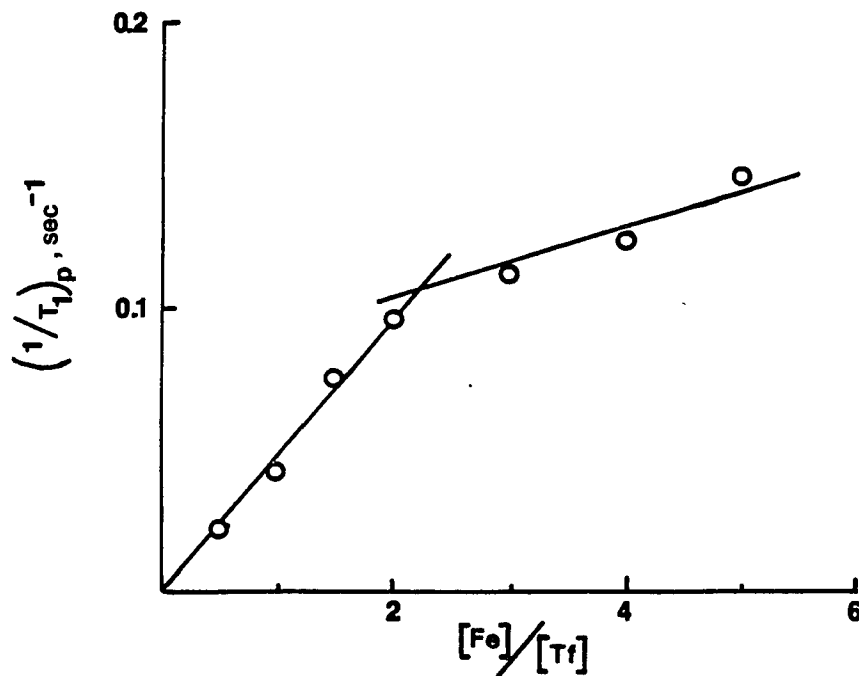
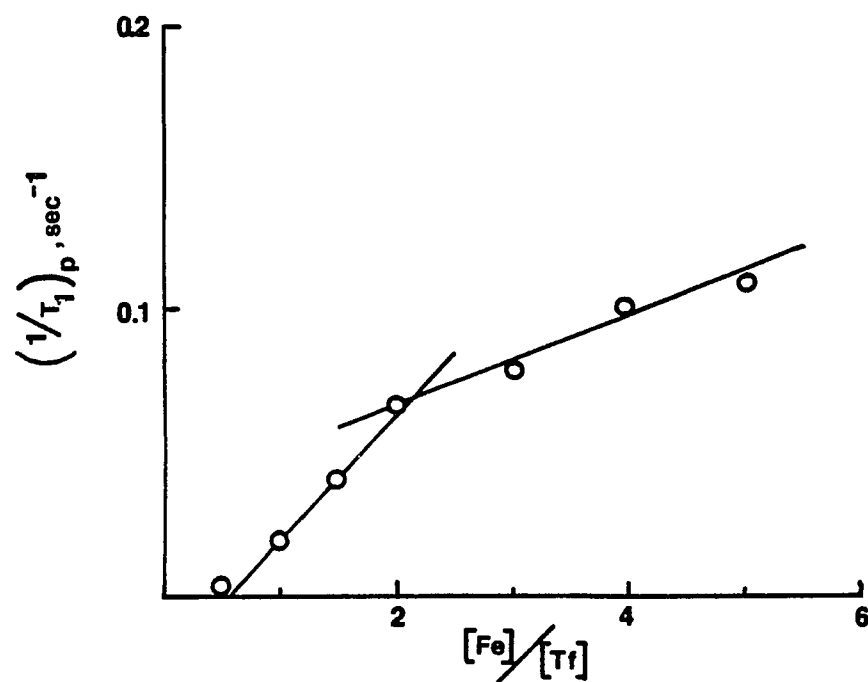


Figure 4.9.  $(1/T_1)_p$  vs  $[Fe]/[Tf]$  obtained from titration of 20  $\mu\text{M}$  apotransferrin in 0.25 M ATP, 0.09 M HEPES, 0.01 M  $\text{NaHCO}_3$ , 10%  $\text{D}_2\text{O}$  at pH 7.5 with 0.1 M Fe(II). A = gamma phosphorus, B = beta phosphorus.

$(PP_i) = 4.15$  s for 0.10 M pyrophosphate compared to 0.866 s in the presence of the protein and 10 mM  $HCO_3^-$ .

Linear relationships between  $1/T_{1p}$  and diferric transferrin concentration with pyrophosphate concentration fixed and  $1/T_{1p}$  and pyrophosphate concentration with diferric transferrin concentration fixed are obtained (Figures 4.10 and 4.11). The data, plotted according to the Dahlquist-Raftery equation with  $n = 1$ , is shown in Figures 4.12 and 4.13. The two independent sets of data give an association constant for pyrophosphate with diferric transferrin of  $204\text{ M}^{-1}$  and  $266\text{ M}^{-1}$ . The values are reasonable for anion binding to a protein. Cooperativity of pyrophosphate binding is not observed under these conditions. Previous EPR measurements with pyrophosphate which did display positive cooperativity were made at pH 7.5 raising the question that a positively charged amino acid constituting an anion binding site might be titrated in the pH range 7 to 9.

#### Distance Calculation

As discussed above, if this system is in the rapid exchange case, the value of  $T_{1app}$  can be obtained from the Dahlquist-Raftery plots. Two cases are of interest in equation 4.2, i.e.,  $t_M \ll T_{1M}$  giving  $T_{1app} = T_{1M}$  and  $t_M \gg T_{1M}$  giving  $T_{1app} = t_M$ . In the latter case the only information that can be obtained from the Dahlquist-Raftery plots is the exchange rate of ATP on transferrin (86, 87). If the former case holds, the value of  $T_{1M}$  can be used to calculate the metal-anion distance provided

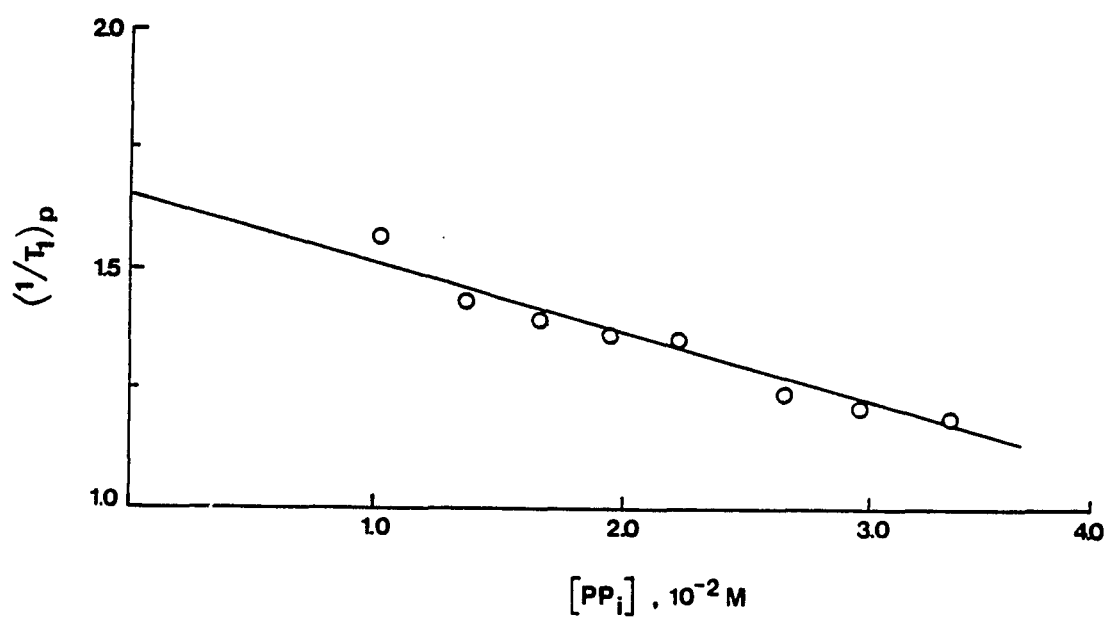


Figure 4.10  $(1/T_1)_p$  vs  $[PP_i]$  obtained from titration of 56  $\mu\text{M}$  diferric transferrin in 0.1 M HEPES, 0.01 M  $\text{NaHCO}_3$ , 10%  $\text{D}_2\text{O}$  with a 0.10 M pyrophosphate solution at pH 9.0.



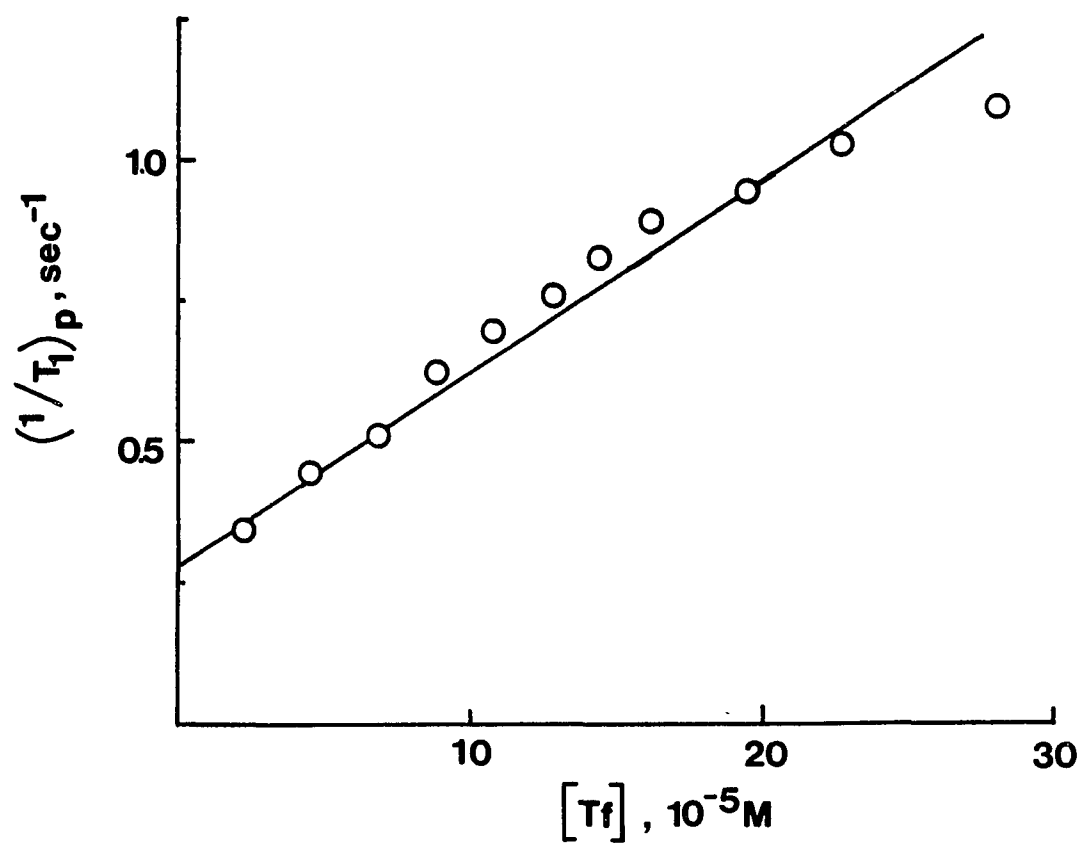


Figure 4.11.  $(1/T_1)_p$  vs  $[Tf]$  obtained from titration of 0.10 M pyrophosphate with a 1 mM diferric transferrin, 0.1 M HEPES, 0.01 M  $\text{NaHCO}_3$ , 0.1 M pyrophosphate solution at pH 9.0.

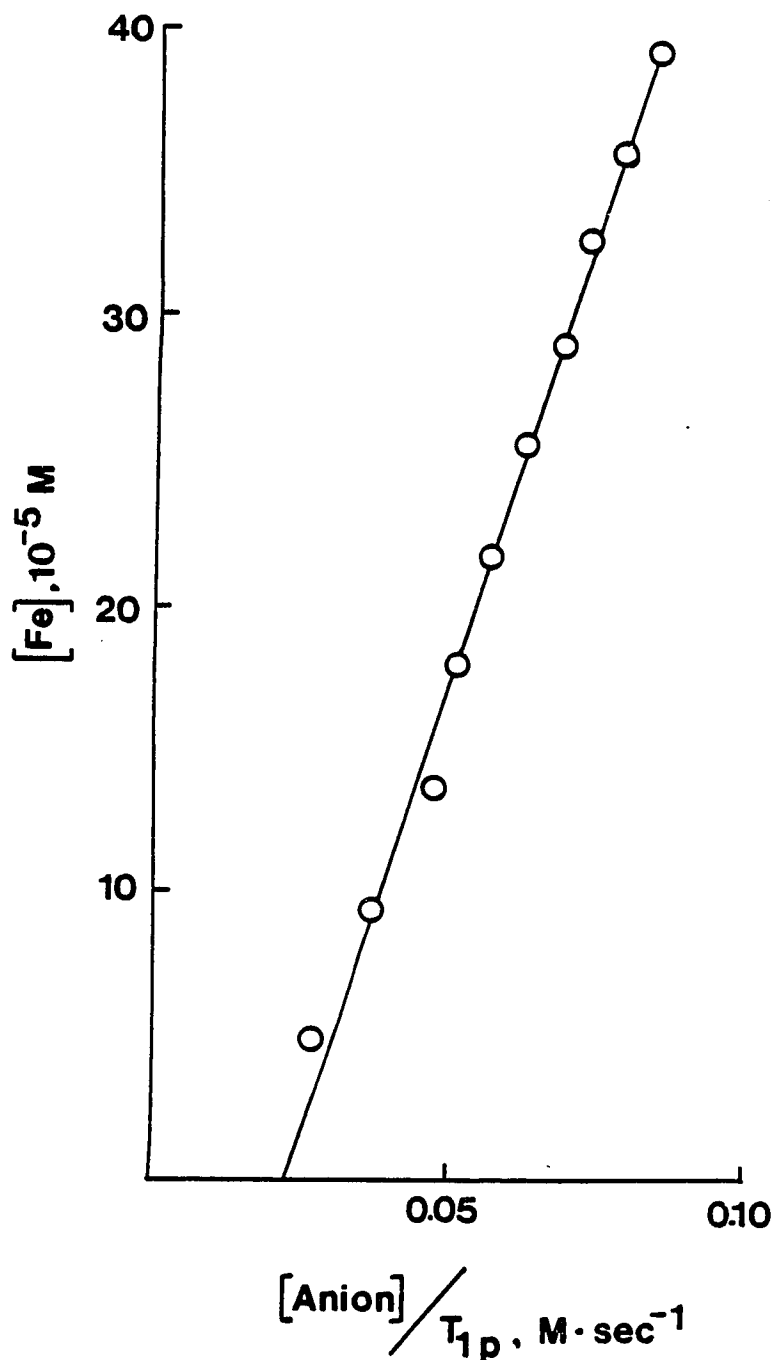


Figure 4.12. Dahlquist-Raftery plot of data shown in Figure 4.11 for  $n = 1$ . The slope of the line is equal to  $(1/T_1)_{app}$  and the intercept to  $-1/K$ .  $m = 371 \pm 41 \text{ s}^{-1}$ ,  $K = 204 \pm 31 \text{ M}^{-1}$ .

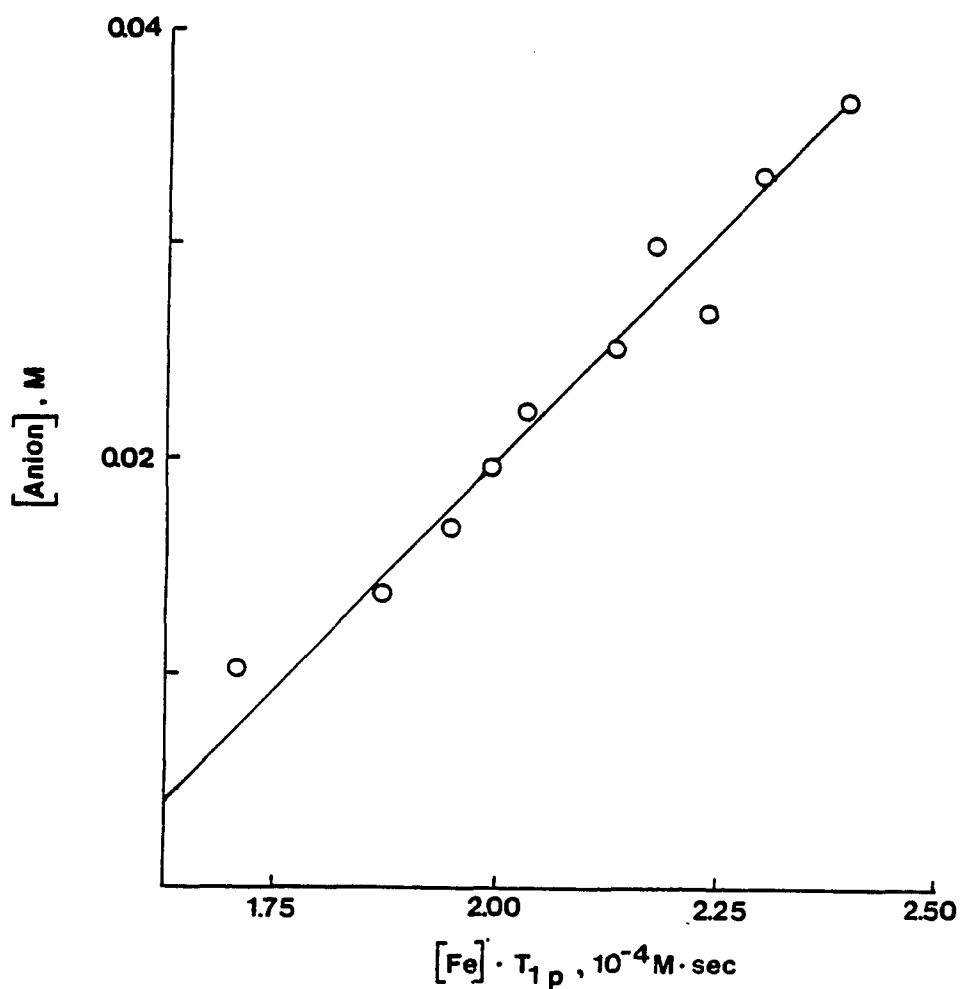


Figure 4.13. Dahlquist-Raftery plot of data shown in Figure 4.10 for  $n = 1$ . The slope of the line is equal to  $(1/T_1)_{\text{app}}$  and the intercept to  $-1/K$ .  $m = 395 \pm 52 \text{ s}^{-1}$ ,  $K = 266 \pm 38 \text{ M}^{-1}$ .

the correct correlation time is known (87). We assume that the rotational correlation time is the appropriate one. The distance can be calculated from the Solomon-Blombergen equation (88, 89).

$$\frac{1}{T_{1M}} = \frac{2}{15} \frac{(S)(S+1)\gamma^2\beta^2g^2}{r^6} \left( \frac{3t_c}{1 + \omega_I^2 t_c^2} \right) \quad (4.4)$$

where  $S$  is the electron spin ( $S = 5/2$ ),  $\gamma$  is the magnetogyric ratio for  $^{31}\text{P}$ ,  $g$  is the electron  $g$  factor ( $g = 2.0$ ),  $\beta$  is the Bohr magneton,  $\omega_I$  is the Larmor precession frequency of the  $^{31}\text{P}$  nucleus, and  $r$  the metal-anion distance.

Using a rotational correlation time of 31 ns (obtained from vanadyl EPR spectroscopy) and assuming the values of  $T_{1\text{app}}$  obtained from nonlinear regression and the Dahlquist-Raftery plots (Figures 4.12 and 4.13) are equal to  $T_{1M}$ , i.e.,  $T_{1M} \gg t_M$ , the metal-anion distances tabulated in Table 4.2 were calculated. We are also assuming here that the correlation time is the same for all nuclei and is independent of pH. Obviously more studies are needed before any more definite conclusions can be made about the metal-anion distance.

### Discussion

This study demonstrates the potential of NMR spectroscopy for studying the interaction of small molecular weight substrates with diferric transferrin. More work is clearly indicated in-

Table 4.2  
Calculated Metal-Anion Distances<sup>a</sup>

<u>Anion (peak)</u>	<u>r (Å)</u>
ATP ( $\alpha$ )	12
ATP ( $\beta$ )	9
ATP ( $\gamma$ )	9
HP <sub>2</sub> O <sub>7</sub>	9 <sup>b</sup>

- a) Calculated by assuming a rotational correlation of 31 ns is the process dominating  $T_{1M}$
- b) Represents the average distance of pyrophosphate phosphorous nuclei.

cluding a detailed titration of ATP with transferrin as a function of temperature and protein concentration. Such a study would allow one to measure  $T_{1M}$  directly as well as providing a measure of the thermodynamic properties,  $\Delta G$ ,  $\Delta H$ , and  $\Delta S$  of anion association with diferric transferrin. A study of the pH dependence of the  $T_1$ 's of ATP would also indicate whether an amino acid residue, which constitutes an anion binding site, is being titrated between pH 7 and 9.

## CHAPTER V

### SUMMARY

The work presented in this dissertation has helped to elucidate the effects that small molecular weight inorganic anions have on the metal centers of transferrin. Using EPR difference spectroscopy we have demonstrated that there are specific anion binding sites on transferrin which when occupied affect the electronic environment of the iron centers. There are two such sites in each domain of the protein and anions bind cooperatively to these sites. Such an observation is unique to nonstereospecific anion interaction with proteins. The binding constants have been determined.

A competitive binding study between transferrin and pyrophosphate has provided thermodynamic information about the ability of pyrophosphate to remove iron from transferrin in vivo, a potential early step in the metabolism of iron. The first direct dependence of iron binding and free bicarbonate concentration is also documented. This result confirms the long standing assumption that bicarbonate will not bind strongly in the absence of iron.

A preliminary investigation of ATP and pyrophosphate binding to diferric transferrin is presented. Using the technique of paramagnetic enhancement of relaxation rates, ATP and pyrophosphate have been shown to bind within the influence of the paramagnetic Fe(III) centers and that both centers are affected.

The studies presented here have provided insight into the chemistry of transferrin as well as raising new and intriguing questions about this unique protein; finding the answers to these questions should provide challenging and stimulating research in the future.



## REFERENCES

## REFERENCES

1. Fletcher, A.; Huehns, E.R.; Nature 1968, 218, 1211.
2. Sussman, M.; "Iron in Biochemistry and Medicine," Academic Press, Inc., N.Y., 1974, 650 pp.
3. Aisen, P.; Aasa, R.; Malmstrom, B.G.; Vanngard, T. J. Biol. Chem. 1967, 242, 2484.
4. Price, E.M.; Gibson, J.F. Biochem. Biophys. Res. Commun. 1972, 46, 646.
5. Williams, S.C.; Woodworth, R.C. J. Biol. Chem. 1973, 248, 5848.
6. Schlabach, M.R.; Bates, G.W. J. Biol. Chem. 1975, 250, 2182
7. Feeny, R.E.; Kamatsu, S.K. Structure and Bonding 1966, 1, 150.
8. Llinas, M.; Structure and Bonding 1973, 17, 135.
9. Chasteen, N.D.; Coord. Chem. Rev. 1977, 22, 1.
10. Aisen, P.; "Inorganic Biochemistry, IV" Elsevier, N.Y., 1973, 280 pp.
11. Morgan, E.H.; "Iron in Biochemistry and Medicine," Academic Press, Inc., N.Y., 1974, 29 pp.
12. Aisen, P. and Listowsky, L.; Ann. Rev. Biochem. 1980, 49, 357.
13. Macgillivray, R.T.; Mendez, E.; Brew, K.; "Proteins of Iron Metabolism," Grune & Stratton, N.Y., 1977, 133 pp.
14. Williams, J.; Biochemistry 1974, 141, 745.
15. Williams, J.; Biochemistry 1975, 149, 237.
16. Brock, J.H.; Arzabe, F.R.; FEBS Letts., 1976, 69, 63.
17. Lineback-Zins, J.; Brew, K; J. Biol. Chem. 1980, 255, 708.
18. Macgillivray, R.T.; Mendez, E.; Sinha, S.K.; Sutton, M.R.; Lineback-Zins, J.; Brew, K.; Proc. Nat. Acad. Sci., U.S.A. 1982, 79, 2504.

19. Williams, J.; Elleman, T.C.; Kingston, I.B.; Wilkins, A.G.; Kuhn, K.A.; *Eur. J. Biochem.* 1982, 122, 297.
20. Metz-Boutique, M.H.; Jolles, J.; Mazurier, J.; Spik, G.; Montreuil, B.; Jolles, P.; *Biochimie.* 1978, 60, 557.
21. Delucas, L.J.; Suddath, F.L.; Gams, R.A.; Bugg, C.E.; *J. Mol. Biol.* 1978, 123, 285.
22. Baker, E.N.; Remball, S.V.; *J. Mol. Biol.* 1977, 111, 207.
23. Gorinsky, B.; Horsburgh, C.; Lindley, P.F.; Moss, D.S.; Parkar, M.; and Watson, J.L.; *Nature* 1979, 281, 157.
24. Cannon J.C.; Chasteen, N.D.; "Proteins of Iron Storage and Transport in Biochemistry and Medicine," North Holland, Amsterdam, 1975, 67 pp.
25. Tan, A.T.; Woodworth, R.C.; *Biochemistry* 1969, 8, 3711.
26. Tan, A.T.; Woodworth, R.C.; *J. Polymer Sci., Part C.* 1970, 599.
27. Casey, J.D.; Chasteen, N.D.; *J. Inorg. Biochem.* 1980, 13, 111.
28. Luk, C.K.; *Biochemistry* 1971, 10, 2838.
29. Bezukoravainy, A.; Grohlich, D.; *Biochim. Biophys. Acta.* 1976, 426, 385.
30. Prados, R.; Boggess, R.K.; Martin, B.B.; Woodworth, R.C.; *Bioinorg. Chem.* 1975, 4, 135.
31. Tomimatsu, Y.; Kint, S.; Scherer, J.R.; *Biochem. Biophys. Res. Commun.* 1973, 54, 1067.
32. Tomimatsu, Y.; Kint, S.; Scherer, J.R.; *Biochemistry* 1976, 15, 4918.
33. Aasa, R.; Aisen, P.; *J. Biol. Chem.* 1968, 243, 2399.
34. Aisen, P.; Leibman, A.; Reich, R.A.; *J. Biol. Chem.* 1966, 241, 1666.
35. Campbell, R.F.; Chasteen; *J. Biol. Chem.* 1977, 252, 5996.
36. Harris, D.C.; Gray, G.; Aisen, P.; *J. Biol. Chem.* 1974, 249, 5261.
37. Najarian, R.C.; Harris, D.C.; Aisen, P.; *J. Biol. Chem.* 1978, 253, 38.
38. Zweier, J.L.; Wooton, J.B.; Cohen, J.S.; *Biochemistry* 1981,

- 20, 3505.
39. Bates, G.W.; Schlabach, M.R.; J. Biol. Chem. 1975, 250, 2177.
  40. Chasteen, N.D.; White, L.K.; Campbell, R.F.; Biochemistry 1977, 16, 363.
  41. Zweier, J.L.; Aisen, P.; J. Biol. Chem. 1977, 252, 6090.
  42. Chasteen, N.D.; Campbell, R.C.; White, L.K.; "Proteins of Iron Metabolism," Stratton, N.Y., 1977, 187 pp.
  43. Aisen, P.; Leibman, A.; Zweier, J.; J. Biol. Chem. 1978, 253, 1930.
  44. Price, M.; Gibson, J.F.; Biochem. Biophys. Res. Commun. 1972, 46, 646.
  45. Bates, G.W.; Schlabach, M.R.; J. Biol. Chem. 1973, 248, 3228.
  46. Williams, J.; Moreton, K.; Biochem. J. 1980, 185, 483.
  47. Williams, J.; Chasteen, N.D.; Moreton, K.; Biochem. J. 1982, 201, 527
  48. Chasteen, N.D.; Williams, J.; Biochem. J. 1981, 193, 717.
  49. Baldwin, D.A.; deSousa, M.R.; Biochem. Biophys. Res. Commun. 1981, 99, 1101.
  50. Carver, F.J.; Frieden, E.; Biochemistry 1978, 17, 167.
  51. Morgan, E.H.; Biochim. Biophys. Acta. 1979, 580, 312.
  52. Aasa, R.; J. Biochem. Biophys. Res. Commun. 1972, 49, 806.
  53. Aasa, R.; J. Chem. Phys. 1970, 52, 3919.
  54. Carrington, A.; McLachlan, A.D.; "Introduction to Magnetic Resonance," Harper & Row, Inc., N.Y., 1967.
  55. Price, E.M.; Gibson, J.; Biol. Chem. 1972, 247, 8031.
  56. Chasteen, N.D.; Campbell, L.K.; White, L.K.; Casey, J.D.; "Proteins of Iron Metabolism," Grune & Stratton, N.Y., 1977.
  57. Mann, K.G.; Fish, W.W.; Cox, A.C.; Tanford, C.; Biochemistry 1970, 9, 1348.
  58. Williams, J.; Private Communication.

59. Linjse, S.S.; van der Kraan, A.M.; J. Inorg. Biochem. 1981, 15, 329.
60. Williams, J.; "Proteins of Iron Storage and Transport in Biochemistry and Medicine," North Holland, Amsterdam, 1975.
61. White, L.K.; Chasteen, N.D.; J. Phys. Chem. 1979, 82, 279.
62. Aisen, P.; Pinkowitz, R.A.; Liebman, A.; Ann. N.Y. Acad. Sci. 1973, 222, 337.
63. Bezhorovainy, A.; "Biochemistry of Non-Heme Iron," Plenum Press, N.Y., 1980.
64. Record, M.T.; Anderson, C.F.; Lohman, T.M.; Quart. Rev. Biophys. II 1978, 2, 103.
65. Chasteen, N.D.; Malik, N.; to be published.
66. Warner, H; Weber J.; J. Am. Chem. Soc. 1953, 75, 5094.
67. Konopka, K.; Mareschal, J.; Crichton, R.R.; Biochim. Biophys. Acta. 1981, 677, 417.
68. Morgan, E.H.; Appleton, T.C.; Nature 1969, 223, 1371.
69. Octave, J.N.; Schneider, Y.J.; Hoffman, P.; Trouet, A.; Crichton, R.R.; FEBS Letts. 1979, 108, 127.
70. Rama, R.; Octave, J.N.; Schneider, Y.J.; Sibille, J.C.; Linet, J.N.; Mareschal, J.C.; Trouet, A.; Crichton, R.R.; FEBES Letts. 1981, 127, 204.
71. Crichton, R.R.; FEBS Letts. 1973, 34, 125.
72. Ankel, E.; Petering, D.H.; Biochem. Pharmacology 1980, 29, 1833.
73. Harris, D.C.; Haroutunian, P.V.; Gutmann, S.M.; Brit. J. Haematology 1977, 37, 302.
74. Kojima, N.; Bates, G.W.; J. Biol. Chem. 1979, 254, 8847.
75. Morgan, E.H.; Biochim. Biophys. Acta. 1977, 499, 169.
76. Egyed, A.; Biochim. Biophys. Acta. 1975, 411, 349.
77. Konopka, K.; Romslo, I.; Eur. J. Biochem. 1981, 117, 239.
78. Konopka, K.; Mareschal, J.C.; Crichton, R.R.; Biochem. Biophys. Res. Commun. 1980, 96, 1408.

79. Fitzgerald, J.J.; Chasteen, N.D.; Biochemistry 1974, 13, 4338.
80. Banerjee, S.; Mitra, S.K.; Science and Culture 1956, 16, 530.
81. Rogers, R.; Reynolds, J.; J. Am. Chem. Soc. 1949, 71, 208.
82. Bates, G.W.; Private Communication.
83. Smith, R.M.; Martell, A.E.; "Critical Stability Constants, I-IV," Plenum Press, N.Y. 1975.
84. James, T.L.; "Nuclear Magnetic Resonance in Biochemistry," Academic Press, N.Y., 1975.
85. Harris, D.C.; Gray, G.A.; Aisen, P.; J. Biol. Chem. 1974, 249, 5261.
86. Dahlquist, F.W.; Raftery, M.A.; Biochemistry, 1968, 1, 3269; Bigbee, W.L.; Dahlquist, F.W.; Biochemistry 1977, 16, 3798.
87. Mildvan, A.S.; Cohen, M.; Adv. Enzym. 1970, 33, 1.
88. Solomon, I.; Phys. Rev. 1955, 99, 559.
89. Solomon, I.; Blombergen, J.N.; J. Chem. Phys. 1956, 25, 261.